UNIVERSITÀ DEGLI STUDI DEL PIEMONTE ORIENTALE

School of Medicine

Department of Health Sciences

Corso di Dottorato di Ricerca in Scienze e Biotecnologie Mediche

Ciclo XXXIV

Academic Years 2019-2021

High Expression of Lysosomal Cathepsin D Inhibits Neuroblastoma Cell Growth, Migration and Invasion, and Confers Better Prognosis in Neuroblastoma Patients

SSD (Settore Scientifico Disciplinare) della tesi: MED 04

Coordinators

Prof. Dr. Marisa Gariglio

Prof. Dr. Sandra D'Alfonso

Mentor

Prof. Dr. Ciro Isidoro

Ph.D. Student

Eleonora Secomandi

TABLE OF CONTENTS

STATEMENT OF ORIGINAL AUTHORSHIP

The work contained in this thesis has not been previously submitted to meet requirements for an award at this or any higher education institution. To the best of knowledge and belief, the thesis contains no material previously published or written by another person except where due to reference is made.

Preface

I have done my Ph.D. studies in Medical Sciences and Biotechnology at Università del Piemonte Orientale (Laboratory of Molecular Pathology, Department of Health Sciences, Novara) under the mentorship of Prof. Ciro Isidoro.

During my studies, I focused on the role of the lysosomal protease cathepsin D in neuroblastoma growth and progression.

On this subject, I have first-authored two original articles in peer reviewed journals, one it is published in *International Journal of Molecular Sciences,* and one is under revision in *Cells* Journal. These two articles are included in this thesis. Also, I have first authored one review article that is under submission to *Cells* Journal.

In addition, I participated to other ongoing lab projects dealing with relevance of autophagy in cancer progression, and in osteogenic differentiation of human gingival mesenchymal stem cells. During a visit to the laboratory of Tumeur/Ingénierie Cellulaire et Génique of Univ. Bourgogne Franche-Comté, Besançon (France), I have studied the anti-fibrotic effects of Halofuginone in keloid fibroblasts. Recently, I have been involved in the study of the role of autophagy in Lymphoma response to chemo-immunotherapy (paper submitted to *Cells* journal). Altogether, during my PhD internship I have co-authored seven papers published plus two more submitted/under submission. One additional paper will arise from the work thesis (see chapter on Cathepsin D and Annexin2), which will be soon submitted. The first pages of these papers are appended at the end of the thesis, in the Appendix section.

Neuroblastoma (NB) is one of the most common extracranial solid tumors of childhood and it accounts for 15% of cancer-related deaths. NB is an embryonal malignancy arising during fetal or early postnatal life from neural crest-derived sympathetic cells. It is commonly found in the adrenal medulla or along the sympathetic chain.

Neuroblastoma shows heterogeneous clinical phenotypes with different rate of aggressiveness and responsiveness to therapies. The broad *spectrum* of clinical manifestations ranges from spontaneous regression, maturation into a benign ganglioneuroma or, in the worst cases, into an aggressive and metastatic disease. The International Neuroblastoma Risk Group (INRG) classification system, developed in 2009, classifies NB patients in four risk groups (very low, low, intermediate, and high) based on clinical criteria and expected-5-year event free survival (EFS) rates. The most frequent genetic aberration found in metastatic high-risk NB is *MYCN* amplification, (25% of all cases), predictor of poor prognosis. Approximately 50% of patients with NB have distant metastasis at the time of diagnosis and the 5-year event-free survival rate of patients with high-risk NB is <50%.

Despite recent advances in chemotherapy and surgical care, high-risk NB remains difficult to treat. MYCN drives oncogenic pathways and the inhibition of its transcription results in reduced cell growth even in *MYCN* non-amplified NB cell lines (Kling et al., 2021). This protein stimulates the extracellular release of procathepsin D (proCD), precursor of the lysosomal protease cathepsin D, leading to doxorubicin resistance and increased survival in neuroblastoma cells.

Cathepsin D (CD) is a ubiquitous soluble aspartic endopeptidase found in acidic intracellular compartments. CD accomplishes bulk protein degradation and mediates the activation of hormones and their precursors, as well as the inactivation of mature growth factors through extensive lysosomal degradation. These functions are associated with protein homeostasis and, consequently, cell growth control. Cytoplasmic translocation of CD, under stressful conditions, can drive apoptosis; on the other hand, overexpression of *CTSD* gene, along with defective segregation in the acidic compartments, leads to abnormal secretion of the precursor proCD which elicits oncogenic activities.

In the first part of the work, we reviewed the "state of art" of the current knowledge regarding cathepsin D in respect of the hallmarks of cancer. A better understanding of its multiple functions might provide novel insights into the molecular mechanisms as possible targets for cancer treatment.

In the first original article, we investigated whether cathepsin D plays a role in EGFR-induced growth and progression of neuroblastoma. We found that patients with high *CTSD* and *EGFR* transcript levels showed a better prognosis and longer overall survival than those with high *EGFR* but low *CTSD*. These preliminary data provided the rationale to speculate that CD could be involved in EGFR signaling. We tested this hypothesis in engineered neuroblastoma cells in which cathepsin D was overexpressed or knocked-down. We found that in the absence of cathepsin D, EGF increased SH-SY5Y cell growth, and conversely, cathepsin D overexpression decreased the proliferative potential. Notably, EGF-mediated activation of ERK 1/2 was associated with a downregulation of endogenous CD protein level. This is the first report showing such an effect of EGF on CD expression in cancer cells.
Our findings enrich the knowledge about the molecular mechanisms downstream EGFR and may help the identification of novel key targets and the development of effective therapeutics.

Multicellular spheroids better resemble the *in vivo* tumor condition and mimic the heterogeneity of cancer clones which develop during tumor evolution. Thus, in the second part of the work, we studied the effects of CD in a three-dimensional culture system, and we investigated whether and how this lysosomal protease plays a role in the metastatic process. 3D cell aggregates mimic clusters of circulating cancer cells forming secondary metastasis. We demonstrated a dual role of cathepsin D in

2D and 3D growth of neuroblastoma cells in response to EGF. High cathepsin D expression promoted the survival of NB cells cultivated in suspension as 3D spheroids, whereas it was detrimental for the growth in adherent condition.

Overall, our findings described a novel anti-proliferative role of cathepsin D and may improve the personalization of therapy for neuroblastoma patients using modulators of cathepsin D synthesis and activity.

A third part of my work deals with the role of CD in the chaperone-mediated autophagy of annexin A2, which results in attenuation of the NB cell malignant phenotype (paper in preparation).

Prefazione

Ho svolto l'internato di Ph.D. in Scienze e Biotecnologie Mediche presso l'Università del Piemonte Orientale (Laboratorio di Patologia Molecolare, Dipartimento di Scienze della Salute, Novara) sotto la guida del Professor Ciro Isidoro.
Durante i miei studi, ho analizzato il ruolo della proteasi lisosomiale catepsina D nella crescita e nella progressione del neuroblastoma.

Sono primo autore di due *original articles* sottoposti a revisione paritaria, uno di questi è pubblicato sulla rivista scientifica *International Journal of Molecular Sciences*, il secondo è in fase di revisione sulla rivista *Cells.* Questi due articoli sono inclusi nella tesi. Inoltre, sono primo autore di una *review*, in fase di revisione sulla rivista scientifica *Cells.*

Inoltre, ho partecipato ad altri progetti di laboratorio in corso sulla rilevanza dell'autofagia nella progressione del cancro e nella differenziazione osteogenica delle cellule staminali mesenchimali gengivali umane. Durante una visita al laboratorio di Tumeur/Ingénierie Cellulaire et Génique dell'Univ. Bourgogne Franche-Comté, Besançon (Francia), ho studiato gli effetti antifibrotici dell'alofuginone nei fibroblasti di cheloidi. Recentemente, sono stato coinvolto nello studio del ruolo dell'autofagia nella risposta del linfoma alla chemio-immunoterapia (articolo presentato alla rivista *Cells*). Complessivamente, durante il mio percorso di Dottorato, sono stato co-autore di sette articoli pubblicati più due sottomessi/in sottomissione. Inoltre, un nuovo articolo deriverà dal lavoro presentato in questa tesi (sezione Risultati, capitolo relativo a Catepsina D e Annessina A2) e sarà presto sottomesso alla rivista *Oncogene*. Le prime pagine di questi articoli sono mostrate alla fine della tesi, sella sezione Appendice.

Il neuroblastoma (NB) è uno dei tumori solidi extracranici più comuni dell'infanzia ed è responsabile del 15% dei decessi per cancro nei bambini. NB è una neoplasia embrionale che insorge durante la vita fetale o postnatale precoce e origina nei neuroblasti derivanti dalla cresta neurale. Frequentemente, (70% dei casi) si sviluppa nell'addome, in particolare nelle ghiandole surrenali, ma può localizzarsi anche a livello del torace (19% dei casi), sul collo o sulla colonna vertebrale. Le persone più colpite da neuroblastoma sono i bambini di età inferiore a 5 anni.

Il neuroblastoma mostra condizioni cliniche eterogenee con diversa aggressività e responsività alle terapie. L'ampio spettro delle manifestazioni cliniche include casi di regressione spontanea, maturazione in un ganglioneuroma benigno o, nei casi peggiori, in una malattia aggressiva e metastatica. Il sistema di classificazione dell' "*International Neuroblastoma Risk Group (INRG)",* sviluppato nel 2009, classifica i pazienti in quattro gruppi di rischio (molto basso, basso, intermedio

e alto) in base a criteri clinici e tassi di sopravvivenza a 5 anni, senza ricadute. L'aberrazione genetica più frequente riscontrata in casi di NB metastatico ad alto rischio è l'amplificazione del gene *MYCN* (25% di tutti i casi), indice di prognosi sfavorevole. Circa il 50% dei pazienti presenta metastasi secondarie al momento della diagnosi e il tasso di sopravvivenza per gli individui classificati ad alto rischio è <50%.

Nonostante i recenti progressi nella chemioterapia e nella chirurgia, il neuroblastoma ad alto rischio rimane difficile da curare. MYCN promuove e attiva diversi processi cellulari pro-oncogenici e l'inibizione della sua trascrizione riduce la crescita e contrasta il fenotipo maligno di cellule tumorali. Questa proteina stimola il rilascio nell'ambiente extracellulare del precursore di catepsina D (proCD), evento associato a chemio resistenza e aumento della sopravvivenza dei cloni tumorali.

Catepsina D (CD) è un'endopeptidasi aspartica solubile presente nei compartimenti intracellulari acidi di tutte le cellule di mammifero. CD svolge un ruolo chiave nella degradazione di proteine intra- ed extra-cellulari e di organelli, media l'attivazione di ormoni e dei loro precursori, nonché l'inattivazione dei fattori di crescita maturi attraverso una degradazione lisosoma-mediata. Queste funzioni sono associate al mantenimento dell'omeostasi e, di conseguenza, al controllo della crescita cellulare. La traslocazione di catepsina D nel citoplasma, in condizioni di stress, può indurre l'apoptosi; al contrario, l'overespressione del gene *CTSD*, insieme alla segregazione aberrante della proteina, portano ad una secrezione extracellulare del precursore proCD che possiede attività oncogeniche.

Nella prima parte del lavoro, abbiamo revisionato ed elaborato le attuali conoscenze in merito a catepsina D e agli *Hallmarks of cancer*, attraverso la scrittura di una *review article*. Una migliore comprensione delle sue molteplici funzioni potrebbe fornire nuove informazioni sui meccanismi molecolari alla base del cancro.

Nel primo *original article*, abbiamo studiato il ruolo di catepsina D nella crescita e nella progressione del neuroblastoma. Abbiamo scoperto che i pazienti con alti livelli di *CTSD* ed *EGFR* (mRNA) hanno una prognosi migliore e una sopravvivenza più lunga rispetto a quelli con *EGFR* alto e ridotto *CTSD* mRNA. Questi dati preliminari hanno fornito il razionale adatto per ipotizzare che CD potrebbe essere coinvolta nel *signaling* del recettore transmembrana EGFR. Abbiamo testato questa ipotesi in cellule di neuroblastoma ingegnerizzate, nel nostro laboratorio, in cui catepsina D era overespressa o silenziata mediante shRNA. Abbiamo dimostrato che in assenza di catepsina D, EGF aumentava la crescita delle cellule SH-SY5Y e, al contrario, la sua overespressione ne diminuiva il potenziale proliferativo. In particolare, l'attivazione di ERK 1/2, mediata da EGF, era associata ad una downregolazione di catepsina D endogena. Questa è la prima dimostrazione scientifica che mostra un

tale effetto di EGF sull'espressione di CD nelle cellule tumorali. I nostri risultati arricchiscono le conoscenze riguardanti i meccanismi molecolari *downstream* EGFR che controllano la crescita cellulare.

Gli sferoidi multicellulari riproducono in maniera più similare la condizione del tumore *in vivo* e mimano l'eterogeneità dei cloni tumorali che si formano durante la cancerogenesi. Nella seconda parte del lavoro, abbiamo studiato gli effetti derivanti dall'overespressione e dal silenziamento di catepsina D in un modello cellulare tridimensionale di NB. Gli aggregati 3D mimano i *clusters* di cellule circolanti che formano metastasi. Abbiamo dimostrato che CD esercita un duplice ruolo nel controllo della crescita 2D e 3D di cellule di neuroblastoma, in risposta al fattore EGF. Elevati livelli di CD favoriscono la sopravvivenza di cellule cresciute in sospensione, ma riducono drasticamente la loro proliferazione in adesione. Questo indica che l'espressione di CD possa variare durante il processo di formazione di metastasi.

Complessivamente, i nostri risultati evidenziano e descrivono un ruolo antiproliferativo della proteasi lisosomiale e potrebbero portare ad un miglioramento della personalizzazione della terapia per i pazienti con neuroblastoma, utilizzando stimolatori della sintesi e dell'attività di catepsina D.

Una terza parte del mio lavoro si incentra sullo studio di catepsina D nell'autofagia chaperone-mediata di annessina 2, meccanismo che provoca un'attenuazione del fenotipo maligno di cellule di neuroblastoma umano (articolo in preparazione).

Chapter 1

Introduction

Neuroblastoma: Epidemiology

Neuroblastoma (NB) is the most common early childhood cancer, representing 8%-10% of all tumors, and the most frequent extracranial solid tumor. NB is an embryonal malignancy arising during fetal or early postnatal life from neural crest-derived sympathetic cells and it is commonly found in the adrenal medulla or along the sympathetic chain (Figure 1) (Davidoff, 2021). It affects children aged 0 to 4 years, the mean age at diagnosis is 18 months and 90% of cases are detected before the sixth year of life. NB accounts for approximately 15% of all cancer-related deaths in the pediatric population (Davidoff, 2021). Neuroblastoma's incidence is higher in white infants and slightly more common among male that females, while the overall incidence is 1 per 100,000 children in the United States (Brodeur *et al.,* 2011). NB very rarely occurs in adolescence and adulthood. The disease shows heterogeneous clinical phenotypes with different rate of aggressiveness and responsiveness to adjuvant therapies. The broad *spectrum* of clinical manifestations ranges from spontaneous regression, maturation into a benign ganglioneuroma or, in the worst cases, into an aggressive and metastatic disease. The different disease evolution finds an important support in clinical observations which date back to the 1960s. In 1963, Beckwith and Perrin described microscopic nodules, termed *in situ* neuroblastoma, in autopsies of the adrenal glands of infants died of non-cancer-related death. The presence of these lesions was more than 200-fold higher that the clinical incidence of NB, indicating different plausible scenarios: nodules may spontaneously regress, may remain dormant or transform in benign tumors, or could become clinically apparent and degenerate in malignant conditions (Beckwith and Perrin, 1963). Spontaneous disease regression is frequently observed in patients younger than 1 year of age. The molecular mechanisms involved are still unclear. However, the host immunity seems to play a pivotal role, since the presence of anti-neuronal antibodies is associated with a better prognosis (Raffaghello *et al.,* 2009). Furthermore, the withdrawal of neurotrophic maintenance factors, such as nerve growth factor, may contribute to NB regression. It is possible to group children diagnosed with NB as low-, intermediate- and high-risk, based on clinical features. This classification system allows to establish the correct medical approach and to define the patient's outcome. Overall, the 5-year survival rate for NB-affecting children is approximately 75%, instead the ones younger than 18 months at onset, exhibit a survival rate greater than 85% (Gigliotti *et al.,* 2009; Zhou *et al.,* 2014). Despite recent advances in early diagnosis and multimodal therapeutic approaches, current treatments remain elusive and ineffective for many patients with high-risk disease, with a 5-year survival rate of less than 50% (Siegel *et al.,* 2021). Therapies for these patients

are often highly aggressive and provide minimal benefit in terms of survival rates. The different clinical condition and outcome are influenced by biological factors, including the genetic background, the age, the tumor stage and the site of the primary tumor.

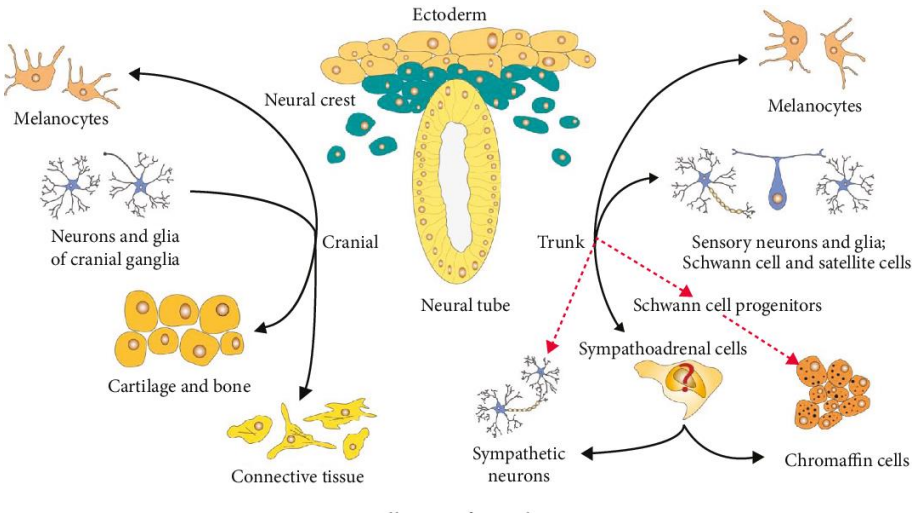

Figure 1. Cell types of neural crest origin (Kholodenko *et al.,* 2018).

Neuroblastoma: Etiology

Approximately 1-2 % of NB cases have a hereditary component, such as the highly penetrant, autosomal dominant germline mutations in *PHOX2B* (associated with neural crest disorders) and alterations in *ALK* gene (Kamihara *et al.,* 2017; Ritenour *et al.,* 2018). This inherited condition leads to an earlier neuroblastoma onset compared to sporadic cases. Other familial syndromes predisposing to cancer, such as Li-Fraumeni Syndrome (especially the R337H pathogenic variant of *TP53*), Beckwith Wiedemann Syndrome with a germline *CDKN1C* mutation, germline RAS pathway gene mutations and Simpson-Golabi-Behmel Syndrome, have been reported to increase the probability of NB development (Scollon *et al.,* 2017). Besides the genetic background, the early stage at diagnosis suggests that the prenatal exposure to chemicals or physical substances, for examples alcohol, cigarette smoke, codeine, hydrocarbons, pesticides, could be risk factors for NB onset. Other genetic abnormalities linked to NB are *MYCN*-amplification, present in 25% of tumors, index of aggressive phenotype and predictor of poor prognosis (Look *et al.,* 1991); deletions of the short arm of chromosome 1 and of the long arm of chromosome 11 (Brodeur, 2003); gain of the long arm of chromosome 17 (Tomioka *et al.,* 2008). In the last decades, advances in genetics and genomics allowed to go more in depth relative to neuroblastoma biology and researchers have identified germline variations predisposing children to familial and sporadic cases, summarized in the review entitled “Genetic Predisposition to Neuroblastoma” (Barr and Applebaum, 2018) (Figure 2).

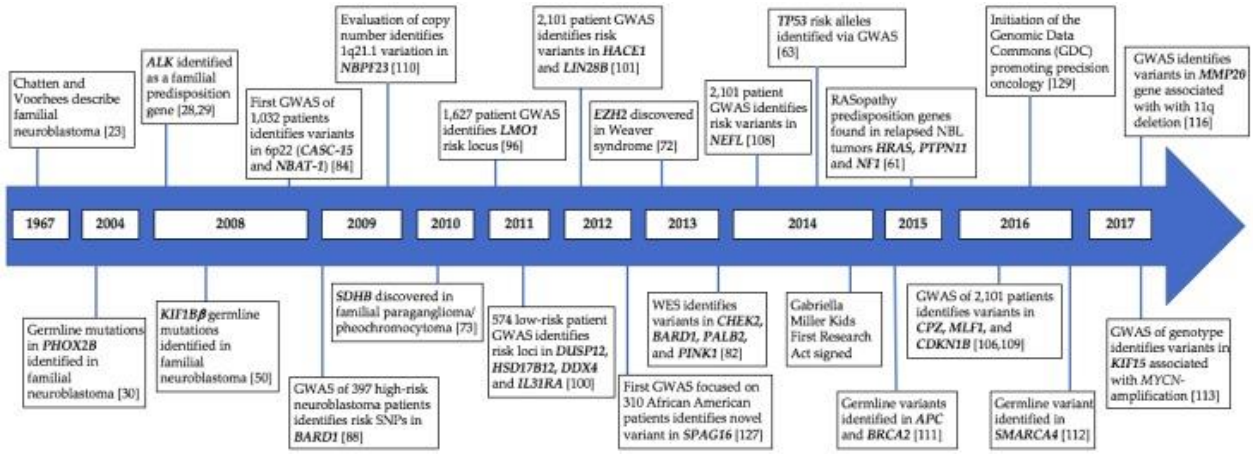

Figure 2. Identification of genetic variants predisposing to neuroblastoma (Barr and Applebaum, 2018).

Neuroblastoma is an embryonal tumor of the sympathetic nervous system arising during fetal or early postnatal life from sympathetic cells (sympathogonia). The neuroectodermal cells originate from the neural crest and during embryonic development they migrate from the dorsolateral side of the spinal neural tube and differentiate into several lineages. Neural (N-) cadherin, member of the cadherin superfamily of adhesion molecules, is crucial for the correct migration of the neural crest cells during early embryonic development. Downregulation of N-cadherin on these cells is essential to allow migration away from the neural tube and contributes to the formation of different tissues (Nieto, 2001). Neural crest cells are the progenitors for the peripheral and enteric nervous systems, the adrenal medulla, melanocytes, smooth muscle, craniofacial cartilage, and bone (Crane and Trainor, 2006). In the last steps of differentiation, most of these progenitor cells undergo apoptosis, and only a small portion of them survive and become fully differentiated with neuronal features and properties (Figure 3). Neuroblastoma originates from stem cells of the sympathoadrenal lineage. Accumulating evidence have highlighted transcription factors and regulators involved in the development of sympathetic lineage as attributable oncogenic drivers, such as MYCN, MASH, ID2, DHAND, HIF, PHOX2 AND TRKA, TRKB, TRKC receptors (Nakagawara *et al.,* 2018). The latter are transmembrane receptors for nerve growth factor (NGF), brain-derived neurotrophic factor (BDNF) and neurotrophin-3 (NT3), respectively. The activation of these pathways positively regulates cell survival and/or differentiation, whereas the inhibition of TRKA activation leads to programmed cell death. For this reason, the amount of free ligand (NGF) has a profound impact on neural crest cell behavior and fate. Even epigenetic alterations and changes could contribute to NB tumorigenesis (Brodeur, 2003).

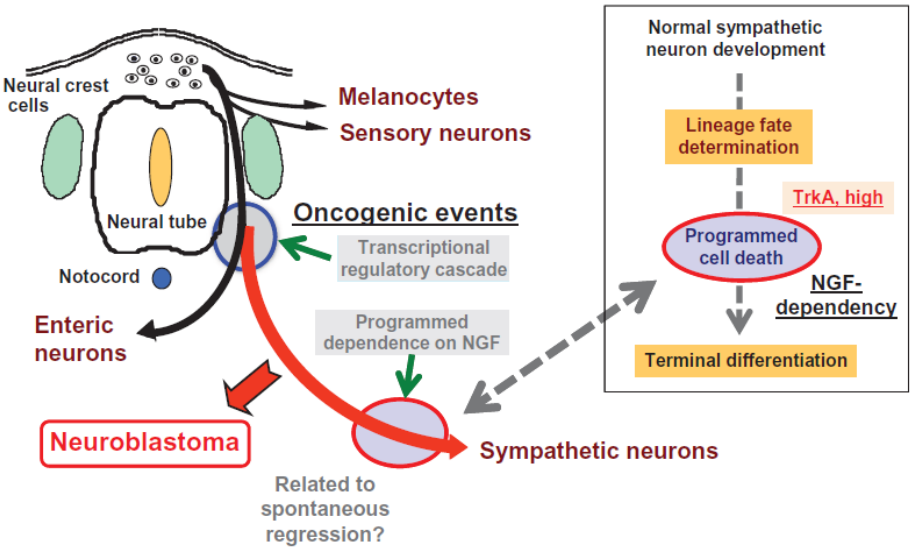

Figure 3. Neural crest cells and NB development (Nakagawara *et al.,* 2018).

Neuroblastoma: Pathology and Clinical Manifestation

Most perinatal cases emerge during the third trimester of gestation and are detected by fetal ultrasound imaging, during routine exams, as solid subdiaphragmatic masses, like cystic components (Nuchtern, 2006). Modern analysis tools, like fetal Magnetic Resonance Imagining (MRI), increase the incidence of early neuroblastoma diagnosis.

Usually, NB arises in a paraspinal location in the abdomen or chest (Brodeur, 2003). Primary tumors develop along the sympathetic nervous system, very frequently in the adrenal medulla and paraspinal ganglia (Figure 4). The involvement of these tumor primary sites correlates with worse prognosis and shorter overall survival, compared to that of primary lesions occurring in others body location (neck, chest, or pelvis). Neuroblastomas typically spread to regional lymph nodes, bone marrow, bones, liver, and skin. Unfortunately, more than 50% of patients are diagnosed with metastatic disease, which leads to secondary syndromes caused by tumor invasion in neural tissues (Nakagawara *et al.,* 2018). The involvement of the central nervous system and lungs are rarely found. Frequent symptoms associated with invasive and metastatic disease are pain, enlarging mass, lymphadenopathy, respiratory distress, hepatomegaly, spinal cord compression, neurological deficits, weight loss, fever and periorbital bruising, due to extravasation of blood into the subcutaneous tissue around the orbit. The presence of tumor masses in the chest can cause dysphagia and dyspnea, due to organ compression, while in the pelvis leads to constipation and difficulty urinating. The skin involvement is detectable as blue subcutaneous nodules known as blueberry muffin syndrome (Colon and Chung, 2011). A small portion of NB patients (1-2%) develops a paraneoplastic syndrome, an indirect consequence of the malignancy, due to the production of autoantibodies recognizing Purkinje cells in

the *cerebellum*, organ controlling movement, motor coordination and balance. Other examples of paraneoplastic syndromes are intractable diarrhea with electrolyte disturbances, due to release of vasoactive intestinal peptide (VIP), encephalomyelitis, or sensory neuropathy (Colon and Chung, 2011).

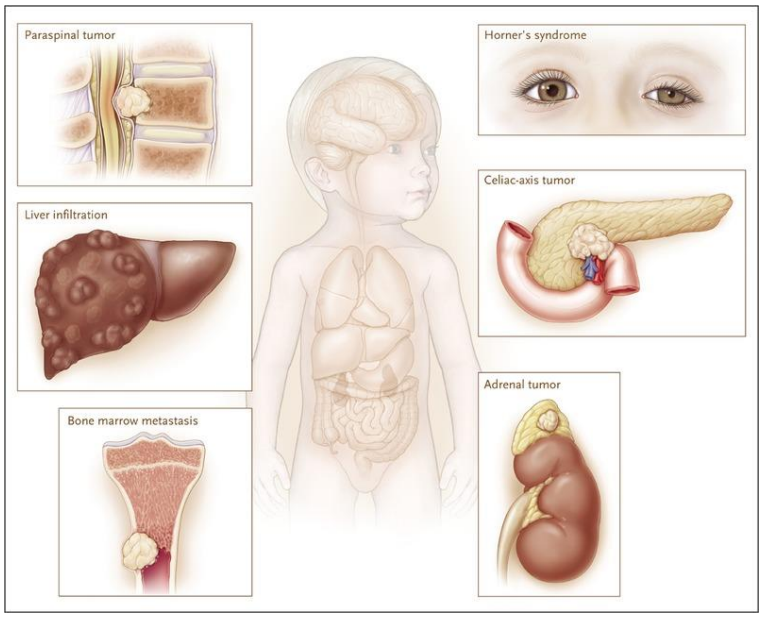

Figure 4. Neuroblastoma primary site and secondary metastasis (Maris, 2010).

Neuroblastoma: Diagnosis

Tumor stage and patient's age at diagnosis are important clinical predictors of outcomes. Early diagnosis associates with better prognosis and reduced mortality. One reason is that lower-stage neuroblastomas are often encapsulated and can be easily removed with surgical interventions, while higher-stage tumors at diagnosis, have already invaded local lymph nodes and distant organs, resulting largely unresectable.

As mentioned before, it is possible to recognize the presence of abnormal masses, in particular adrenal ones, during fetal development, through ultrasonography, a non-invasive technique. Ultrasound imaging and MRI are performed also in postnatal period, to monitor the disease evolution or for a differential diagnosis (Siegel *et al.,* 2002). The diagnostic imaging is the gold standard, indeed a computed tomography scan of the neck, chest, and/or abdomen can simultaneously detect the presence of tumor mass, distant metastasis, and, indirectly, the degree of aggressiveness. Clinical data coming from imaging tools must be accompanied and corroborated by serologic analysis, complete blood count and liver function test. Blood tests include lactate dehydrogenase and ferritin measurements, both with prognostic significance. High serum levels of LDH (>1500 U/ml), ferritin

(>142 ng/ml) and neuron-specific enolase (>100 ng/ml) are associated with advanced tumor stage, relapses, and poor prognosis. These parameters reflect the high proliferative capacity of tumor cells and can be used for monitoring disease evolution and response to therapy (Kim and Chung, 2006). An additional marker for NB diagnosis is the increased level of urine or serum catecholamines or catecholamine metabolites (dopamine, vanillylmandelic acid, and homovanillic acid). These markers are highly specific, given the unique capacity of neuroblastoma cells to secrete the cited products, detected in more than 90% of patients (Kim and Chung, 2006).

To definitively confirm the diagnosis, it is necessary to analyze primary tumor/bone marrow-derived specimens, obtained from the resection of the tumor mass or as an open biopsy for unresectable disease. Once the diagnosis is established, a metaiodobenzylguanidine (MIBG) scintiscan is performed to define tumor staging and monitor the follow-up after therapy administration.

Fluorescent in situ hybridization (FISH) and additional genetic tests, can be performed on tissue samples to note ploidy, gene amplification and other chromosomal aberrations. Knowledge of the genetic abnormalities and molecular alterations responsible for NB tumorigenesis is essential for choosing the correct medical approach and therapeutic intervention. Based on tumor histology, patients are stratified in different categories, according to the "International Neuroblastoma Pathology Classification" (INPC).

Neuroblastoma: Staging and Classification

The International Neuroblastoma Staging System (INSS), first established in 1986 and revised in 1993, classifies NB patients into Stages 1, 2A/2B, 3, 4 and 4S according to the extent of surgical tumor excision at time of diagnosis and the presence of metastasis (Brodeur *et al.,* 1993). Generally, infants younger than 1 year of age display a positive clinical outcome. Tumor bearers diagnosed in advanced stage show a reduced overall survival. In 2009 the International Neuroblastoma Risk Group (INRG) developed a new clinical staging system (INRGSS), for pretreatment risk classification, based on clinical criteria and tumor imaging, rather than on the extent of surgical resection, like the previous one (Monclair *et al.,* 2009). In the novel INRGSS, localized tumors are classified as Stage L1 or L2 depending on the presence or absence of one or more of image-defined risk factors (IDRFs), respectively. In the Stage M are included metastatic tumors, while in Stage MS tumors display metastasis in skin, liver and/or bone marrow in children younger than 18 months of age (Monclair *et al.,* 2009).

Table 1. The International Neuroblastoma Risk Group Staging System (Monclair *et al.,* 2009).

INRG STAGE	DESCRIPTION
L1	Localized tumor, confined to one body compartment (neck, chest, abdomen, pelvis); no involvement of vital structures as defined by IDRFs.
L2	Locoregional tumor with one or more IDRFs.
M	Distant metastatic disease.
MS	Metastatic disease in children younger than 18 months with metastasis confined to skin, liver, and/or bone marrow.

The main genetic alterations, considered as risk factors, are *MYCN* status, DNA index (ploidy), the allelic status at chromosome 11q23 and histopathologic classification. Around 25% of affected infants bear the amplification of *MYCN* oncogene, and this aberration is detected in up to 40% of patients with advanced stage disease. Indeed, the hyperexpression of MYCN protein confers proliferative advantage and a very aggressive phenotype (Brodeur *et al.,* 1984). To be noted, MYCN promotes the transcription of *CTSD* gene and the extracellular secretion of the procathepsin D precursor, from cancer cells, resulting in resistance to doxorubicin-induced apoptosis (Sagulenko *et al.,* 2008). Patients carrying near-triploid tumors manifest a longer overall survival and a better prognosis compared to that of children with others genetic abnormalities, such as chromosome 1p deletion and *MYCN* amplification. The latter anomaly is inversely related to chromosome 11q deletion, considered a high-risk factor (Look *et al.,* 1984; Attiyeh *et al.,* 2005). Based on the genetic background and presence/absence of numerous risk factors, patients are stratified in specific risk groups, depending on the expected 5-year event-free survival (EFS) rate:

- **Very low** (> 85% EFS, 28,2% of patients)
- **Low** (>75% to < = 85% EFS, 26,8% of patients)
- **Intermediate** (> = 50% to 75% EFS, 9% of patients)
- **High** (< 50% EFS, 36,1% of patients)

In general, the overall survival for each of this group is around 90% except for those patients in the high-risk group, that is less than 50% (Siegel *et al.,* 2021).
The guidelines provided by the INRGSS are useful to predict the clinical outcome of NB patients. Besides the risk factors, neuroblastomas can be further divided based on the mitotic index of tumor cells (low, intermediate, high) and the degree of neuroblastic differentiation (undifferentiated, poorly differentiated and differentiated) (Goto *et al.,* 2001).
In summary, we have understood that several factors, like the histopathology of the tumor, the age of the patient and its intrinsic characteristics (genetics and epigenetics) play pivotal role in determining the clinical approach and the prognosis.

Neuroblastoma: Treatments

The standard therapeutic interventions for NB patients essentially include chemotherapy, surgery and/or radiotherapy. Children also need a special psychological support, a constant help concerning physical and cognitive growth and nutritional status. Unfortunately, the medical needs, including effective diagnosis, pharmacological treatments, and supportive care are not equally distributed and accessible around the world. Often, more aggressive neuroblastomas have developed resistance to standard chemotherapy, making this tumor difficult to treat. Multidrug resistant-associated protein 1 (MRP1), encoded by *ABCC1* gene, is an important cause of drug resistance of aggressive NB (Peaston *et al.,* 2001). The survival rate of non-high-risk neuroblastoma is generally high, and exposure to chemotherapy or surgery may be not necessary for these patients. Extensive surgery is often associated with intraoperative and postoperative complications (including bleeding, vascular injuries, sepsis, diarrhea, and damage to organs) particularly in young infants (Azizkhan *et al.,* 1985; Losty *et al.,* 1993). Thus, resection is limited for tumors characterized by a continued growth and aggressive phenotype. Postoperative bowel obstructions occur in 1% to 5% of cases and the overall mortality for young patients underwent to adrenal gland surgery is approximately 2% (Ikeda *et al.,* 1998).
Despite recent advances in early diagnosis and multimodal therapeutic approaches, current treatments remain elusive and ineffective for many patients with high-risk disease, with a 5-year survival rate less than 50% (Siegel *et al.,* 2021), ensuring that this cancer remains an important health problem to manage.
Epidermal growth factor receptor (EGFR) was found overexpressed in neuroblastoma tumor specimens (Tamura *et al.,* 2007), and its signaling was found dysregulated in multi-drug resistant NB cell lines (Meyers *et al.,* 1988). The high expression of EGFR/HER1 has been associated with enhanced tumor growth, invasive potential and chemoresistance in a variety of solid tumors resulting in a worse prognosis for patients (Wells, 1999; Tang and Lippman, 1998).

An attractive approach for cancer treatment is the inhibition of growth factor receptors: the HER1-specific tyrosine kinase inhibitor ZD1839 (Iressa, gefitinib) markedly reduces receptor activation and PI3K/AKT signaling. One limitation of this drug is that it is not effective on MAPK in neuroblastoma (Ho *et al.,* 2005). In addition, alterations of EGFR itself (polymorphisms, variants) and overexpression of HER family ligands (and of certain lncRNAs) are associated with monoclonal antibody resistance and tumor relapse (Braig *et al.,* 2017; Sok *et al.,* 2006; Liao *et al.,* 2015; Li *et al.,* 2019). Getting insight into the molecular mechanism downstream growth factor receptors, may help the identification of novel key targets and the development of personalized therapies.

Neuroblastoma represents a clinical emergency requiring urgent interventions and our work describes for the first time a novel anti-proliferative role of cathepsin D that may be exploited to improve tumor management and treatment.

Cathepsin D: Gene Transcription and Regulation

Human cathepsin D is a soluble aspartic endopeptidase normally resident within the acidic endosomal-lysosomal compartments in all mammalian cells (Barrett, 1979). The protease is also active in secretory inflammatory and lytic granules of mastocytes and lymphocytes, respectively (Dragonetti *et al.,* 2000; Burkhardt *et al.,* 1990). A small amount of CD was found on the plasma-membranes and in the extracellular environment, due to exocytosis (Diment *et al.,* 1988). Cathepsin D is ubiquitously present in human tissues, but its expression differs among the various organs; in particular neurons in the central nervous system (CNS) possess abundant levels of CD (Reid *et al.,* 1986). Human cathepsin D is coded by the *CTSD* gene, located in the short (p) arm of chromosome 11, position (11p) 15.5. The characterization of *CTSD* gene revealed that its promoter presents a mixed structure and features of both housekeeping and a regulated facultative gene (Cavaillès *et al.,* 1993). More precisely, the promoter contains two types of transcription initiation sites: 1) TATA-dependent transcription starting, located around 28 bp downstream from the TATA box; and 2) a TATA-independent transcription initiation site, distant from TATA box and controlled by GC boxes and Sp1 factors. In normal tissues the expression of *CTSD* gene is constitutively controlled from TATA-independent start sites. Overexpression of *CTSD*, along with defective segregation in the acidic compartments, leads to abnormal secretion of the precursor proCD with oncogenic activities; it was largely detected in the culture media and body fluids of tumor bearers (Vignon *et al.,* 1986; Isidoro *et al.,* 1995a; Isidoro *et al.,* 1995b; Reid *et al.,* 1986).

The correlation of CD expression with tumor stage and patient's clinical outcome has been investigated in several cancer types and the extracellular secretion of the precursor is accompanied by the loss of intracellular functions.
The activity of cathepsin D in the wrong time and in the wrong place could be responsible for the acquisition of malignant features driving cancer development and progression.

Biosynthesis of Cathepsin D and Cellular Functions

Human CD is synthesized as a di-glycosylated precursor of approximately 52 kDa in ribosomes attached to the endoplasmic reticulum (ER), which then travers the Golgi complex and is finally delivered by receptors to the endosomal-lysosomal compartment for the last stage of maturation. The multistep processing of cathepsin D biogenesis is expoited a useful reporter to study protein trafficking and maturation along the exocytic-endocytic pathways (Isidoro *et al.,* 1996). The synthesis of cathepsin D (Figure 5) begins into the rough endoplasmic reticulum (RER) and leads to the formation of a pre-pro-enzyme (Faust *et al.,* 1985) composed of 412 amino acids. The short pre-sequence of 20 residues, localized at the N-terminal, is removed while the translation is still ongoing, precisely soon after the translocation across the RER membrane (Erickson and Blobel, 1979). The resulting CD precursor, made up by 392 amino acids, is approximately 52 kDa, and it is still enzymatically inactive. Subsequently, pro-cathepsin D is transported from Golgi complex to the late endosome compartments mainly via mannose-6-phosphate (M6P) pathway (von Figura and Hasilik, 1986; Isidoro *et al.,* 1991). CD mutants lacking one or both sugar chains seem to achieve the correct folding and to maintain enzymatic activity, yet the glycosylation is necessary for their targeting into the lysosome (Fortenberry *et al.,* 1995). In addition, proCD could be delivered to acidic compartments through M6P-independent pathways: one alternative mechanism includes the interaction of proCD with prosaponin, which forms complexes that travel together via membrane association to the acidic organelles (Gopalakrishnan *et al.,* 2004). A second putative molecule responsible for cathepsin D trafficking is sortilin, as substitute of M6P receptor (Canuel *et al.,* 2008). In physiological condition part of the precursor protein can be secreted outside the cell and successively re-endocytosed by M6P-receptors localized at the level of plasma membrane. The endocytosed precursor reaches the early endosomal compartments where the pH allows the dissociation from the receptor. The early endosomes fuse with late endosomes and the precursor can start its processing (Castino and Isidoro, 2008). Here, the acid pH (5-6) allows the limited proteolysis of proCD and the precursor loses its inhibitory pro-peptide (44 amino acids), giving rise to the single chain cathepsin D, enzymatically active. This molecular form, called intermediate, has a molecular weight of 48 kDa and consists of 348 amino acids. The last step of maturation occurs within the lysosome (pH 3.5 - 4.5), where the

intermediate CD is discharged after fusion with the late endosome: here the intermediate CD is finally processed into a double-chain active form, the final mature protein. This is composed of an N-terminal light chain of 13 kDa and a C-terminal heavy chain of 31-33 kDa, bound together through hydrophobic interactions (Baldwin *et al.,* 1993; Gieselmann *et al.,* 1983; Rijnboutt *et al.,* 1992; Delbrück *et al.,* 1994). Mutations occurring in the β-hairpin loop (proteolytic processing region) block the conversion from the intermediate single-chain polypeptide into the mature double-chain form but do not prevent the lysosomal targeting. Moreover, modifications in this amino acid sequence do not affect CD stability or enzymatic activity (Follo *et al.,* 2007).

Cathepsin D is an important endopeptidase and alterations in its synthesis, transport, processing and/or enzymatic activity are correlated with several pathological conditions, (reviewed in Vidoni *et al.,* 2016), and phenotypic abnormalities during embryonic development, as demonstrated in *in vivo* models. More in details, CD knockdown zebrafish *larvae* resulted in several morphological alterations, including failure of yolk absorption, reduced growth of the whole body and of the digestive tract, lack of the swim bladder and microphthalmia associated with defective pigmentation of the retinal epithelium (Follo *et al.,* 2011). Additional evidence reported a crucial role of CD in maintaining the proper development and function of skeletal muscles in zebrafish (Follo *et al.,* 2013). CD is also implicated in embryonic cell death thanks to its ability to trigger apoptosis in the neuroepithelium and in the somitic mesoderm of chicken embryos (Zuzarte-Luis *et al.,* 2007). Cathepsin D orchestrates and directs the development of vital tissues and organs through different mechanisms, mainly affecting the turnover of growth factors and the inactivation of their precursors/inhibitors (Saftig *et al.,* 1995). The extensive lysosomal degradation reduces the pool of active signaling molecules (Berg *et al.,* 1995). On the opposite, the excess of free growth factors leads to the hyperactivation of oncogenic pathways and enhances cell growth, typical features of proliferative disorders such as cancer.

In addition to the proteolytic activity, cytosolic cathepsin D triggers apoptosis in response to cytotoxic/stress agents, such as TNF-α (Démoz *et al.,* 2002), IFN-gamma, Fas/CD95/APO-1 (Deiss *et al.,* 1996), etoposide, 5-fluorouracil, cisplatin (Emert-Sedlak *et al.,* 2005; Castino *et al.,* 2009), 2-phenylethynesulfonamide (Granato *et al.,* 2014), resveratrol (Trincheri *et al.,* 2007), growth factor deprivation (Shibata *et al.,* 1998), oxidative stress (Castino *et al.,* 2007; Roberg and Ollinger, 1998), and sphingosine (Kågedal *et al.,* 2001). The exposure to chemotherapeutic drugs, resveratrol, or reactive oxygen species (ROS), causes the lysosomal leakage and the cytosolic relocation of cathepsin D. In the cytoplasm, it activates pro-apoptotic proteins that increase the mitochondrial permeabilization and the caspase-mediated apoptosis in ovarian cancer and neuroblastoma cells (Castino *et al.,* 2009; Castino *et al.,* 2007). However, the pro-apoptotic or anti-apoptotic functions of

cathepsin D strictly depend on its localization. Indeed, the extracellular precursor proCD increases cell survival via PI3K-AKT signaling activation, and contributes to doxorubicin resistance in neuroblastoma, avoiding apoptosis (Sagulenko *et al.,* 2008). Since the 1980s, scientists described the mitogenic activity of proCD in tumor cell lines, and over the years accumulating evidence highlighted multiple oncogenic functions. In this respect, overexpression and hypersecretion of cathepsin D are often associated with high incidence of metastasis in breast cancer (Masson *et al.,* 2010) and with increased tumor size, grade and chemoresistance in a variety of others solid malignancies (ovarian, glioma, head and neck tumors, melanoma, bladder, prostate, lung, colorectal, liver, and gastric cancers) (Cunat *et al.,* 2004; Leto *et al.,* 2004). Moreover, the extracellular proCD acts as an autocrine and paracrine growth factor for an unknown receptor, triggering RAS/MAPK and PI3K/AKT pathway activation in fibroblasts and in human endothelial cells (Laurent-Matha *et al.,* 2005; Pranjol *et al.,* 2018). This is another example of how CD plays an oncogenic function since a well-organized vascular network supports tumor growth. Therefore, it is fundamental that the protein is correctly segregated to perform its activities in the endosomal-lysosomal compartments, to avoid its aberrant function in the stroma microenvironment.

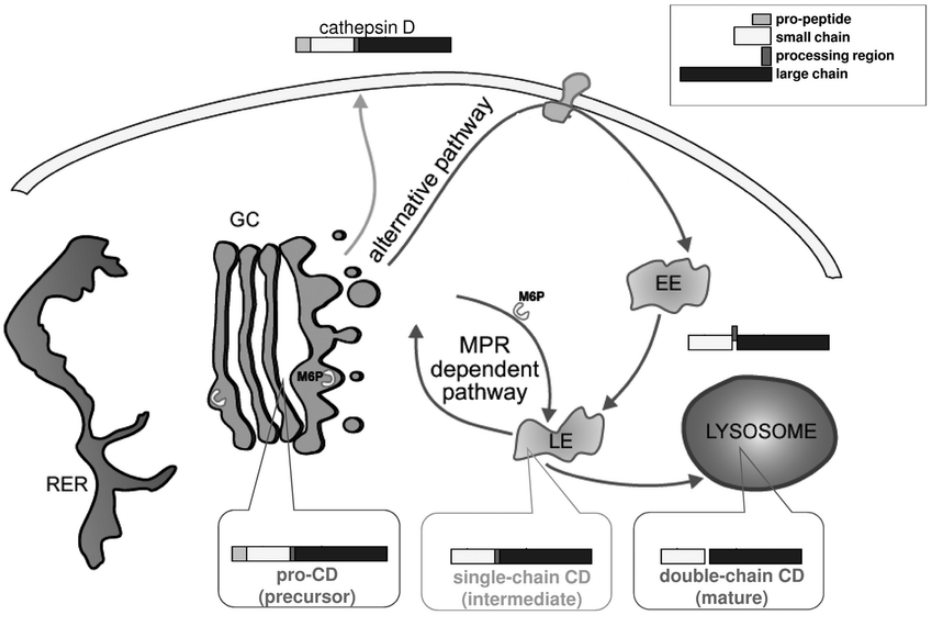

Figure 5. Cathepsin D biosynthesis (Nicotra *et al.,* 2010)

As previously mentioned, lysosomal CD, being a proteolytic enzyme, carries out post-translational modifications on prohormones, growth factors and brain-specific antigens, thus it regulates their turnover (Benes *et al.,* 2008; Minarowska *et al.,* 2007). In other words, cathepsin D indirectly controls cell growth.

The hyperactivation of oncogenic signaling pathways, such as epidermal growth factor receptor/mitogen-activated protein kinase (EGFR/MAPK), as well as the overexpression of EGF family ligands, drive malignant transformation and neuroblastoma progression (Wells, 1999; Tang and Lippman, 1998; Sasaki *et al.,* 2013). Current knowledge describes the involvement of cathepsin S and B in the attenuation of EGFR signaling and in receptor degradation (Huang *et al.,* 2016; Authier *et al.,* 1999). However, no information about the possible involvement of cathepsin D has never been reported. Whether CD plays an active role in EGFR-induced growth and progression of neuroblastoma remains to be elucidated.

In the first part of this thesis, I have reviewed the "state of art" of the current knowledge regarding the role of cathepsin D in the development and progression of cancer, in respect of cell proliferation, invasion and metastasis, angiogenesis, apoptosis, and inflammation, known as hallmarks of cancer (Figure 6).

During the research work, first we interrogated datasets from the TCGA database to determine the clinical relevance of *CTSD* status in pediatric neuroblastoma patients highly expressing *EGFR*. Then, we validated *in vitro* the hypothesis that cathepsin D could be involved in EGFR signaling regulation. Overall, our findings may have a translational relevance and we propose cathepsin D as a possible biomarker for the stratification of neuroblastoma patients in a view of personalized medicine. The identification of a novel prognostic marker may be helpful to improve tumor management and treatments.

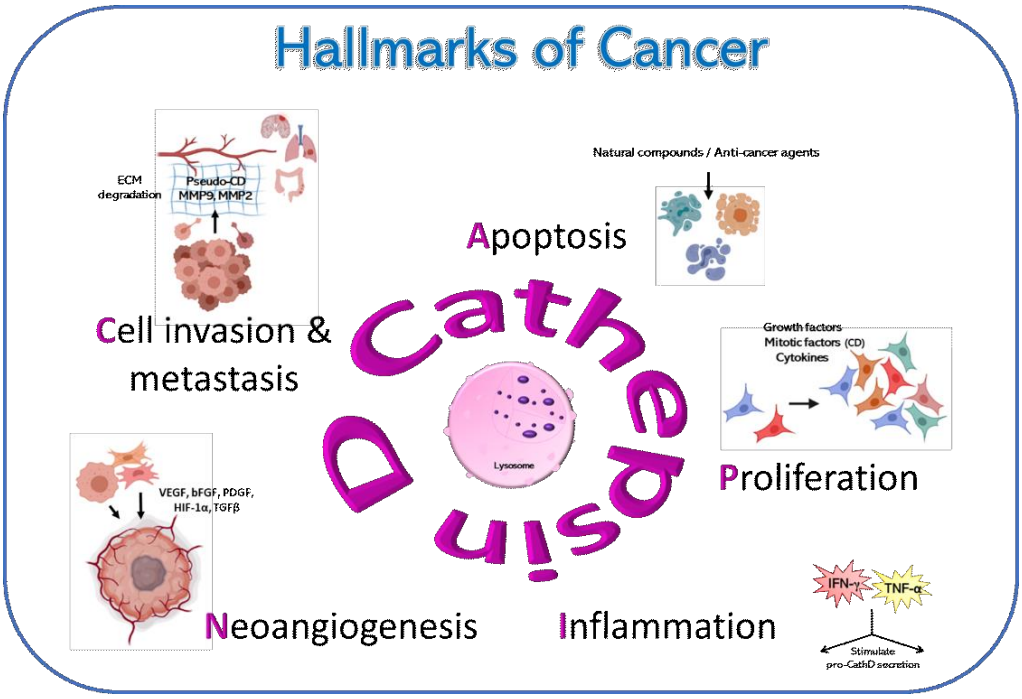

Figure 6. Cathepsin D and Hallmarks of Cancer

Chapter 2
Aims

The aims of the work performed during my Ph.D. study were:

1) To review the literature on the role of lysosomal cathepsin D in cancer.

2) To assess whether cathepsin D plays a role in EGF-induced growth and progression of neuroblastoma.

3) To investigate the biochemical pathways downstream EGFR activation in human SH-SY5Y neuroblastoma cells, engineered for overexpressing or silencing CD expression.

4) To investigate whether and how cathepsin D differently affects the growth of NB cells in suspension as 3D neurospheroids *versus* 2D adherent condition, in response to EGF.

5) To explore the significance of cathepsin D-annexin A2 interaction and to assess whether and how the post-translational modification of annexin A2 affects the malignant phenotypes of neuroblastoma cells.

Chapter 3

Materials and Methods

Materials and Methods reported in this section refer to the manuscript to be submitted.

Here, I will describe more in detail the cellular model employed and the informatic tool used for the quantitative analysis of image data in the measurement of fluorescence intensity.

Cell Culture and Treatments

Human neuroblastoma SH-SY5Y cells were obtained from the American Type Culture Collection (ATCC® CRL-2266™, Rockville, MD) and genetically manipulated in our laboratory under the supervision of Professor Ciro Isidoro. Originally, SH-SY5Y arise from SK-N-SH cells, isolated in 1970 from the biopsy of a four-year old female child affected by neuroblastoma. NB is a malignant neuroendocrine tumor deriving from embryonic neural crest cells, from which physiologically originate the adrenal medulla and ganglia of the sympathetic nervous system. Morphologically, SH-SY5Y cells assume a neuronal-like phenotype with a non-polarized body and short neurites. They were maintained in standard conditions (37°C, 95 v/v% air: 5 v/v% CO_2) in 50% Minimum Essential Medium (MEM, cod. M2279, Sigma-Aldrich Corp., St Luis, MO, USA) and 50% Ham's F12 Nutrient Mixture (HAM, cod. N4888, Sigma-Aldrich Corp.), containing 10% heated-inactivated Fetal Bovine Serum (FBS, cod. ECS0180L; Euroclone S.p.A., Milan, Italy), supplemented with 1% Glutamine (cod. G7513, Sigma-Aldrich Corp.) and 1% w/v of Penicillin/Streptomycin (cod. P0781, Sigma-Aldrich Corp.). For this study, we employed three engineered clones of SH-SY5Y neuroblastoma cells (Sham, KD-CD and Over CD) (Figure 7). The clone generation procedure is described in Secomandi, Salwa *et al.,* 2022.
Alternatively, the cells were cultured in Earle's Balanced Salt Solution (EBSS, cod. E2888, Sigma-Aldrich Corp.), containing 1% glucose, without fetal bovine serum. Cultured cells were treated, where specifically indicated, with 20 ng/ml Epidermal Growth Factor (EGF, cod. E5036; Sigma-Aldrich Corp.), dissolved in 10 mM acetic acid, or Pepstatin A (PstA, cod. P4265; Sigma-Aldrich Corp.), used at 100 μM as a final concentration.

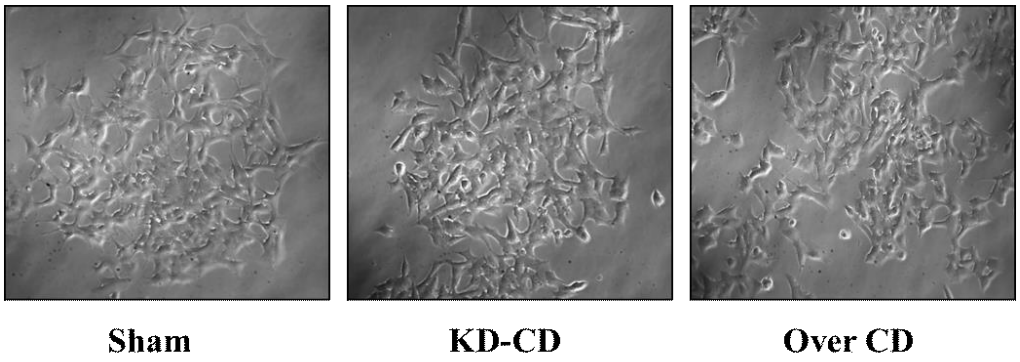

Figure 7. Images of SH-SY5Y transgenic clones.

Antibodies

The following primary antibodies (used in the last paper to be submitted) were employed for western blotting: mouse anti-β-tubulin (1:1000, cod. T5201; Sigma-Aldrich Corp.), mouse anti-β-actin (1:2000, cod. A5441; Sigma-Aldrich Corp.), rabbit anti-annexin A2 full-length (1:1000, cod. PA5-88522; Invitrogen, Waltham, MA, USA), mouse anti-phospho (Tyr23) annexin A2 (1:250, cod. sc-135753; Santa Cruz Biotechnology), mouse anti-annexin A2 (C-10) (1:500, cod. sc-28385; Santa Cruz Biotechnology), mouse anti-cathepsin D (1:100, cod. IM03; Calbiochem), mouse anti-HSC70 (1:250, cod. sc-32239; Santa Cruz Biotechnology), mouse anti-STAT3 (1:500, cod. 9139; Cell Signaling), rabbit anti-phospho (Tyr705) STAT3 (1:500, cod. 9145; Cell Signaling), rabbit anti-cyclin D1 (1:500, cod. 2978; Cell Signaling). Secondary antibodies employed for immunoblotting were purchased from the following sources: Horse Radish Peroxidase-conjugated goat anti-mouse IgG (1:10,000, cod. 170–6516; Bio-Rad, Hercules, CA, USA), Horse Radish Peroxidase-conjugated goat anti-rabbit IgG (1: 10,000, cod. 170–6515: Bio-Rad, Hercules, CA, USA). The following primary antibodies were employed for immunofluorescence: rabbit anti-LAMP2 (1:100, cod. PRS3627; Sigma-Aldrich Corp.), rabbit anti-phospho (Tyr705) STAT3 (1:100, cod. 9145; Cell Signaling), mouse anti-phospho (Tyr23) annexin A2 (1:100, cod. sc-135753; Santa Cruz Biotechnology), mouse anti-annexin A2 (C-10) (1:100, cod. sc-28385; Santa Cruz Biotechnology), rabbit anti-annexin A2 full-length (1:50, cod. PA5-88522; Invitrogen), mouse anti-HSC70 (1:250, cod. sc-32239; Santa Cruz Biotechnology), mouse anti-cathepsin D (1:100, cod. IM03; Calbiochem), rabbit anti-TWIST1 (1:500, cod. 69366, Cell Signaling). Secondary antibodies used for immunofluorescence were purchased from the following sources: goat-Anti Rabbit IgG Alexa FluorTM Plus 488 (1:1000, cod. A32731; Invitrogen) and Goat-Anti Mouse IgG Alexa FluorTM Plus 555 (1:1000, cod. A32727; Invitrogen).

Western blotting

SH-SY5Y Sham, KD-CD and Over CD clones were plated at a density of 50,000 cells/cm^2 on sterile P35 Petri dishes and let adhere. Treatment with EGF, PstA or incubation with EBSS were performed when the confluence reached approximately 80%. Cells were harvested in RIPA Buffer (0.5% Deoxycholate, 1% NP-40, 0.1% Sodium Dodecyl Sulfate in PBS solution) supplemented with protease inhibitor cocktail and phosphatase inhibitors (sodium fluoride and sodium orthovanadate) and homogenized using an ultrasonic cell disruptor XL (Misonix, Farmingdale, NY, US). All reagents were supplied by Sigma-Aldrich Corporation. Protein content concentration was determined with a Bradford assay and samples were denaturized with 5X Leammli sample buffer at 95°C for 10 minutes. Equal amounts of protein (30 μg of total cell homogenates) were separated by SDS-PAGE and transferred onto PVDF membrane (cod.162-0177; BioRad, Hercules, CA, USA). Filters were blocked with 5% not-fat dry milk (cod. sc-2325; Santa Cruz Biotechnology) solution containing 0.2% Tween-20 for 1 hour at room temperature (RT). Subsequently, membranes were incubated with specific primary antibodies overnight at 4°C, followed by incubation with secondary HRP-conjugated antibodies (goat anti-mouse and goat anti-rabbit) for 1 hour at room temperature. The bands were detected using Enhanced Chemiluminescence reagents (ECL, cod. NEL105001EA; Perkin Elmer, Waltham, MA, USA) and developed with the ChemiDoc XRS instrument (BioRad, Hercules, CA, USA). Intensity of the bands was estimated by densitometry using Quantity One Software (BioRad, Hercules, CA, USA).

Immunofluorescence

SH-SY5Y clones were seeded separately onto sterile coverslips at the density of 30,000 cells/cm^2, let adhere and grow before treatment. KD-CD and Over CD were cocultured together at a density of 20,000 cells/cm^2 for each clone. The cell monolayers were scratched using a sterile pipette yellow tip and then washed with 1X PBS to remove the cell debris. Treatment was performed as appropriately indicated. At the end of the experiment, the coverslips were fixed in ice-cold methanol, permeabilized with 0.2% Triton-PBS and then re-fixed with methanol. After washing with 1X PBS, coverslips were incubated with specific primary antibodies, dissolved in 0.1% Triton PBS + 10% FBS, overnight at 4°C. The following day, the coverslips were washed with 0.1% Triton-PBS and incubated for 1 hour at room temperature with Goat-Anti Rabbit IgG Alexa FluorTM Plus 488 or Goat-Anti Mouse IgG Alexa FluorTM Plus 555 secondary antibodies, as appropriate. Nuclei were stained with the UV fluorescent dye DAPI (4′,6-diamidino-2-phenylindole). Secondary antibodies and DAPI were dissolved in 0.1% Triton-PBS + 10% FBS. Thereafter, coverslips were mounted onto glasses using

SlowFade antifade reagent (cod. S36936; Life Technologies, Paisley, UK) and data acquired by fluorescence microscope (Leica DMI6000, Leica Microsystems, Wetzlar, Germany). For each experimental condition, different microscopic fields were randomly selected. Scale bar = 20 μm; magnification = 63x.

Co-Immunoprecipitation Assay

SH-SY5Y cells were seeded onto sterile P60 Petri dishes at a density of 100,000 cells/cm^2 and let adhere and grow before treatments. In each plate, 10 minutes before the end of the treatment, 0.5 M 3-3'-dithiodipropionic acid di-(N-hydroxysuccinimide ester), a chemical cross-linker, was added into the medium. Then, the culture media were collected and centrifuged at 2000 rpm for 5 minutes. The supernatant was aspirated, the pellet resuspended in 350 μL of PBS 1X, again centrifuged and kept on ice. Sample collection was performed by scraping the Petri dishes with 350 μl of RIPA Buffer supplemented with protease inhibitor cocktail and phosphatase inhibitors (sodium fluoride and sodium orthovanadate) and homogenized using an ultrasonic cell disruptor. The cell lysates were stored at -20°C. Protein concentration was determined by BCA assay. The samples (500 μg) were incubated with anti-CD primary antibody or anti-Annexin A2 full-length antibody for 2 hours at 4°C, under rotation. The dilution factors are reported in the previous section (Antibodies). The immunocomplexes were captured by adding 50 μl of Sepharose G beads (cod. P3296; Sigma-Aldrich Corp.), under rotation at 4°C over-night. The bead-bound immunocomplexes were precipitated by centrifugation (1000 g) and eluted with 80 μl of Leammli buffer 1X at 95°C for 10 minutes. Equal volume of eluate was loaded onto SDS-containing polyacrylamide gels and immunoblotted with specific antibodies to reveal the presence of immunoprecipitates.

***In vitro* Protease Assay**

To further assess and demonstrate the CD-mediated proteolytic cleavage of annexin A2, an *in vitro* protease assay was performed. SH-SY5Y KD-CD cells were seeded in sterile P60 at a density of 100,000 cells/cm^2 and employed as substrate homogenates for the unaltered annexin A2 protein and the lack of cathepsin D. Cells were collected with RIPA Buffer supplemented with phosphatase inhibitors. Cathepsin D was immunoprecipitated from Over CD cell homogenates. Immunocomplexes were eluted with Leammli buffer 1X in a final volume of 20 μl. 100 μg of samples (SH-SY5Y Sham incubated with Pepstatin A, SH-SY5Y KD-CD control condition, EBSS- and EGF-treated cells), were incubated with equal amount (100 μg) of immunoprecipitated cathepsin D. Protease reaction was carried out for 3 hours at 37°C. At the end, samples were boiled at 95°C in Leammli buffer 5X and then separated by SDS-PAGE. As control, Leammli buffer 5X was added in

4 eppendorf containing 100 µg of Sham PstA, KD-CD Co, KD-CD EBSS, KD-CD EGF total lysates. Immunoblots were developed using anti-annexin A2 full-length and anti-cathepsin D primary antibodies.

siRNA Transfection and Clonogenic Assay

SH-SY5Y KD-CD cells were seeded into P35 Petri dishes at the density of 50,000 cells/cm^2 and let adhere. When cells reached the 80% of confluence, transfection with 150 pmol/µl siRNA ANXA2 and 150 pmol/µl siRNA Co-Duplex was performed using Lipofectamine™ 3000 Transfection Reagent (cod. L3000-15, Invitrogen). The siRNA-Lipofectamine complexes were prepared in 125 µl of OptiMEM I Reduced Serum Medium (cod. 11058021, Invitrogen) with 150 pmol/µl of siRNA and 7.5 µl of Lipofectamine™ 3000. After 6 h of incubation, the medium was replaced with a serum-containing culture medium (10% FBS), and the cells were cultivated for further 21 hours to allow protein silencing. Subsequently, KD-CD cells were collected, counted and then 2000 cells/P35 were seeded for each experimental condition. The experiment was carried out for 10 days to allow colony formation (Thongchot *et al.,* 2021). Treatment with 20 ng/ml EGF in fresh culture medium was performed every 48 hours. A second transfection was executed on KD-CD cells after 5 days of culture. At the end of the experiment, the medium was removed, cells were washed with 1X PBS and then fixed with methanol for 20 minutes at room temperature. Next, another wash with 1X PBS was performed and subsequently colonies were stained with 0.5% crystal violet solution for 30 minutes. Finally, P35 were washed with distilled water (until the background becomes clear) and dried at room temperature. Each Petri dish was photographed, and the number of colonies formed was estimated by photometric measurements and CellCounter software (v0.2.1.).

Wound-Healing Migration Assay

Cells were seeded in P35 Petri dishes at the density of 80,000 cells/cm^2 and cultured until confluence. The cell monolayers were scratched with a sterile pipette yellow tip to produce a straight line, and the debris washed out with culture medium (Morani *et al.,* 2014). Medium and substances for treatment were renovated every 24 hours. The open gap was photographed with a camera at phase contrast microscope (magnification 5x) at the indicated times. The rate of healing was estimated by ImageJ software based on the area (in which the length is predetermined, and the wideness varies) free of cells. Data are calculated for three different fields per each condition in three separate experiments. SH-SY5Y KD-CD cells were transfected with siRNA ANXA2 and Co-Duplex before the scratching, as described in the previous paragraph.

Transwell *in Vitro* Cell Migration Assay

Cells were plated in Petri dishes at a density of 25,000 cells/cm^2 and cultured until reaching 80% confluence. Cell monolayers were cultured as appropriate, and treatments were renovated the following day. After 48 hours of culture, cells were trypsinized, collected and counted. For each experimental condition, 50,000 cells were resuspended in serum-free medium supplemented with the corresponding treatment and loaded into individual uncoated inserts containing 8.0 μM pore-size polycarbonate membrane (cod. 3422; Corning Incorporated Costar, New York, NY, USA). Each insert was placed in a 24-well plate containing complete media (10% FBS) and the plate was placed in the incubator. After 24 h (collectively 72 hours of treatment), cells that had migrated to the underside of the inserts were washed in 1X PBS, fixed in methanol for 30 min, washed again with 1X PBS and then processed for immunofluorescence double staining CD / TWIST1. Incubation with the secondary antibodies was performed the day after, for 1 hour, at room temperature. Inserts were cut and mounted onto slides using SlowFade antifade reagent and photographed with fluorescence microscope (Leica DMI6000, Leica Microsystems, Wetzlar, Germany). For each experimental condition, different microscopic fields were randomly selected, and representative images were shown. Scale bar = 20 μm; magnification = 63x.

Bioinformatic Analysis

Kaplan–Meier curves, correlation studies and biological process were obtained by extracting clinical data from the TCGA database (www.portal.gdc.cancer.gov/, last accessed on 29 April 2021). RNA-seq and corresponding clinical data (including overall survival status, INSS stage and mRNA expression of 21,578 group of genes) of Pediatric Neuroblastoma patients (TARGET 2018, that comprised 248 patients after filtering out dataset without enough survival information) were downloaded from the cBioportal.org. Patients were grouped based on the level of mRNA expression i.e., low *versus* high groups were defined relative to the median expression level of overall patient cohort. Pearson and Spearman's correlation analysis were performed to identify the genes correlated with *ANXA2*. TBtools (https://github.com/CJ-Chen/TBtools/) was used to identify the differentially expressed genes (DEGs) in correlation with *CTSD*, represented as Volcano plot. To identify the DEGs, cut-off criteria was set based on Spearman's correlation value (i.e., correlation coefficient value greater than + 0.25 (positively correlated) or lower than − 0.25 (negatively correlated) and *p*-value < 0.00001 (-log10(p-value) threshold was fixed above 5.0). DAVID bioinformatics functional annotation tool (https://david.ncifcrf.gov/summary.jsp) was used to analyze Gene Ontology (GO) biological processes and Kyoto Encyclopedia of Genes and Genomes (KEGG) pathway were obtained with the help of positively - differentially expressed genes. Data are presented in bar graphs

displaying the number of transcripts belonging to negatively associated biological processes. Scatter plots were employed to represent the correlation between the expression of relevant biomarkers in the patient cohort. Pearson correlation analysis were performed to identify the correlation between *ANXA2* and *STAT3* genes. Regression was estimated by calculating Pearson's correlation coefficients (r) and the relative *p*-values. *ANXA2* and *STAT3* were grouped based on the level of mRNA expression in neuroblastoma patients. The correlation of *ANXA2* and *STAT3* was performed after sub-classification of mRNA expression based on the level of Z-score values as high (upper 25% of z-score values) and low (below 75% of z-score values), respectively. *CTSD* mRNA expression was defined relative to the median expression level of all patients in the form of a box-plot and used to investigate the relationship between dichotomized *ANXA2* and *STAT3* groups. To reduce the potential bias from dichotomization, *CTSD* mRNA expression was measured in the *ANXA2* and *STAT3* different expression groups and were compared using t-test (Welch Two Sample t-test) by R. All cut-off values were set before the analysis, and all the tests were two-tailed. All statistical analysis were performed using R (3.6.1 version, The R Foundation for Statistical Computing, Vienna, Austria) and SAS software (9.4. version, SAS Institute Inc., Cary, NC, USA). The log-rank test has been used to determine the statistical significance. The p-value ≤ 0.05 was considered as significant. Survival analysis was performed using SAS for the *ANXA2* and *STAT3* mRNA expression level-based groups. Survival curves of these three groups were estimated by the Kaplan–Meier plots and compared using the Cox regression model assuming an ordered trend for the three groups as described previously. The log-rank test has been used to determine the statistical significance. The p-value < 0.05 was significant.

Statistical Analysis

Statistical analysis was performed with GraphPad Prism 6.0 software (San Diego, CA, USA). Bonferroni's multiple comparison test after one-way/two-way ANOVA analysis (unpaired, two-tailed) was employed. Significance was considered as follow: **** $p < 0.0001$; *** $p < 0.001$; ** $p < 0.01$; * $p < 0.05$. Data are reported as average ± S.D.

Image J Freeware Software

In this thesis, the ImageJ freeware software was employed as a technique for quantitative analysis of data in the measurement of Intensity Density (INT.DEN) of the fluorescence signal. Quantification of fluorescence was performed on single channel in the case of the unique staining, or on the two-channels merge in the case of double-staining to estimate the co-localization of two proteins. The processing direction of using the software is briefly explained as below.

First, start to open a*.TIF file in ImageJ and follow the next steps:

To analyze "one single channel":

- Select the TIF file correspond your signal target (channel blue corresponds "image_A", whereas channel red corresponds "image_N21");
- Image Adjust Threshold (Thresholding method = Default; Threshold color = Red; Color space = HSB) Click to "Select"
- Go to the Menu Analyze Measure
- Finally appear a table of Results The term "INT.DEN" is the value of the intensity of fluorescence

To analyze "two-channels":

- Select the TIF file correspond your signal target, in this specific case is the "Overlay_Maximum";
- Image Adjust Threshold Color (Thresholding method = Default; Threshold color = White; Color space = RGB; click off "pass" of the channel blue if you desire to quantify the yellow signal obtained from the overlay between the channel red and green)
- Click to "Select"
- Go to the Menu Analyze Measure
- Finally appear a table of Results The term "INT.DEN" is the value of the intensity of fluorescence.

Chapter 4

Results

High Expression of the Lysosomal Protease Cathepsin D Confers Better Prognosis in Neuroblastoma Patients by Contrasting EGF-Induced Neuroblastoma Cell Growth

Secomandi E, Salwa A, Vidoni C, Ferraresi A, Follo C, Isidoro C. High Expression of the Lysosomal Protease Cathepsin D Confers Better Prognosis in Neuroblastoma Patients by Contrasting EGF-Induced Neuroblastoma Cell Growth. Int J Mol Sci. 2022 Apr 26;23(9):4782. doi: 10.3390/ijms23094782. PMID: 35563171; PMCID: PMC9101173.

SYNOPSIS

Neuroblastoma is the most common early childhood cancer, representing 8%-10% of all tumors, and the most frequent extracranial solid cancer. NB is an embryonal malignancy arising during fetal or early postnatal life from neural crest-derived sympathetic cells and it is commonly found in the adrenal medulla or along the sympathetic chain. NB accounts for approximately 15% of all cancer-related deaths in the pediatric population. Despite the advances in early diagnosis and therapeutic innovations, it remains difficult to treat and for high-risk disease the 5-year survival rate is less than 50%. The most frequent genetic aberration found in metastatic high-risk NB is *MYCN* amplification, (25% of all cases), which correlates with undifferentiated, aggressive phenotype and poor prognosis. Among various *MYCN* target genes, the lysosomal protease cathepsin D was also identified. In addition to increased *CTSD* transcription, MYCN stimulates the secretion of a specific precursor (proCD, 52 kDa) from neuroblastoma cells, with oncogenic activities.

Cathepsin D is a ubiquitous soluble aspartic endopeptidase normally found in acidic intracellular compartments. Its protein synthesis begins in the rough endoplasmic reticulum as preprocathepsin D, proceeds towards Golgi complex until late endosomes, mainly via mannose-6-phosphate pathway. The last step of maturation occurs in lysosomes where the intermediate CD is processed into the double-chain active form (31 kDa). Mature CD accomplishes protein degradation, promotes the macromolecular turnover, and it sustains cell homeostasis. On the opposite, secreted extracellular cathepsin D elicits oncogenic activities.

The present study reported that NB patients bearing high level of CD benefit from a better prognosis. *In silico* transcriptome analysis revealed that patients with high *EGFR* and high *CTSD* levels had a better prognosis compared to patients bearing high *EGFR* and low *CTSD.* Accordingly, two-thirds of patients at INSS Stage 4 had low *CTSD*, indicating that neuroblastomas with CD deficiency grow and progress faster. Therefore, we argued that in neuroblastomas highly expressing CD, the protease is retained intracellularly and can control protein homeostasis and, consequently, the cell cycle. Consistent with this interpretation, overexpression of *CTSD* gene negatively correlated with a subset of genes associated with cell cycle and proliferation, including *CCNB2*, *CCNA2*, *CDK1*, and *CDK6.* We validated *in vitro* our hypothesis, and we found that the addition of exogenous EGF strongly enhanced the proliferation of CD knockdown cells. SH-SY5Y overexpressing CD showed a higher expression of p21 and were less responsive to EGF stimulation. Notably, EGF-mediated activation of ERK 1/2 was associated with a downregulation of endogenous CD protein level.

This is the first report showing such an effect of EGF on CD expression in cancer cells. Stimulators of cathepsin D synthesis and activity, such as the nutraceutical resveratrol, could be exploited as adjuvant therapy for neuroblastomas low expressing cathepsin D and not responding to the EGFR inhibitors.

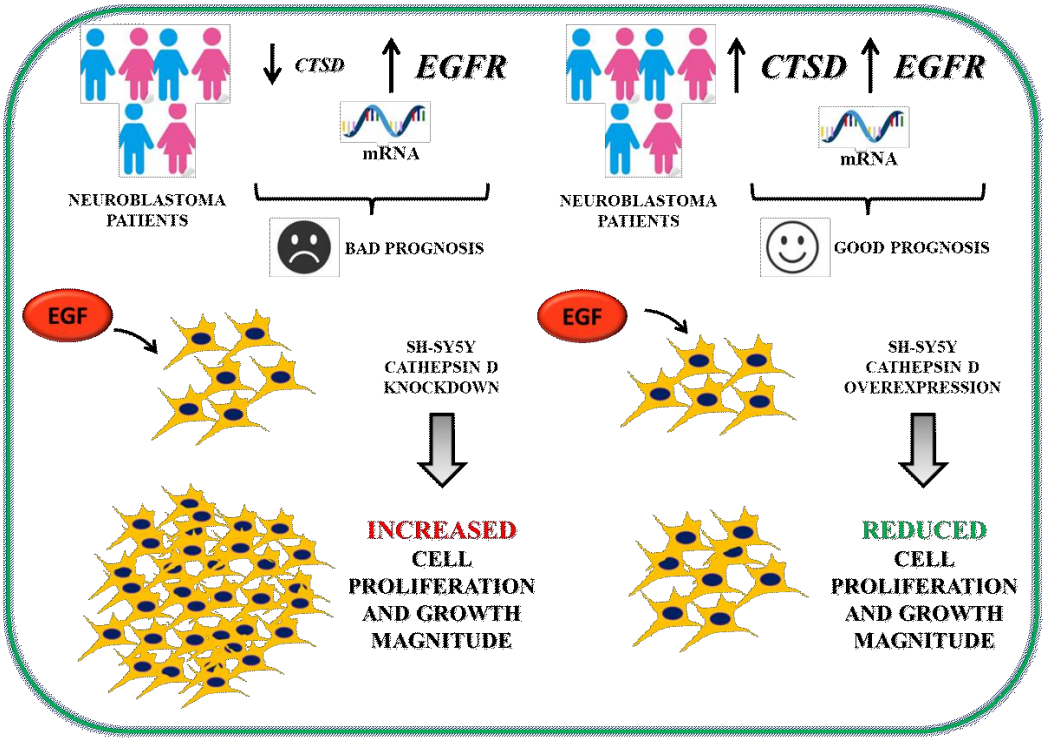

Figure 8. High expression of cathepsin D confers better prognosis in neuroblastoma patients by contrasting EGF-induced neuroblastoma cell growth.

International Journal of
Molecular Sciences

MDPI

Article

High Expression of the Lysosomal Protease Cathepsin D Confers Better Prognosis in Neuroblastoma Patients by Contrasting EGF-Induced Neuroblastoma Cell Growth

Eleonora Secomandi †, Amreen Salwa †, Chiara Vidoni, Alessandra Ferraresi, Carlo Follo and Ciro Isidoro *

Laboratory of Molecular Pathology, Department of Health Sciences, Università del Piemonte Orientale "A. Avogadro", Via Solaroli 17, 28100 Novara, Italy; eleonora.secomandi@uniupo.it (E.S.); salwa.amreen@uniupo.it (A.S.); chiara.vidoni@med.uniupo.it (C.V.); alessandra.ferraresi@med.uniupo.it (A.F.); follocarlo@gmail.com (C.F.)

* Correspondence: ciro.isidoro@med.uniupo.it; Tel.: +39-032-166-0507; Fax: +39-032-162-0421

† These authors contributed equally to this work.

Abstract: Neuroblastoma is a malignant extracranial solid tumor arising from the sympathoadrenal lineage of the neural crest and is often associated with *N-MYC* amplification. Cathepsin D has been associated with chemoresistance in N-MYC-overexpressing neuroblastomas. Increased EGFR expression also has been associated with the aggressive behavior of neuroblastomas. This work aimed to understand the mechanisms linking EGFR stimulation and cathepsin D expression with neuroblastoma progression and prognosis. Gene correlation analysis in pediatric neuroblastoma patients revealed that individuals bearing a high *EGFR* transcript level have a good prognosis only when *CTSD* (the gene coding for the lysosomal protease Cathepsin D, CD) is highly expressed. Low *CTSD* expression was associated with poor clinical outcome. *CTSD* expression was negatively correlated with *CCNB2*, *CCNA2*, *CDK1* and *CDK6* genes involved in cell cycle division. We investigated the biochemical pathways downstream to EGFR stimulation in human SH-SY5Y neuroblastoma cells engineered for overexpressing or silencing of CD expression. Cathepsin D overexpression decreased the proliferative potential of neuroblastoma cells through downregulation of the pro-oncogenic MAPK signaling pathway. EGFR stimulation downregulated cathepsin D expression, thus favoring cell cycle division. Our data suggest that chemotherapeutics that inhibit the EGFR pathway, along with stimulators of cathepsin D synthesis and activity, could benefit neuroblastoma prognosis.

Keywords: cancer; lysosomes; prognosis; cell cycle; EGF; growth factor

Citation: Secomandi, E.; Salwa, A.; Vidoni, C.; Ferraresi, A.; Follo, C.; Isidoro, C. High Expression of the Lysosomal Protease Cathepsin D Confers Better Prognosis in Neuroblastoma Patients by Contrasting EGF-Induced Neuroblastoma Cell Growth. *Int. J. Mol. Sci.* **2022**, *23*, 4782. https://doi.org/10.3390/ijms23094782

Academic Editor: Jacek Z. Kubiak

Received: 5 April 2022
Accepted: 25 April 2022
Published: 26 April 2022

1. Introduction

Neuroblastoma (NB) is the most common extracranial solid tumor of childhood, accounting for 15% of cancer-related deaths in children. NB is an embryonal malignancy arising during fetal or early postnatal life from neural crest-derived sympathetic cells. It is commonly found in the adrenal medulla or along the sympathetic chain [1]. The broad spectrum of clinical manifestations ranges from spontaneous regression, maturation into a benign ganglioneuroma or, in the worst cases, into an aggressive and metastatic disease [2]. Despite recent advances in early diagnosis and multimodal therapeutic approaches, current treatments remain elusive and ineffective for many patients with high-risk disease, with a 5-year survival rate of less than 50% [3]. A frequent genetic aberration, occurring in 25% of all NB cases and predicting poor outcome, is *MYCN* amplification [1]. *MYCN* drives oncogenic pathways, and the inhibition of its transcription results in reduced NB cell growth, even in non-*MYCN*-amplified NB cell lines [4]. Overexpression of N-MYC protein stimulates the extracellular release of procathepsin D (proCD) precursor, leading to doxorubicin resistance and increased cancer cell survival [5]. Cathepsin D is a ubiquitous soluble aspartic endopeptidase found in acidic intracellular compartments [6]. CD

accomplishes bulk protein degradation and mediates the activation of hormones and their precursors as well as the inactivation of mature growth factors through extensive lysosomal degradation [7]. Accordingly, CD-deficient mice and CD-knockdown zebrafish larvae show severe congenital malformations and premature death [8,9]. The defective intracellular sorting and the escape from lysosomal targeting led to aberrant secretion of cathepsin D precursor [10,11], an event associated with increased tumor size, grading and chemoresistance in a variety of malignancies [12,13].

Epidermal growth factor receptor (EGFR) was found to be overexpressed in NB tumor specimens [14], and its signaling was found to be dysregulated in multi-drug resistant NB cell lines [15]. Current knowledge points to the involvement of cathepsin S and B in the attenuation of EGFR signaling and in receptor degradation [16,17]. Whether cathepsin D plays an active role in EGFR-linked growth and progression of neuroblastoma remains to be elucidated. In the present study, we interrogated datasets from the TCGA database to determine the clinical relevance of *CTSD status* in pediatric neuroblastoma patients highly expressing *EGFR*. We found that patients with high *CTSD* and *EGFR* transcript levels showed a better prognosis and longer overall survival than those with high *EGFR* but low *CTSD*. These preliminary data provided the rationale to speculate that cathepsin D could be involved in EGFR regulation of neuroblastoma growth. We tested this hypothesis in engineered neuroblastoma cells in which cathepsin D was overexpressed or knocked down. We found that in the absence of cathepsin D, EGF increased SH-SY5Y cell growth, and conversely, cathepsin D overexpression attenuated EGF-promoted cell proliferation. Notably, EGF-mediated activation of ERK 1/2 was associated with a downregulation of endogenous CD protein level.

The present work demonstrates, for the first time, a novel antiproliferative role of cathepsin D that may be exploited to improve neuroblastoma management and treatment.

2. Results

2.1. High CTSD Expression Correlates with Better Prognosis in Pediatric Neuroblastoma Patients

First, we focused on the prognostic value of *CTSD* in pediatric neuroblastoma patients, and we found that the 75% of patients at INSS Stage 4 showing low *CTSD* expression had the worst prognosis. A smaller cohort of individuals with high *CTSD* expression manifested a better outcome (Figure 1A,B). The median overall survival for patients with high *CTSD* expression was 67 months, while the median survival for patients with low *CTSD* expression was 60 months (p value = 0.1166, not significantly different). At first diagnosis, most patients present with neuroblastoma expressing low *CTSD*, which is associated with metastatic tumors at Stage 4 (Figure 1C).

2.2. High CTSD Expression Increases the Overall Survival of Neuroblastoma Patients Highly Expressing EGFR Transcript

EGFR/HER1, a receptor protein involved in cellular growth and invasiveness, is found frequently overexpressed or aberrantly activated in human neuroblastoma cells, and its inhibition or decreased phosphorylation causes tumor growth suppression and apoptosis in neuroblastomas [14,18–20]. Therefore, we extended our studies of *EGFR* expression to evaluate its relationship with *CTSD*. The mRNA expression of *CTSD* and *EGFR* were positively correlated (Figure 2A). This finding was unexpected and somehow counterintuitive, given the above data showing better a prognosis in patients bearing a neuroblastoma expressing *CTSD*.

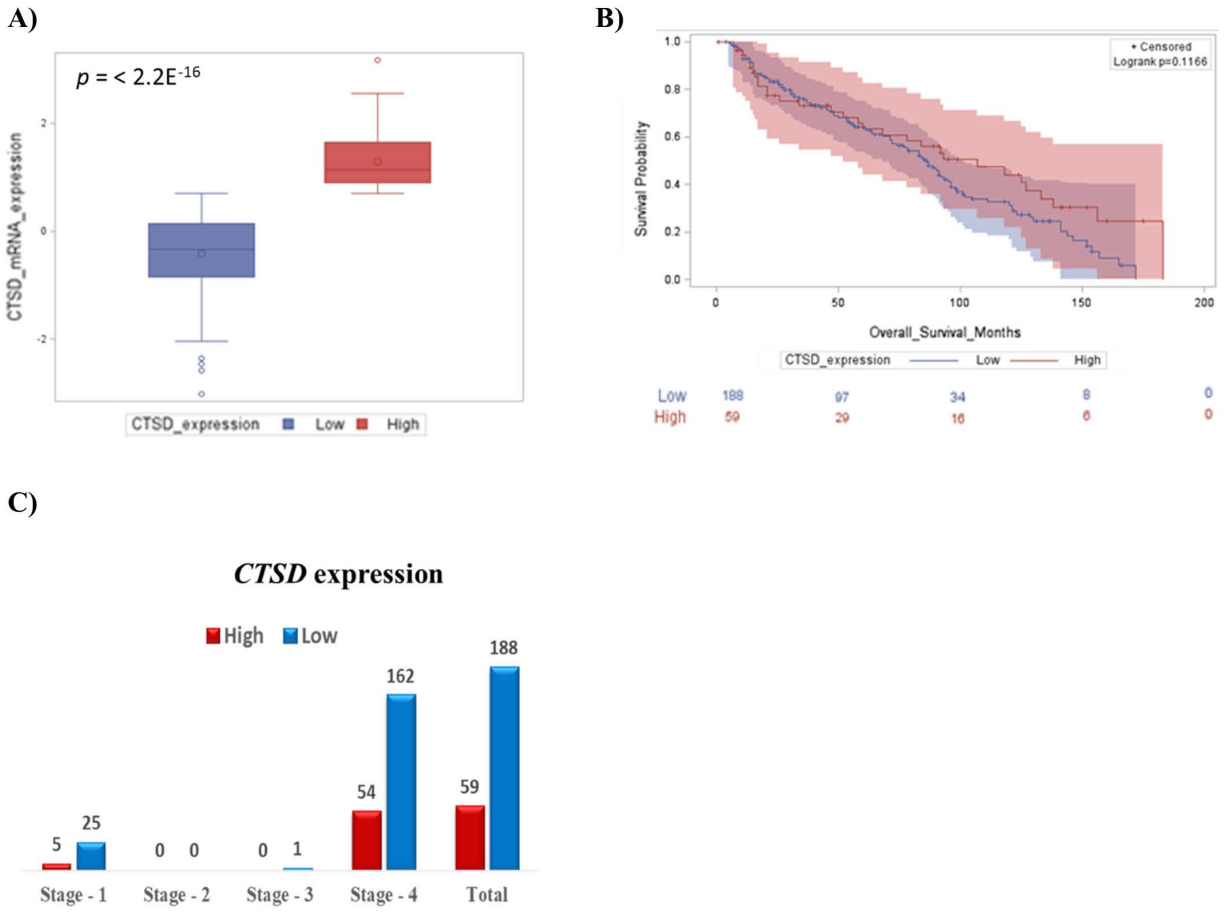

Figure 1. Neuroblastoma patients bearing high *CTSD* transcript level show a better prognosis. (**A**) Box-plot showing the distribution of *CTSD* expression. (**B**) Kaplan–Meier plot representing the overall survival of neuroblastoma patients according to *CTSD* expression levels (high and low). (**C**) Low expression of *CTSD* correlates with INSS Stage 4 in neuroblastoma patients.

We grouped the cases with high and low expression, and we analyzed the prognostic value in combinatorial groups of tumors based on the respective levels of mRNA expression of *CTSD* and *EGFR*, as follows: High/High, High/Low and Low/High (Figure 2B). Kaplan–Meier overall survival curves indicated that patients with high *CTSD* mRNA expression, and with either high or low *EGFR* expression, had the better prognosis, while the group bearing low *CTSD* mRNA expression and high *EGFR* exhibited the worst prognosis (Figure 2C). These data suggest that in patients overexpressing *EGFR*, the different clinical outcome is strictly influenced by *CTSD status*.

2.3. CTSD Gene Expression Negatively Correlates with Genes Involved in Cell Division

To obtain an insight into the functional role of *CTSD* in pediatric neuroblastoma patients, we performed an *in silico* transcriptomic analysis of the genes correlated to it. We retrieved the RNA-seq data (mRNA expression profile) from the TCGA database (TARGET, 2018) and performed a co-expression analysis to identify the most significant differentially expressed genes (DEGs) that were positively (up-regulated genes in red dots) and negatively (down-regulated genes in blue dots) correlated with *CTSD* in patients' samples, as represented in the Volcano plot (Figure 3A). We then focused on the genes inversely correlated with high expression of *CTSD*. Notably, the main biological processes regulated by the genes negatively correlated with *CTSD* included mitosis, cell cycle progression, G1/S and G2/S cell cycle transition, nuclear division and DNA replication (Figure 3B). To substantiate this finding, we determined the correlation between the expression of *CTSD* and the genes involved in cell cycle progression. We found that the mRNA expression of

CTSD was significantly negatively correlated with *CCNB2* (G2/mitotic-specific cyclin-B2), *CCNA2* (cyclin-A2), *CDK1* (cyclin-dependent kinase 1) and *CDK6* (cyclin-dependent kinase 6) (Figure 3C–F).

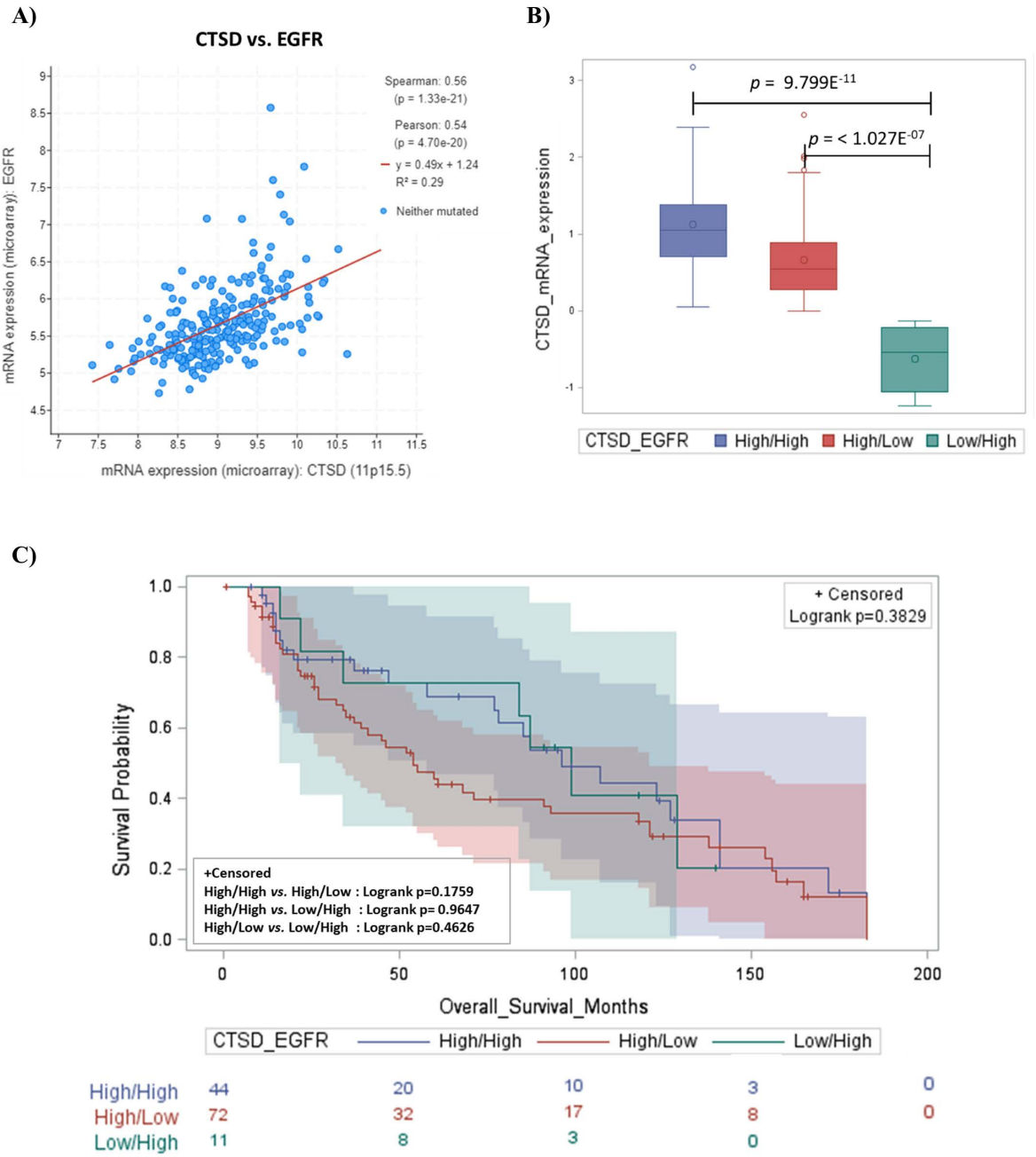

Figure 2. *CTSD* positively correlates with *EGFR* expression and patients exhibit a better prognosis. (**A**) Scatter plot showing the positive correlation between *CTSD* and *EGFR* expression. (**B**) Boxplot representing the distribution of *CTSD* mRNA expression level in different combinations of *CTSD* and *EGFR*—high/high, high/low and low/high groups, respectively. (**C**) Kaplan–Meier plot representing the overall survival of neuroblastoma patients according to combination of *CTSD* and *EGFR*—high/high, high/low, and low/high groups, respectively. Log-rank *p* value for each combination is reported in the box.

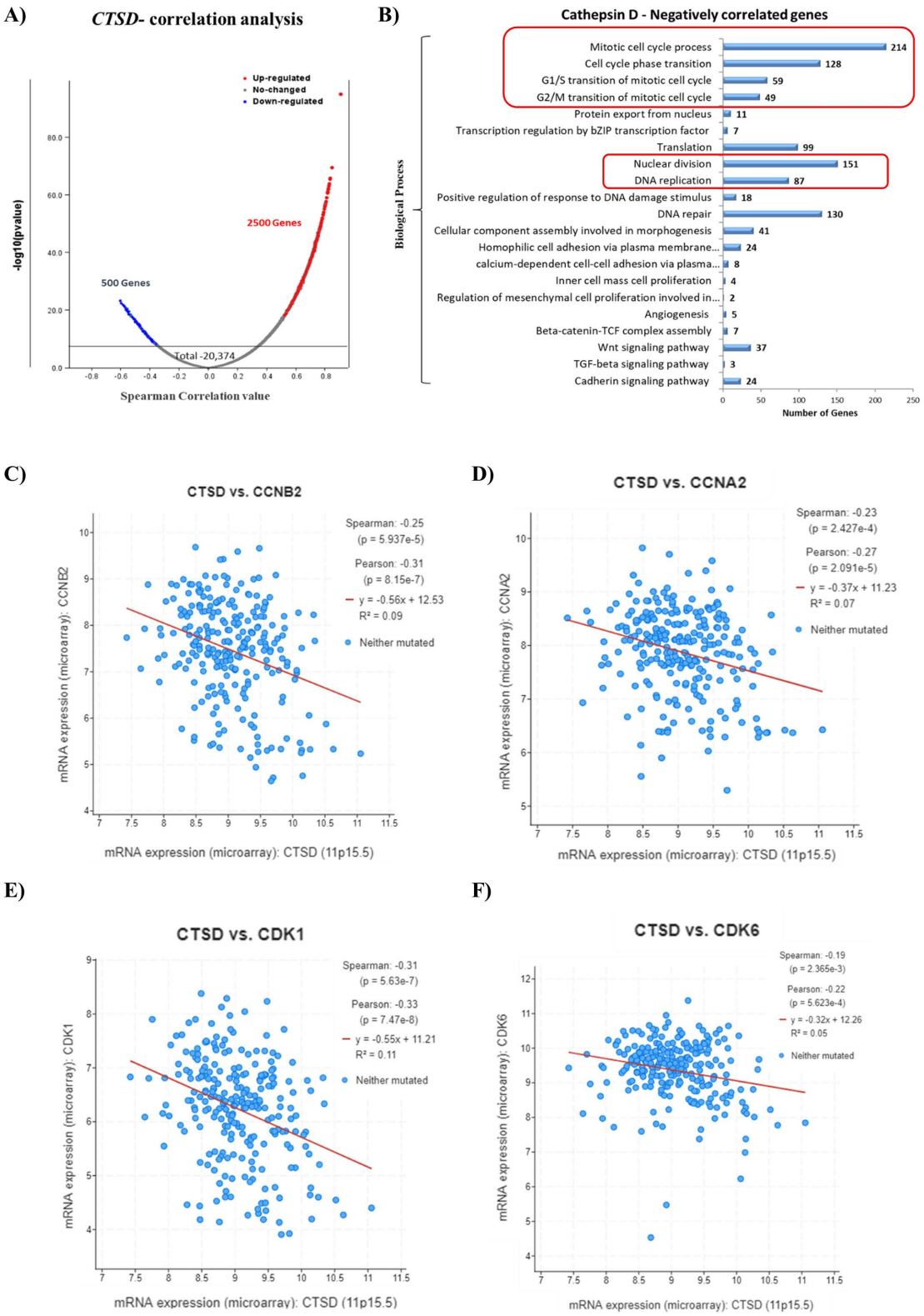

Figure 3. High *CTSD* expression inversely correlates with genes involved in cell cycle progression. (**A**) Volcano plot displaying the differential expressed genes (DEGs). Red dots represent *CTSD*-positively correlated genes, while blue dots represent *CTSD*-negatively correlated genes. (**B**) Graph reporting the negatively correlated biological processes with *CTSD*. (**C**–**F**) Scatter plots showing the negative correlation between *CTSD* and *CCNB2*, *CCNA2*, *CDK1*, *CDK6*, respectively.

2.4. Generation of Transgenic SH-SY5Y Clones Stably Over-Expressing or Silenced for Cathepsin D

To investigate the role of cathepsin D in determining neuroblastoma growth we sought to genetically manipulate its expression. For this, we generated stable transfectants of human neuroblastoma SH-SY5Y cells in which CD was either overexpressed or silenced. We generated several clones and used the ones with the best desired outcome. Sham-transfected cells, which behaved as untransfected cells, served as controls. We employed the Tet-On gene expression system, in which either the overexpression or the knockdown of CD was switched on in the presence of tetracycline. The pcDNA™4/TO or pENTR™/H1/TO vectors were used, in combination with pcDNA6/TR© plasmid, respectively, for generating CD overexpressing- or downregulated- clones. SH-SY5Y were initially transfected with the pcDNA6/TR© vector. Following selection with 0.4 mg/mL blasticidin, cells stably expressing the Tet repressor were used as the host for the pcDNA™4/TO or pENTR™/H1/TO constructs described below. The vectors are shown in Figure 4. As an internal control for endogenous CD level, the Sham clone was produced by transfecting SH-SY5Y cells with the pENTR™/H1/TO empty vector. In double transfected cells, following tetracycline addition to the culture media, the Tet repressor was switched off, and either the overexpression or the knockdown of CD was enabled.

2.4.1. Construction of pENTR™/H1/TO Plasmids for Cathepsin D Knockdown

For CD knockdown, we constructed three pENTR™/H1/TO plasmids carrying three different shRNA specific for human CD. Two double strand oligonucleotides, encoding for two different shRNA for human CD, were designed using the BLOCK-iT RNAi Designer tool (https://rnaidesigner.thermofisher.com/rnaiexpress/ (accessed on 15 January 2018): shRNA486 (complementary to the bp 486–506 of cathepsin D mRNA) and shRNA879 (complementary to the bp 879–899 of cathepsin D mRNA). As a positive control, a double strand oligonucleotide encoding for a previously validated shRNA (complementary to the bp 1163–1182 of cathepsin D mRNA) [21] was also employed in our study. Stable double transfectants clones (clone 5 pENTR/™H1/TO-shRNA486, clone 4 pENTR™/H1/TO-shRNA879 and clone 1 pENTR™/H1/TO-shRNA Ohri) were then selected with 0.8 mg/mL zeocin. Oligonucleotides sequences are shown in Table 1.

Oligonucleotides were cloned into the pENTR™/H1/TO plasmid following the manufacturer's protocol (BLOCK-iT Inducible H1 RNAi Entry vector kit, Invitrogen, Waltham, MA, USA). Briefly, DNA oligonucleotides were annealed to generate double strand oligonucleotides and inserted into the pENTR™/H1/TO vector using T4 DNA ligase. The plasmids obtained were subjected to DNA sequencing to check for correct insertion of the oligonucleotides into the vector (shown in Figure S1). Next, the plasmids were transfected in SH-SY5Y, and the efficiency of hCD downregulation by each shRNA was assessed by CD immunoblotting (Figure 4B). The shRNA 486 was the most efficient shRNA in downregulating the aspartic protease. For this reason, pENTR™/H1/TO 486 was employed for the generation of tetracycline-inducible CD knockdown SH-SY5Y cells.

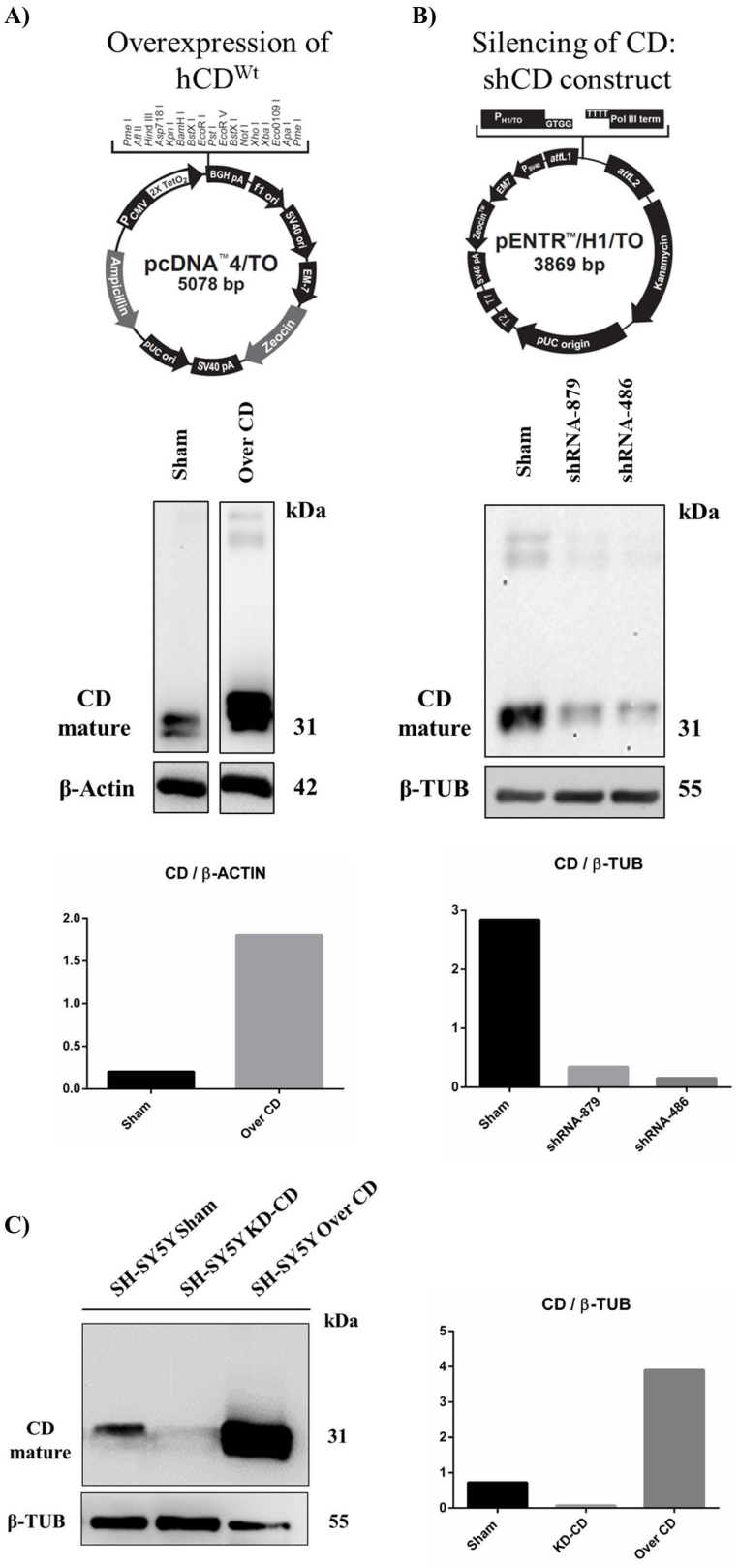

Figure 4. Generation and validation of transgenic SH-SY5Y clones. pcDNA™4/TO (**A**) and pENTR™/H1/TO (**B**) vectors used for cathepsin D overexpression and silencing, respectively. Below, western blot analysis of CD expression is shown. (**C**) Western blot of cathepsin D in SH-SH5Y Sham, 486 (KD-CD) and Over CD clones. Densitometry of the bands is reported in the histogram.

Table 1. Oligonucleotide sequences of both top and bottom strands of shRNA 879, 486 and Ohri are shown. Nucleotides for the directional cloning of the double strand oligonucleotides into the pENTR™/H1/TO vector are shown in italics.

shRNA	Oligo Strand	Sequence
879	Top	5′-*cacc*GCACAGACTCCAAGTATTACACGAATGTAATACTTGGAGTCTGTGC
	Bottom	5′-*aaaa*GCACAGACTCCAAGTATTACATTCGTGTAATACTTGGAGTCTGTGC
486	Top	5′-*cacc*GGATCCACCACAAGTACAACACGAATGTTGTACTTGTGGTGGATCC
	Bottom	5′-*aaaa*GGATCCACCACAAGTACAACATTCGTGTTGTACTTGTGGTGGATCC
Ohri	Top	5′-*cacc*GGCAAAGGCTACAAGCTGTTTCAAGAGAACAGCTTGTAGCCTTTGCC
	Bottom	5′-*aaaa*GGCAAAGGCTACAAGCTGTTCTCTTGAAACAGCTTGTAGCCTTTGCC

2.4.2. Construction of pcDNA™4/TO Plasmid for Cathepsin D Overexpression

Human CD cDNA [11] was subcloned into the pcDNA4™/TO vector. pcDNA 3.1 Zeo (-) carrying wild type cDNA of human CD was digested with EcoRI and the resulting CD cDNA was inserted into pcDNA4™/TO linearized with EcoRI. The plasmid was then transfected in SH-SY5Y and the efficiency of hCD overexpression was determined by CD immunoblotting (Figure 4A).

Finally, the selected clones used for the subsequent studies were assayed for their level of CD expression. As shown in Figure 4C, the KD-CD and Over-CD clones expressed approximately ten times less and ten times more, respectively, the level of mature (enzymatically active) CD than that expressed in the Sham clone. It should be noted that in the SH-SY5Y knockdown clone, CD was barely detectable (Figure 4C).

2.5. Overexpression of Cathepsin D Reduces, While Downregulation of Cathepsin D Enhances, the Proliferative Potential of Transgenic SH-SY5Y Clones

We assessed the proliferative potential of the transfectant clones using a colony-forming assay (as detailed in Materials and Methods section). Cells were seeded at a starting density of 2000 cells/well and allowed to grow for 10 days, with the culture medium renewed every 48 h. Quantification of colony formation (Figure 5A) showed that the clonogenic potential was markedly increased in KD-CD cells (2.3 times higher than Sham and 4.0 times higher than Over CD), and markedly decreased in CD-overexpressing cells (halved compared to Sham). Prompted by this finding, we assayed the cell cycle distribution of the cells in the transfectant clones (Figure 5B). In the KD-CD cell population an increased proportion of cells were found in S phase (7.3%), and even more in G2/M phase (23.58%), compared to that observed in Over CD cell population (where the proportions were 5.48% in S phase and 15.5% in G2/M phase). The latter showed a higher proportion of cells arrested in G0/G1 phase (45.52% versus 36.68% in KD-CD cells and 40.72% in Sham cells). Taken together, these data demonstrate that the level of CD expression impacts on the proliferative ability of neuroblastoma cells, and validate the bioinformatic data showing a strong inverse correlation between the expression of *CTSD* and genes involved in cell cycle progression (Figure 3C–F).

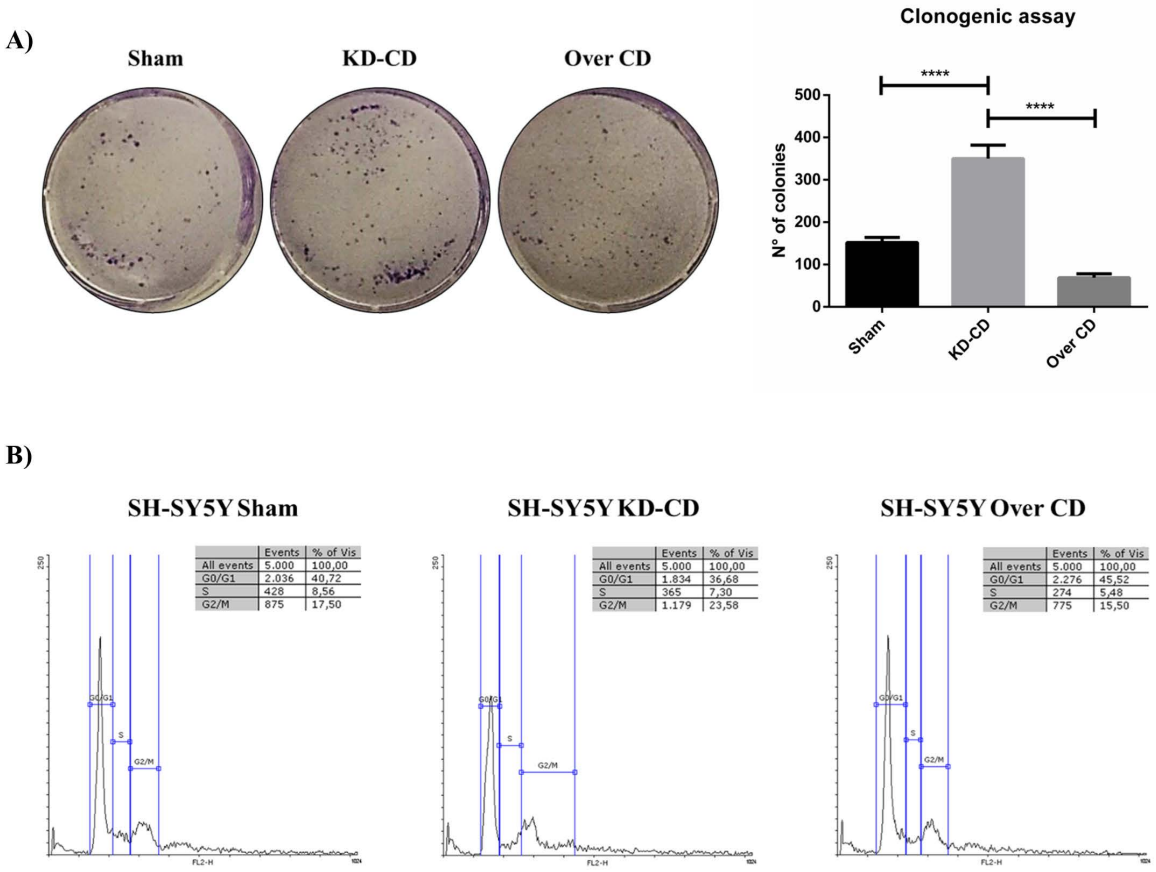

Figure 5. SH-SY5Y Sham, KD-CD and Over CD clones show different growth rates depending on CD expression levels. (**A**) Clonogenic assay and representative graph of the new colonies formed during 10 days of culture. Cells were seeded in 6-well plates and stained with 0.5% crystal violet solution. Images were acquired and colony counting was performed using CellCounter software. Cell growth and number of colonies were estimated through photometric measurements using CellCounter software and are shown in the graph. Data ± S.D. are representative of three independent replicates. Significance was considered as follows: **** $p < 0.0001$. (**B**) Cell cycle analysis performed at 72 h. The percentage of cell populations in different cell cycle phases is reported. Quantification was performed using Flowing software 2.0.

2.6. Epidermal Growth Factor Stimulates the Proliferation of KD-CD SH-SY5Y Transgenic Cells While Overexpression of CD Contrasts Its Activity

Bioinformatic analysis showed that overall survival was far better in neuroblastoma patients bearing a tumor expressing high level of CD, irrespective of the level of *EGFR* expression (Figure 2). At this point, we used our CD transgenic clones to test the hypothesis that CD could dampen the proliferative signal downstream to EGFR.

We analyzed the behavior of SH-SY5Y cells in response to EGF at a concentration of 20 ng/mL, which is in the range of cell growth stimulation with no toxic side effects in neuroblastomas [22].

Cell growth assay demonstrated that EGF stimulated the growth of the Sham cultures, and to a much greater extent, also that of the KD-CD clone, evident from 24 h incubation onward, whereas the Over CD clone was relatively insensitive to EGF stimulation (Figure 6A). These data were corroborated by immunofluorescence staining of Ki-67, a proliferative nuclear marker, and of p21 $^{Waf/Cip1}$, a cyclin-dependent kinase inhibitor that prevents entering the cell cycle (Figure 6B). Consistent with the cell growth data, EGF induced the expression of Ki-67 and decreased the expression of p21. Notably, p21 was basally expressed at a higher level in Over CD cells compared to their Sham and KD-CD counterparts, suggesting an arrest in G1/S transition, and consistent with decreased cell growth.

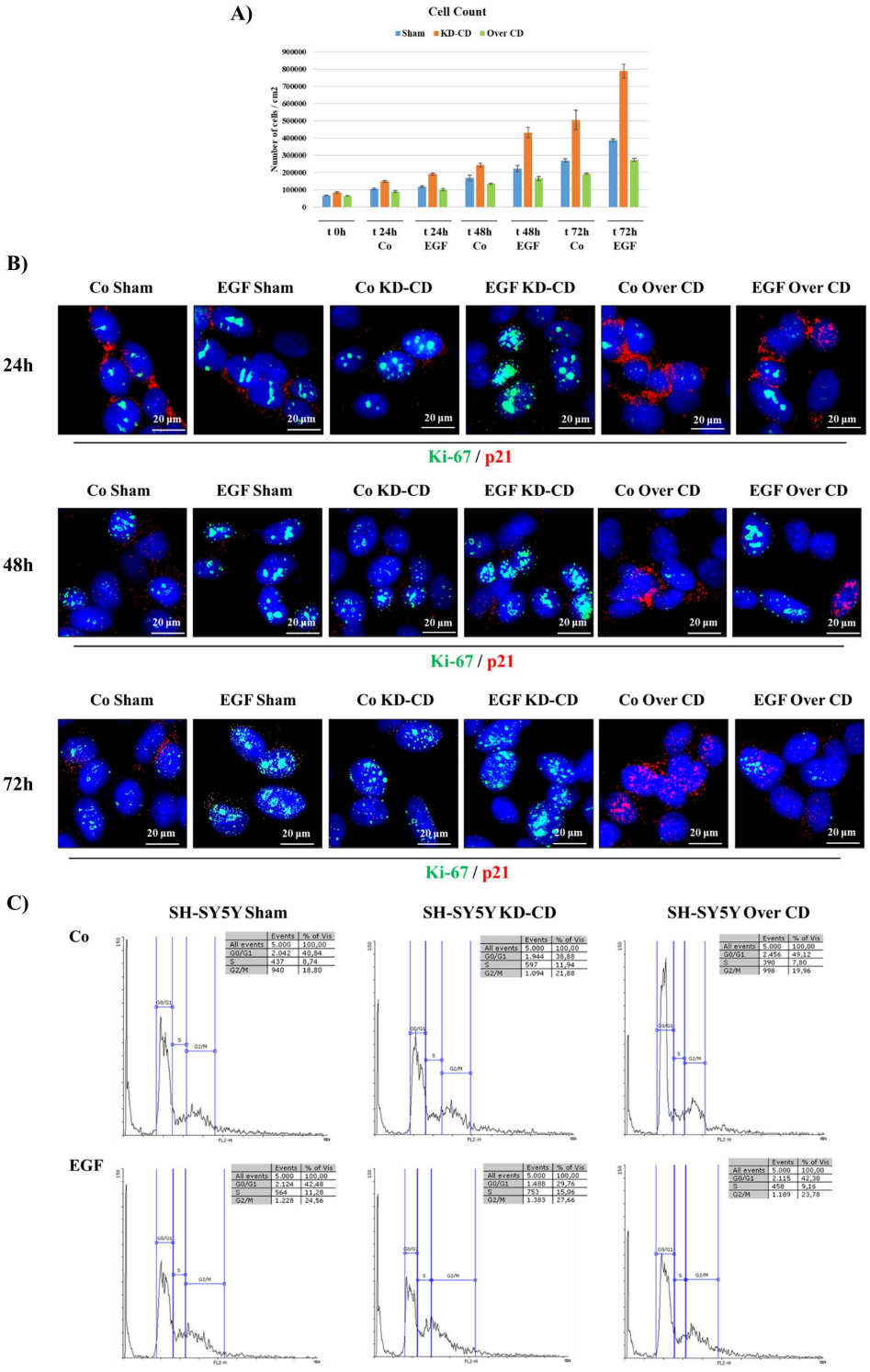

Figure 6. SH-SY5Y KD-CD cells are more sensitive to EGF and show a faster growth compared to CD-overexpressing cells. Assessment of cell proliferation following 20 ng/mL EGF treatment. (**A**) The figure shows a graphical representation of cell count, performed in triplicate for each experimental condition. The treatment was repeated every 24 h, until the end point of 72 h. Time zero is referring to the first day of treatment. (**B**) Immunofluorescence double staining at 24, 48, 72 h. Cells were stained for Ki-67 (green)/p21 (red). Scale bar = 20 µm; magnification = 63X. Representative images of different fields for each experimental condition are shown. (**C**) Cell cycle analysis performed on SH-SY5Y clones after 72 h of EGF. The percentage of cell populations in different cell cycle phases is reported. Quantification was performed by Flowing software 2.0.

The cytofluorimetric analysis of the cell cycle was in accordance with above findings (Figure 6C). EGF stimulation in KD-CD resulted in a substantial decrease in the percentage of cells in the G0/G1 phase (−9%), with a corresponding increase in S (+3%) and G2/M phases (+6%), compared to the control condition. The increment was higher in KD-CD than in the other two clones. The fraction of cells in G2/M phase following treatment with EGF was 24.56% in Sham, 27.66% in KD-CD and 23.78% in Over CD. Interestingly, in the EGF-treated Sham culture, we observed that the fraction of cells in S phase (11.28%) was closer to that of untreated KD-CD (11.94%).

2.7. EGF Reduces Cathepsin D Protein Level and Increases ERK 1/2 Phosphorylation in SH-SY5Y Neuroblastoma Cells

The data above suggested that EGF can modulate cell proliferation in the Sham and KD-CD clones, and to a much lesser extent, in the Over CD clone. We suspected that such a differential effect was related to the ability of EGF to modulate endogenous CD, whose expression was shown to correlate with cell cycle genes. Therefore, we determined the duplication time of the Sham and KD-CD clones with or without EGF stimulation. EGF reduced the doubling time of Sham cells by approximately 23% (from 39 h to 30 h), and of KD-CD cells by approximately 30% (from 27 h to 19 h) (Table 2). Intriguingly, supplementation of EGF to the Sham culture made these cells proliferate, with a doubling time (29.9 ± 1.9 h) close to that of untreated KD-CD cells (26.8 ± 1.2 h). This prompted us to hypothesize that EGFR stimulation could result in CD downregulation. To test this hypothesis, we measured the CD protein content in EGF-treated Sham at different time points. The western blotting data demonstrate that CD was in fact downregulated in neuroblastoma cells challenged with EGF (Figure 7A).

Table 2. Doubling time calculated for SH-SY5Y Sham and KD-CD clones.

Clone	Doubling Time
Co Sham	38.6 ± 4.8
EGF Sham	29.9 ± 1.9
Co KD-CD	26.8 ± 1.25
EGF KD-CD	19.05 ± 1.23

Finally, we assayed the activation of the cell proliferation signaling pathway downstream to EGFR. In particular, we focused on the ERK pathway as this is the main mitogenic signaling triggered by EGF [23]. As confirmation, an increased phosphorylation of ERK 1/2 was observed in cells exposed to EGF (Figure 7B).

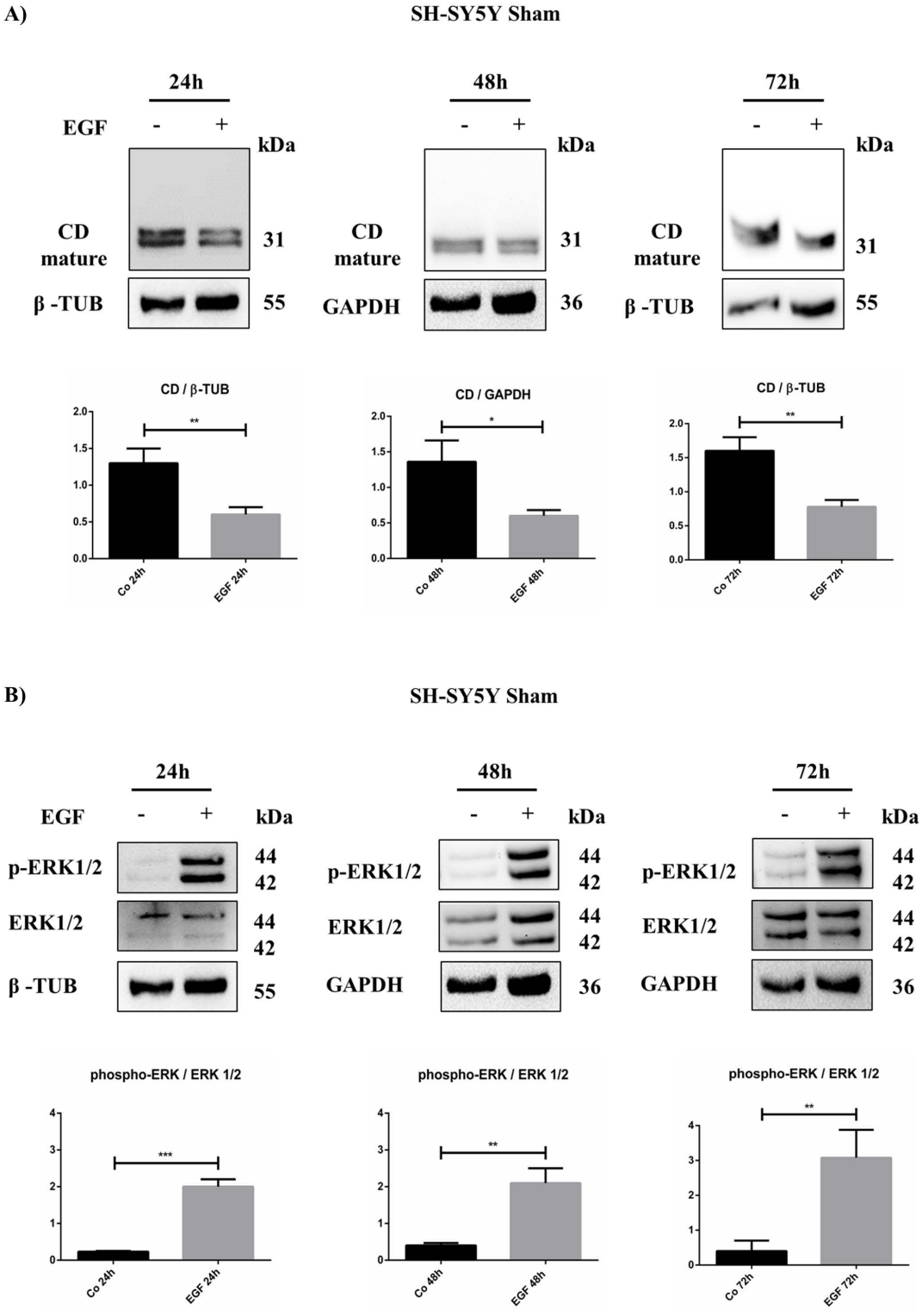

Figure 7. EGF downregulates intracellular cathepsin D in SH-SY5Y Sham. SH-SY5Y cells were treated for 24, 48, and 72 h. (**A**) Time course of cathepsin D expression analyzed through western blotting. (**B**) Western blot of phospho-ERK 1/2 and total protein in Sham cell homogenates at different time points (24, 48, and 72 h) in the presence/absence of EGF. The filters were probed with β-tubulin and GAPDH as loading control. Significance was considered as follows: *** $p < 0.001$; ** $p < 0.01$; * $p < 0.05$.

3. Discussion

CD is an aspartic protease resident in acidic compartments, where it accomplishes the degradation of extracellular proteins internalized by endocytosis or phagocytosis, as well as that of intracellular proteins delivered to lysosomes by autophagy [24]. This function is associated with protein homeostasis and, consequently, cell growth control [10,25]. Under cytotoxic and stressful conditions, cytoplasmic relocation of mature CD from the lysosomes can drive apoptosis [26–32]. On the other hand, overexpression of the *CTSD* gene, along with defective segregation in the acidic compartments, leads to abnormal secretion of the precursor proCD, which can be found in the culture media and body fluid of tumor bearers [13,33–36]. In contrast, hypersecretion of proCD elicits oncogenic activities. Extracellular proCD acts as an autocrine and paracrine growth factor for an unknown receptor, triggering RAS/MAPK and PI3K/AKT pathway activation in fibroblasts and human endothelial cells [37,38]. A well-organized vascular network supports tumor growth and favor metastasis. proCD may undergo autoactivation in the acidic tumor microenvironment, thus favoring cancer cell invasion and neo-angiogenesis through the degradation of the extracellular matrix (ECM), liberating growth factors [13,39]. In this context, secreted CD exerts a pro-angiogenic activity by processing the precursors of VEGF-C and VEGF-D, releasing active growth factors [40]. Therefore, it is fundamental that CD is correctly segregated to perform its function in the endosomal–lysosomal compartments, to avoid its aberrant secretion. In neuroblastoma cells, secreted proCD exerted an anti-apoptotic activity, promoted cell survival and contributed to doxorubicin resistance [5]. Here, we report that patients bearing a neuroblastoma that expresses a high level of the lysosomal protease CD benefit from a better prognosis. Further, *in silico* transcriptome analysis revealed that neuroblastoma patients with high *EGFR* and high *CTSD* levels had a better prognosis compared to patients bearing high *EGFR* and low *CTSD*. Accordingly, two-thirds of patients at INSS Stage 4 present with a low level of *CTSD* expression, indicating that neuroblastomas with CD deficiency grow and progress faster than neuroblastomas that express a high level of CD. Therefore, we argued that in neuroblastomas highly expressing CD, the protease is retained intracellularly and can control protein homeostasis and, consequently, the cell cycle. Consistent with this interpretation, overexpression of the *CTSD* gene negatively correlated with a subset of genes associated with cell cycle and proliferation, including *CCNB2*, *CCNA2*, *CDK1*, and *CDK6*.

We validated our hypothesis using transgenic human SH-SY5Y neuroblastoma cells in which CD was either stably overexpressed (under the CMV promoter) or knocked down (by specific short-hairpin RNA). The addition of exogenous EGF leads to receptor activation and enhances NB cell proliferation [20]. SH-SY5Y overexpressing CD showed a higher expression of p21 and were less responsive to EGF stimulation, whereas SH-SY5Y knocked down for CD were basally more proliferative and more responsive to EGF stimulation. Notably, Sham-transfected SH-SY5Y cells, which retain the ability to modify protein level, responded to EGF challenge by increasing cell proliferation, along with downregulating the level of endogenous CD. To our knowledge this is the first report showing such an effect of EGF on CD expression in cancer cells.

The EGF family of growth factors are potent inducers of angiogenesis in vitro and in vivo, and EGFR ligands are frequently released in the tumor microenvironment from cancer and non-cancer cells [41]. The existing crosstalk between these cells is crucial for sustaining tumor growth and for promoting angiogenesis. In fact, the heparin-binding EGF-like growth factor (HB-EGF), when released in the tumor microenvironment, induces endothelial cell proliferation in solid cancers and in multiple myeloma [42–44]. The pharmacological inhibition of HB-EGF-EGFR signaling with erlotinib results in anti-angiogenic effects, inhibits cancer cell growth both in vitro and in vivo, and prevents multiple myeloma progression [44].

The inhibition of growth factor receptors is an attractive approach for treating cancers. However, while the HER1-specific tyrosine kinase inhibitor ZD1839 (Iressa, gefitinib) markedly reduces receptor activation and PI3K/AKT signaling, it is not effective on MAPK

in neuroblastoma [20]. In addition, alterations of EGFR itself (polymorphisms, variants), overexpression of HER family ligands, and lncRNAs are associated with monoclonal antibody resistance and tumor relapse [45–48]. Developing insight into the molecular mechanisms of downstream growth factor receptors may help the identification of novel key targets and the development of effective therapeutics.

In this context, it is of relevance that ERK 1/2 activation by EGFR was reduced in the neuroblastoma cells overexpressing CD. Thus, our data may have translational application for the personalization of therapy for neuroblastomas in patients stratified for the expression of *N-MYC*, *EGFR* and *CTSD*. These patients could in fact benefit from a therapy combining an inhibitor of the EGFR signal with a drug inducing the expression and/or stimulating the activity of CD, such as, for instance, the nutraceutical resveratrol [29]. Worthy of note, the latter modulates autophagy [49], interrupts the metabolic crosstalk between cancer and stromal cells [50,51], and suppresses neo-angiogenesis [52,53]. Notably, the anticancer effectiveness of RV, with no toxic side effects, has been reported in several ongoing clinical trials (recorded on clinicaltrial.gov, accessed on 21 April 2022) [54].

Our findings encourage in vitro testing of the effects of resveratrol as adjuvant therapy for neuroblastomas low-expressing cathepsin D and not responding to the EGFR inhibitor gefitinib [55].

4. Materials and Methods

4.1. Cell Culture and Treatment

Human neuroblastoma SH-SY5Y cells were obtained from the American Type Culture Collection (cod. CRL-2266, ATCC, Rockville, MD, USA). SH-SY5Y cells were maintained under standard conditions (37 °C, 95 *v*/*v*% air: 5 *v*/*v*% CO_2) in 50% Minimum Essential Medium (MEM, cod. M2279, Sigma-Aldrich Corp., St. Louis, MO, USA) and 50% Ham's F12 Nutrient Mixture (HAM, cod. N4888, Sigma-Aldrich Corp.), containing 10% heat-inactivated Fetal Bovine Serum (FBS, cod. ECS0180L; Euroclone S.p.A., Milan, Italy), supplemented with 1% Glutamine (cod. G7513, Sigma-Aldrich Corp.) and 1% *w/v* of Penicillin/Streptomycin (cod. P0781, Sigma-Aldrich Corp.). Cultured cells were treated, where specifically indicated, with 20 ng/mL Epidermal Growth Factor (EGF, cod. E5036; Sigma-Aldrich Corp.) dissolved in 10 mM acetic acid. SH-SY5Y stable transfectant clones (Sham, knockdown CD (KD-CD) and Over CD), representing different CD protein levels, were engineered in our laboratory. Plasmids and reagents employed for clone generation were purchased from Invitrogen, Waltham, MA, USA.

4.2. Cell Counting, Doubling Time and Cell Cycle Analysis

Cells were plated into 12-well plates (50,000 cells/cm^2), allowed to adhere for 24 h, and then treated with 20 ng/mL EGF where appropriately indicated. At each time point, cells were trypsinized, collected, and then the cell suspensions were diluted 1:1 with Trypan Blue solution for counting. Time zero refers to the start of treatment, 24 h after plating. Medium was refreshed every day. Cell counting was performed in triplicate for each experimental condition. Doubling time (Dt) was calculated using the free software Doubling Time Online Calculator (http://www.doubling-time.com/compute.php (accessed on 15 July 2021). Cells were fixed in 70% ice-cold ethanol and stored at −20 °C till the start of cytofluorometric analysis. Cells were incubated with RNAse for 30 min at 37 °C, and the DNA was subsequently stained with propidium iodide (PI, 50 µg/mL; cod. P4170, Sigma Aldrich). The stained cells were then analyzed by using a FacScan flow cytometer (FACSCalibur, Becton, Dickinson, Eysins, Switzerland). For each sample, a fraction of 5000 events was assessed. Cytofluorimetric data were elaborated through Flowing software (v2.5.1).

4.3. Clonogenic Assay

For clonogenic assay, cells were seeded into 6-well (MW6) plates at a density of 2000 cells/well, and treated with 20 ng/mL EGF. The cells were cultivated for 10 days to

allow colony formation [56]. At the end of the experiment, the medium was removed, cells were washed with 1X PBS, and then fixed with methanol for 20 min at room temperature. Next, another wash with 1X PBS was performed, and subsequently colonies were stained with 0.5% crystal violet solution for 30 min. Finally, MW6 plates were washed with distilled water (until the background became clear) and dried at room temperature. Each well was photographed, and the number of colonies formed was estimated by photometric measurements and CellCounter software (v0.2.1.).

4.4. Antibodies

The following primary antibodies were employed for western blotting: mouse anti-β-tubulin (1:1000, cod. T5201; Sigma-Aldrich Corp.), mouse anti-β-actin (1:2000, cod. A5441; Sigma-Aldrich Corp.), rabbit anti-GAPDH (1:1000, cod. G9545; Sigma-Aldrich Corp.), mouse anti-cathepsin D (1:100, cod. IM03; Calbiochem, St. Louis, MO, USA), rabbit anti phospho-ERK 1/2 (Thr202/Tyr204, Thr185/Tyr187) (1:500, cod. 05-797R; Millipore, Burlington, MA, USA) and mouse anti-ERK1/2 (1:500, cod. 05-1152; Millipore). Secondary antibodies employed for immunoblotting were purchased as follows: Horse Radish Peroxidase-conjugated goat anti-mouse IgG (1:10,000, cod. 170–6516; Bio-Rad, Hercules, CA, USA) and Horse Radish Peroxidase-conjugated goat anti-rabbit IgG (1: 10,000, cod. 170–6515: Bio-Rad, Hercules, CA, USA). The following primary antibodies were employed for immunofluorescence: mouse anti-p21 (1:100, cod. sc-817; Santa Cruz Biotechnology, Dallas, TX, USA) and rabbit anti-Ki-67 (1:100, cod. HPA001164; Sigma-Aldrich). Secondary antibodies used for immunofluorescence were purchased as follows: goat-Anti Rabbit IgG Alexa FluorTM Plus 488 (1:1000, cod. A32731; Invitrogen) and Goat-Anti Mouse IgG Alexa FluorTM Plus 555 (1:1000, cod. A32727; Invitrogen).

4.5. Western Blotting

SH-SY5Y Sham, KD-CD and Over CD clones were plated at a density of 50,000 cells/cm^2 on sterile P35 Petri dishes and allowed to adhere. Cells were harvested in RIPA Buffer (0.5% Deoxycholate, 1% NP-40, 0.1% Sodium Dodecyl Sulfate in PBS solution) supplemented with protease inhibitor cocktail and phosphatase inhibitors (0.5 M sodium fluoride NaF and 0.2 M sodium orthovanadate Na_3VO_4), and homogenized using an ultrasonic cell disruptor XL (Misonix, Farmingdale, NY, USA). All reagents were supplied by Sigma-Aldrich Corp. Protein content concentration was determined using a Bradford assay and samples were denatured with 5X Leammli sample buffer at 95 °C for 10 min. Equal amounts of protein (30 μg of total cell homogenates) were separated by SDS-PAGE and transferred onto a PVDF membrane (cod.162-0177; BioRad, Hercules, CA, USA). Filters were blocked with 5% non-fat dry milk (cod. sc-2325; Santa Cruz Biotechnology) solution containing 0.2% Tween-20 for 1 h at room temperature (RT). Subsequently, membranes were incubated with specific primary antibodies overnight at 4 °C, followed by incubation with secondary HRP-conjugated antibodies (goat anti-mouse (cod. 170-6516) and goat anti-rabbit (cod. 170-6515)) for 1 h at room temperature. The bands were detected using Enhanced Chemiluminescence reagents (ECL, cod. NEL105001EA; Perkin Elmer, Waltham, MA, USA) and developed with a ChemiDoc XRS instrument (BioRad, Hercules, CA, USA). Intensity of the bands was estimated by densitometry using Quantity One Software (BioRad, Hercules, CA, USA).

4.6. Immunofluorescence

SH-SY5Y cell clones were seeded onto sterile coverslips at a density of 40,000 cells/cm^2, and allowed to adhere and grow before treatment. At the end of the experiment, the coverslips were fixed in ice-cold methanol, permeabilized with 0.2% Triton-PBS, and then re-fixed with methanol. After washing with 1X PBS, coverslips were incubated overnight at 4 °C with specific primary antibodies dissolved in 0.1% Triton PBS + 10% FBS. The following day, the coverslips were washed three times with 0.1% Triton-PBS and incubated for 1 h at room temperature with Goat-Anti Rabbit IgG Alexa FluorTM Plus 488 or Goat-Anti Mouse IgG Alexa FluorTM Plus 555 secondary antibodies, as appropriate. Nuclei were stained with

the UV fluorescent dye DAPI (4′,6-diamidino-2-phenylindole). Secondary antibodies and DAPI were dissolved in 0.1% Triton-PBS + 10% FBS. Thereafter, coverslips were mounted onto glasses using SlowFade antifade reagent (cod. S36936; Life Technologies, Paisley, UK) and data acquired by fluorescence microscopy (Leica DMI6000, Leica Microsystems, Wetzlar, Germany). For each experimental condition, different microscopic fields were randomly selected.

4.7. Bioinformatic Analysis

Kaplan–Meier curves, correlation studies and biological processes were obtained by extracting clinical data from the TCGA database (www.portal.gdc.cancer.gov/, last accessed on 13 December 2021). RNA-seq and corresponding clinical data (including overall survival *status*, INSS stage and mRNA expression of 20,040 group of genes) of pediatric neuroblastoma patients (TARGET 2018, comprising 248 patients after filtering out datasets with insufficient survival information) were downloaded from the cBioportal.org [57]. Patients were grouped based on the level of mRNA expression; low versus high groups were defined relative to the median expression level of the overall patient cohort. The correlation between the mRNA expression of the relevant biomarker *CTSD*, and the INSS Stage is represented in histograms. Pearson's and Spearman's correlation analyses were performed to identify the genes correlated with *CTSD*.

TBtools (https://github.com/CJ-Chen/TBtools/ (accessed on 4 December 2021)) was used to identify differentially expressed genes (DEGs) in correlation with *CTSD*, represented as a Volcano plot. To identify the DEGs, the cut-off criteria were set based on Spearman's correlation values (i.e., correlation coefficient value greater than +0.45 (positively correlated) or lower than −0.45 (negatively correlated) and p-value < 0.0001 (−log10 (p-value) threshold was fixed above 5.0)).

DAVID bioinformatics functional annotation tool (https://david.ncifcrf.gov/summary.jsp (accessed on 20 December 2021) was used to analyze Gene Ontology (GO) biological processes and Kyoto Encyclopedia of Genes and Genomes (KEGG) pathways were obtained with the help of negatively-differentially expressed genes. Data are presented in bar graphs displaying the number of transcripts belonging to negatively associated biological processes.

Scatter plots were employed to represent the correlation between the expression of relevant biomarkers in the patient cohort. Pearson's correlation analyses were performed to identify the correlation between *CTSD* and *CCNB2*, *CCNA2*, *CDK1* and *CDK6* genes. Regression was estimated by calculating Pearson's correlation coefficients (r) and the relative p-values.

CTSD and *EGFR* were grouped based on the level of mRNA expression in the neuroblastoma patients. The correlation of *CTSD* and *EGFR* was determined after sub-classification of mRNA expression based on the level of Z-score values, as high (all positive z-score values) and low (all negative z-score values), respectively. Low versus high mRNA expression was defined relative to the median expression level of all patients in the form of a box plot, and used to investigate the relationship between dichotomized *CTSD* and *EGFR* expression. To reduce potential bias from dichotomization, the mRNA expression of *CTSD* and *EGFR* were compared using a t-test (Welch Two Sample t-test) by R. All cut-off values were set before the analysis, and all the tests were two-tailed.

All statistical analyses were performed using R (3.6.1 version, The R Foundation for Statistical Computing, Vienna, Austria) and SAS software (9.4. version, SAS Institute Inc., Cary, NC, USA). The log-rank test was used to determine statistical significance. p-value ≤ 0.05 was considered to be significant. Survival analysis was performed using SAS for the following: *CTSD* expression and mRNA expression level-based groups of *CTSD* and *EGFR*. Survival curves of these two groups were estimated using Kaplan–Meier plots and compared using the Cox regression model, assuming an ordered trend for the three groups as described previously. The log-rank test was used to determine the statistical significance. p-value < 0.05 was considered significant.

4.8. Statistical Analysis

Statistical analysis was performed with GraphPad Prism 6.0 software (San Diego, CA, USA). Bonferroni's multiple comparison test after one-way ANOVA analysis (unpaired, two-tailed) was employed. Significance was considered as follows: **** $p < 0.0001$; *** $p < 0.001$; ** $p < 0.01$; * $p < 0.05$. Data are reported as average ± S.D. Unpaired *t*-test analysis was also employed.

Supplementary Materials: The following supporting information can be downloaded at: https://www.mdpi.com/article/10.3390/ijms23094782/s1.

Author Contributions: Conceptualization, E.S. and C.I.; software, A.S.; investigation, E.S., C.V., A.F. and C.F.; data curation, A.S.; writing—original draft preparation, E.S. and A.S.; writing—review and editing, C.I.; visualization, E.S, C.V. and A.F.; supervision, C.I. All authors have read and agreed to the published version of the manuscript.

Funding: This research received no external funding.

Institutional Review Board Statement: Not applicable.

Informed Consent Statement: Not applicable.

Data Availability Statement: Not applicable.

Acknowledgments: ES and AS are recipients of a PhD fellowship granted by the Italian Ministry of Education, University and Research (MIUR, Rome, Italy). The fluorescence microscope was donated by Comoli, Ferrari & SpA (Novara, Italy). Thanks to Associazione per la Ricerca Medica Ippocrate-Rhazi (ARM-IR, Novara, Italy) for the support.

Conflicts of Interest: The authors declare no conflict of interest.

References

1. Davidoff, A.M. Neonatal Neuroblastoma. *Clin. Perinatol.* **2021**, *48*, 101–115. [CrossRef] [PubMed]
2. Monclair, T.; Brodeur, G.M.; Ambros, P.F.; Brisse, H.J.; Cecchetto, G.; Holmes, K.; Kaneko, M.; London, W.B.; Matthay, K.K.; Nuchtern, J.G.; et al. The international neuroblastoma risk group (INRG) staging system: An INRG task force report. *J. Clin. Oncol.* **2009**, *27*, 298–303. [CrossRef] [PubMed]
3. Siegel, R.L.; Miller, K.D.; Fuchs, H.E.; Jemal, A. Cancer Statistics, 2021. *CA Cancer J. Clin.* **2021**, *71*, 7–33. [CrossRef] [PubMed]
4. Kling, M.J.; Griggs, C.N.; McIntyre, E.M.; Alexander, G.; Ray, S.; Challagundla, K.B.; Joshi, S.S.; Coulter, D.W.; Chaturvedi, N.K. Synergistic efficacy of inhibiting MYCN and mTOR signaling against neuroblastoma. *BMC Cancer* **2021**, *21*, 1–13. [CrossRef]
5. Sagulenko, V.; Muth, D.; Sagulenko, E.; Paffhausen, T.; Schwab, M.; Westermann, F. Cathepsin D protects human neuroblastoma cells from doxorubicin-induced cell death. *Carcinogenesis* **2008**, *29*, 1869–1877. [CrossRef]
6. Barrett, A.J. Cathepsin D: The Lysosomal Aspartic Proteinase. In *Ciba Foundation Symposium-Aetiology of Diabetes Mellitus and Its Complications (Colloquia on Endocrinology)*; Excerpta Medica: New York, NY, USA, 2008; Volume 15, pp. 37–50. [CrossRef]
7. Berg, T.; Gjøen, T.; Bakke, O. Physiological functions of endosomal proteolysis. *Biochem. J.* **1995**, *307*, 313–326. [CrossRef]
8. Saftig, P.; Hetman, M.; Schmahl, W.; Weber, K.; Heine, L.; Mossmann, H.; Köster, A.; Hess, B.; Evers, M.; Von Figura, K. Mice deficient for the lysosomal proteinase cathepsin D exhibit progressive atrophy of the intestinal mucosa and profound destruction of lymphoid cells. *EMBO J.* **1995**, *14*, 3599–3608. [CrossRef]
9. Follo, C.; Ozzano, M.; Mugoni, V.; Castino, R.; Santoro, M.; Isidoro, C. Knock-Down of Cathepsin D Affects the Retinal Pigment Epithelium, Impairs Swim-Bladder Ontogenesis and Causes Premature Death in Zebrafish. *PLoS ONE* **2011**, *6*, e21908. [CrossRef]
10. Isidoro, C.; Demoz, M.; De Stefanis, D.; Baccino, F.M.; Bonelli, G. Synthesis, maturation and extracellular release of procathepsin D as influenced by cell proliferation or transformation. *Int. J. Cancer* **1995**, *63*, 866–871. [CrossRef]
11. Isidoro, C.; Grässel, S.; Baccino, F.M.; Hasilik, A. Determination of the Phosphorylation, Uncovering of Mannose 6-Phosphate Groups and Targeting of Lysosomal Enzymes. *Clin. Chem. Lab. Med. (CCLM)* **1991**, *29*, 165–171. [CrossRef]
12. Cunat, S.; Hoffmann, P.; Pujol, P. Estrogens and epithelial ovarian cancer. *Gynecol. Oncol.* **2004**, *94*, 25–32. [CrossRef]
13. Nicotra, G.; Castino, R.; Follo, C.; Peracchio, C.; Valente, G.; Isidoro, C. The dilemma: Does tissue expression of cathepsin D reflect tumor malignancy? The question: Does the assay truly mirror cathepsin D mis-function in the tumor? *Cancer Biomarkers* **2010**, *7*, 47–64. [CrossRef]
14. Tamura, S.; Hosoi, H.; Kuwahara, Y.; Kikuchi, K.; Otabe, O.; Izumi, M.; Tsuchiya, K.; Iehara, T.; Gotoh, T.; Sugimoto, T. Induction of apoptosis by an inhibitor of EGFR in neuroblastoma cells. *Biochem. Biophys. Res. Commun.* **2007**, *358*, 226–232. [CrossRef]
15. Meyers, M.B.; Shen, W.P.V.; Spengler, B.A.; Ciccarone, V.; O'Brien, J.P.; Donner, D.B.; Furth, M.E.; Biedler, J.L. Increased epidermal growth factor receptor in multidrug-resistant human neuroblastoma cells. *J. Cell. Biochem.* **1988**, *38*, 87–97. [CrossRef]

16. Huang, C.-C.; Lee, C.-C.; Lin, H.-H.; Chang, J.-Y. Cathepsin S attenuates endosomal EGFR signalling: A mechanical rationale for the combination of cathepsin S and EGFR tyrosine kinase inhibitors. *Sci. Rep.* **2016**, *6*, 29256. [CrossRef]
17. Authier, F.; Métioui, M.; Bell, A.W.; Mort, J.S. Negative Regulation of Epidermal Growth Factor Signaling by Selective Proteolytic Mechanisms in the Endosome Mediated by Cathepsin B. *J. Biol. Chem.* **1999**, *274*, 33723–33731. [CrossRef]
18. Zheng, C.; Shen, R.; Li, K.; Zheng, N.; Zong, Y.; Ye, D.; Wang, Q.; Wang, Z.; Chen, L.; Ma, Y. Epidermal growth factor receptor is overexpressed in neuroblastoma tissues and cells. *Acta Biochim. Et Biophys. Sin.* **2016**, *48*, 762–767. [CrossRef]
19. Hatziagapiou, K.; Braoudaki, M.; Karpusas, M.; Tzortzatou-Stathopoulou, F. Evaluation of antitumor activity of gefitinib in pediatric glioblastoma and neuroblastoma cells. *Clin. Lab.* **2011**, *57*, 22029196.
20. Ho, R.; Minturn, J.E.; Hishiki, T.; Zhao, H.; Wang, Q.; Cnaan, A.; Maris, J.; Evans, A.E.; Brodeur, G.M. Proliferation of Human Neuroblastomas Mediated by the Epidermal Growth Factor Receptor. *Cancer Res.* **2005**, *65*, 9868–9875. [CrossRef]
21. Ohri, S.S.; Vashishta, A.; Proctor, M.; Fusek, M.; Vetvicka, V. Depletion of procathepsin D gene expression by RNA interference – A potential therapeutic target for breast cancer. *Cancer Biol. Ther.* **2007**, *6*, 1081–1087. [CrossRef]
22. Chiu, B.; Mirkin, B.; Madonna, M.B. Mitogenic and Apoptotic Actions of Epidermal Growth Factor on Neuroblastoma Cells Are Concentration-Dependent. *J. Surg. Res.* **2006**, *135*, 209–212. [CrossRef]
23. Carraway, K.L.; Carraway, C.A.C. Signaling, mitogenesis and the cytoskeleton: Where the action is. *BioEssays* **1995**, *17*, 171–175. [CrossRef] [PubMed]
24. Castino, R.; Démoz, M.; Isidoro, C. Destination 'Lysosome': A target organelle for tumour cell killing? *J. Mol. Recognit.* **2003**, *16*, 337–348. [CrossRef] [PubMed]
25. Lockwood, T.D.; Shier, W.T. Regulation of acid proteases during growth, quiescence and starvation in normal and transformed cells. *Nature* **1977**, *267*, 252–254. [CrossRef] [PubMed]
26. Emert-Sedlak, L.; Shangary, S.; Rabinovitz, A.; Miranda, M.B.; Delach, S.M.; Johnson, D.E. Involvement of cathepsin D in chemotherapy-induced cytochrome *c* release, caspase activation, and cell death. *Mol. Cancer Ther.* **2005**, *4*, 733–742. [CrossRef] [PubMed]
27. Castino, R.; Peracchio, C.; Salini, A.; Nicotra, G.; Trincheri, N.F.; Démoz, M.; Valente, G.; Isidoro, C. Chemotherapy drug response in ovarian cancer cells strictly depends on a cathepsin D-Bax activation loop. *J. Cell. Mol. Med.* **2009**, *13*, 1096–1109. [CrossRef] [PubMed]
28. Demoz, M.; Castino, R.; Cesaro, P.; Baccino, F.M.; Bonelli, G.; Isidoro, C. Endosomal-Lysosomal Proteolysis Mediates Death Signalling by TNFα, Not by Etoposide, in L929 Fibrosarcoma Cells: Evidence for an Active Role of Cathepsin D. *Biol. Chem.* **2002**, *383*, 1237–1248. [CrossRef] [PubMed]
29. Trincheri, N.F.; Nicotra, G.; Follo, C.; Castino, R.; Isidoro, C. Resveratrol induces cell death in colorectal cancer cells by a novel pathway involving lysosomal cathepsin D. *Carcinogenesis* **2006**, *28*, 922–931. [CrossRef]
30. Castino, R.; Bellio, N.; Nicotra, G.; Follo, C.; Trincheri, N.F.; Isidoro, C. Cathepsin D–Bax death pathway in oxidative stressed neuroblastoma cells. *Free Radic. Biol. Med.* **2007**, *42*, 1305–1316. [CrossRef]
31. Roberg, K.; Ollinger, K. Oxidative stress causes relocation of the lysosomal enzyme cathepsin D with ensuing apoptosis in neonatal rat cardiomyocytes. *Am. J. Pathol.* **1998**, *152*, 1151–1156.
32. Shibata, M.; Kanamori, S.; Isaharaa, K.; Ohsawaa, Y.; Konishia, A.; Kametakaa, S.; Watanabe, T.; Ebisub, S.; Ishidoc, K.; Kominamic, E.; et al. Participation of Cathepsins B and D in Apoptosis of PC12 Cells Following Serum Deprivation. *Biochem. Biophys. Res. Commun.* **1998**, *251*, 199–203. [CrossRef]
33. Vignon, F.; Capony, F.; Ghambon, M.; Freiss, G.; Garcia, M.; Rochefort, H. Autocrine Growth Stimulation of the MCF 7 Breast Cancer Cells by the Estrogen-Regulated 52 K Protein. *Endocrinology* **1986**, *118*, 1537–1545. [CrossRef]
34. Isidoro, C.; Demoz, M.; De Stefanis, D.; Mainferme, F.; Wattiaux, R.; Baccino, F.M. Altered intracellular processing and enhanced secretion of procathepsin D in a highly deviated rat hepatoma. *Int. J. Cancer* **1995**, *60*, 61–64. [CrossRef]
35. Isidoro, C.; Démoz, M.; De Stefanis, D.; Baccino, F.M.; Bonelli, G. High levels of proteolytic enzymes in the ascitic fluid and plasma of rats bearing the Yoshida AH-130 hepatoma. *Invasion Metastasis* **1995**, *15*, 8621267.
36. A Reid, W.; Valler, M.J.; Kay, J. Immunolocalization of cathepsin D in normal and neoplastic human tissues. *J. Clin. Pathol.* **1986**, *39*, 1323–1330. [CrossRef]
37. Laurent-Matha, V.; Maruani-Herrmann, S.; Prébois, C.; Beaujouin, M.; Glondu, M.; Noel, A.; Alvarez-Gonzalez, M.L.; Blacher, S.; Coopman, P.; Baghdiguian, S.; et al. Catalytically inactive human cathepsin D triggers fibroblast invasive growth. *J. Cell Biol.* **2005**, *168*, 489–499. [CrossRef]
38. Pranjol, Z.I.; Gutowski, N.J.; Hannemann, M.; Whatmore, J.L. Cathepsin D non-proteolytically induces proliferation and migration in human omental microvascular endothelial cells via activation of the ERK1/2 and PI3K/AKT pathways. *Biochim. Et Biophys. Acta* **2018**, *1865*, 25–33. [CrossRef]
39. Benes, P.; Vetvicka, V.; Fusek, M. Cathepsin D—Many functions of one aspartic protease. *Crit. Rev. Oncol. Hematol.* **2008**, *68*, 12–28. [CrossRef]
40. Jha, S.K.; Rauniyar, K.; Chronowska, E.; Mattonet, K.; Maina, E.W.; Koistinen, H.; Stenman, U.-H.; Alitalo, K.; Jeltsch, M. KLK3/PSA and cathepsin D activate VEGF-C and VEGF-D. *eLife* **2019**, *8*, e44478. [CrossRef]
41. Sasaki, T.; Hiroki, K.; Yamashita, Y. The Role of Epidermal Growth Factor Receptor in Cancer Metastasis and Microenvironment. *BioMed Res. Int.* **2013**, *2013*, 1–8. [CrossRef]

42. Ongusaha, P.P.; Kwak, J.C.; Zwible, A.J.; Macip, S.; Higashiyama, S.; Taniguchi, N.; Fang, L.; Lee, S.W. HB-EGF Is a Potent Inducer of Tumor Growth and Angiogenesis. *Cancer Res.* **2004**, *64*, 5283–5290. [CrossRef]
43. Yagi, H.; Yotsumoto, F.; Miyamoto, S. Heparin-binding epidermal growth factor–like growth factor promotes transcoelomic metastasis in ovarian cancer through epithelial-mesenchymal transition. *Mol. Cancer Ther.* **2008**, *7*, 3441–3451. [CrossRef] [PubMed]
44. Rao, L.; Giannico, D.; Leone, P.; Solimando, A.G.; Maiorano, E.; Caporusso, C.; Duda, L.; Tamma, R.; Mallamaci, R.; Susca, N.; et al. HB-EGF–EGFR Signaling in Bone Marrow Endothelial Cells Mediates Angiogenesis Associated with Multiple Myeloma. *Cancers* **2020**, *12*, 173. [CrossRef]
45. Braig, F.; Kriegs, M.; Voigtlaender, M.; Habel, B.; Grob, T.; Biskup, K.; Blanchard, V.; Sack, M.; Thalhammer, A.; Ben Batalla, I.; et al. Cetuximab Resistance in Head and Neck Cancer Is Mediated by EGFR-K_{521} Polymorphism. *Cancer Res.* **2016**, *77*, 1188–1199. [CrossRef] [PubMed]
46. Sok, J.C.; Coppelli, F.M.; Thomas, S.; Lango, M.N.; Xi, S.; Hunt, J.L.; Freilino, M.L.; Graner, M.W.; Wikstrand, C.J.; Bigner, D.D.; et al. Mutant Epidermal Growth Factor Receptor (EGFRvIII) Contributes to Head and Neck Cancer Growth and Resistance to EGFR Targeting. *Clin. Cancer Res.* **2006**, *12*, 5064–5073. [CrossRef]
47. Liao, H.-W.; Hsu, J.-M.; Xia, W.; Wang, H.-L.; Wang, Y.-N.; Chang, W.-C.; Arold, S.T.; Chou, C.-K.; Tsou, P.-H.; Yamaguchi, H.; et al. PRMT1-mediated methylation of the EGF receptor regulates signaling and cetuximab response. *J. Clin. Investig.* **2015**, *125*, 4529–4543. [CrossRef] [PubMed]
48. Li, Z.; Chen, Y.; Ren, W.; Hu, S.; Tan, Z.; Wang, Y.; Chen, Y.; Zhang, J.; Wu, J.; Li, T.; et al. Transcriptome Alterations in Liver Metastases of Colorectal Cancer After Acquired Resistance to Cetuximab. *Cancer Genom. Proteom.* **2019**, *16*, 207–219. [CrossRef] [PubMed]
49. Vidoni, C.; Ferraresi, A.; Secomandi, E.; Vallino, L.; Dhanasekaran, D.N.; Isidoro, C. Epigenetic targeting of autophagy for cancer prevention and treatment by natural compounds. *Semin. Cancer Biol.* **2020**, *66*, 34–44. [CrossRef]
50. Thongchot, S.; Ferraresi, A.; Vidoni, C.; Loilome, W.; Yongvanit, P.; Namwat, N.; Isidoro, C. Erratum to "Resveratrol interrupts the pro-invasive communication between Cancer associated Fibroblasts and Cholangiocarcinoma cells" [Cancer Letters 430C (2018) 160–171]. *Cancer Lett.* **2018**, *434*, 206–207. [CrossRef]
51. Buhrmann, C.; Shayan, P.; Brockmueller, A.; Shakibaei, M. Resveratrol Suppresses Cross-Talk between Colorectal Cancer Cells and Stromal Cells in Multicellular Tumor Microenvironment: A Bridge between In Vitro and In Vivo Tumor Microenvironment Study. *Molecules* **2020**, *25*, 4292. [CrossRef]
52. Brâkenhielm, E.; Cao, R.; Cao, Y. Suppression of angiogenesis, tumor growth, and wound healing by resveratrol, a natural compound in red wine and grapes. *FASEB J.* **2001**, *15*, 1798–1800. [CrossRef]
53. Wu, H.; He, L.; Shi, J.; Hou, X.; Zhang, H.; Zhang, X.; An, Q.; Fan, F. Resveratrol inhibits VEGF-induced angiogenesis in human endothelial cells associated with suppression of aerobic glycolysis via modulation of PKM2 nuclear translocation. *Clin. Exp. Pharmacol. Physiol.* **2018**, *45*, 1265–1273. [CrossRef]
54. Cottart, C.-H.; Nivet-Antoine, V.; Laguillier-Morizot, C.; Beaudeux, J.-L. Resveratrol bioavailability and toxicity in humans. *Mol. Nutr. Food Res.* **2009**, *54*, 7–16. [CrossRef]
55. Rössler, J.; Odenthal, E.; Geoerger, B.; Gerstenmeyer, A.; Lagodny, J.; Niemeyer, C.M.; Vassal, G. EGFR inhibition using gefitinib is not active in neuroblastoma cell lines. *Anticancer. Res.* **2009**, *29*, 1327–1333.
56. Thongchot, S.; Vidoni, C.; Ferraresi, A.; Loilome, W.; Khuntikeo, N.; Sangkhamanon, S.; Titapun, A.; Isidoro, C.; Namwat, N. Cancer-Associated Fibroblast-Derived IL-6 Determines Unfavorable Prognosis in Cholangiocarcinoma by Affecting Autophagy-Associated Chemoresponse. *Cancers* **2021**, *13*, 2134. [CrossRef]
57. Salwa, A.; Ferraresi, A.; Chinthakindi, M.; Vallino, L.; Vidoni, C.; Dhanasekaran, D.; Isidoro, C. *BECN1* and *BRCA1* Deficiency Sensitizes Ovarian Cancer to Platinum Therapy and Confers Better Prognosis. *Biomedicines* **2021**, *9*, 207. [CrossRef]

Dual Role of Cathepsin D in 2D and 3D Growth of Neuroblastoma Cells in Response to EGF

Eleonora Secomandi, Giulia Camurani, Chiara Vidoni, Andrea Esposito, Alessandra Ferraresi, Ciro Isidoro. Dual role of cathepsin D in 2D and 3D growth of neuroblastoma cells in response to EGF. *Cells*. 2022 June 1. Under revision.

SYNOPSIS

Neuroblastoma is the most common extracranial solid tumor of childhood, accounting for 15% of all cancer-related deaths in the pediatric population. It shows a heterogeneous clinical behavior and often adverse outcomes. The overall survival of children with high-risk disease is around 50%, despite the aggressive treatment protocols consisting of intensive chemotherapy, surgery, radiation therapy and EGFR inhibitors. The hyperactivation of oncogenic signaling pathways, such as epidermal growth factor receptor/mitogen-activated protein kinase (EGFR/MAPK), as well as the overexpression of EGF family ligands, exert an important role in NB growth and progression. In this respect, the pharmacologic inhibition of EGFR is a widely used clinical approach, but often it remains ineffective and gives rise to drug resistance. A better understanding of the regulatory mechanism downstream growth factor receptors may help the identification of novel therapeutic targets.

Recently, we demonstrated that lysosomal cathepsin D contrasts neuroblastoma cell proliferation. The high expression of CD reduced the sensitivity to EGF stimulation and diminished ERK 1/2 activation in a 2D cellular model. Our *in vitro* studies are in accordance with data retrieved from *in silico* transcriptome analysis in which NB patients with high *EGFR* and high *CTSD* levels showed a better prognosis and longer overall survival.

In this work we took a step forward and we asked whether and how the expression of CD differentially affects the growth of NB cells in adherent condition and in suspension as 3D neurospheres. During cancer progression, clonal evolution leads to a mixture of clones with different genetic background and proteome; neurospheres may resemble clusters of metastatic cells which disseminate in secondary sites. To mimic tumor heterogeneity, we cocultured in various proportion transgenic clones silenced for, or overexpressing CD, in response to EGF. Intracellular cathepsin D was differentially modulated in 2D and 3D models: high protein expression inhibited the growth of adherent NB cells, whereas it conferred a survival and growth advantage to spheroids grown in suspension. The downregulation of CD is necessary for allowing adherence and anchorage-dependent growth, in fact KD-CD cells were highly proliferating and took the growth advantage over the other (Over CD clone) in 2D coculture

condition. Interestingly, when spheroids were switched to grow on solid substrate, mimicking the adhesion in a metastatic site, KD-CD grew faster and acquired the proliferative advantage. Noteworthy, in Sham-transfected cells, which retained the ability to modulate protein level, intracellular CD increased when they were grown in suspension, and decreased when cultivated in adherent condition.

Thus, we conclude that cathepsin D expression might be epigenetically modulated during the metastatic process. To the best of our knowledge, this is the first report describing such a role of cathepsin D in cancer.

Overall, our findings uncovered a novel function of CD and may have a translational impact for the stratification of patients in a view of personalized therapy.

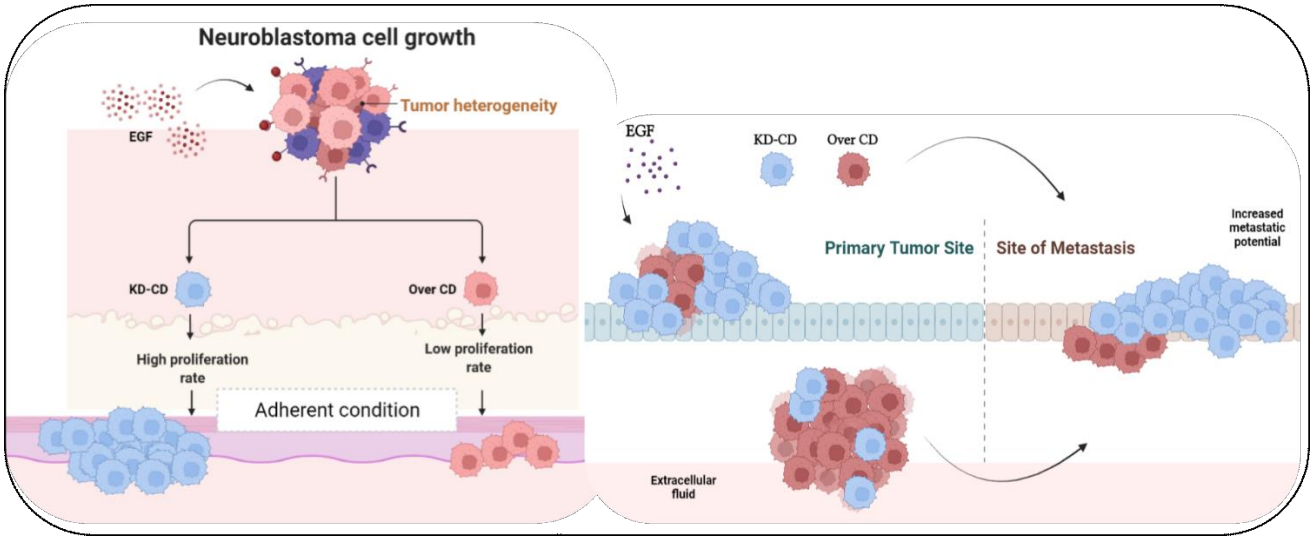

Figure 9. Dual role of cathepsin D in 2D and 3D growth of neuroblastoma cells in response to EGF.

cells

MDPI

Research Article

Dual role of cathepsin D in 2D and 3D growth of neuroblastoma cells in response to EGF

Eleonora Secomandi [1], Giulia Camurani [1], Chiara Vidoni [1], Andrea Esposito [1], Alessandra Ferraresi [1] and Ciro Isidoro[1,*]

[1] Laboratory of Molecular Pathology, Department of Health Sciences, Università del Piemonte Orientale "A. Avogadro", Via Solaroli 17, 28100 Novara, Italy; eleonora.secomandi@uniupo.it (E.S.); giuliacamurani@gmail.com (G.C.); chiara.vidoni@med.uniupo.it (C.V.); andrea.esposito@uniupo.it (A.E.); alessandra.ferraresi@med.uniupo.it (A.F.);

* Correspondence: ciro.isidoro@med.uniupo.it; Tel.: +39-032-166-0507; Fax: +39-032-162-0421

Abstract: Neuroblastoma (NB) is an embryonal tumor arising from the sympathetic central nervous system. The epidermal growth factor (EGF) plays a role in neuroblastoma growth and metastatic behavior. Recently, we have demonstrated that cathepsin D (CD) contrasts EGF-induced neuroblastoma cell growth by downregulating EGFR/MAPK signaling. In the metastatic process adherent cells detach to form clusters of suspended cells that once reached the metastatic site adhere and form secondary colonies. Here, we asked whether CD differentially affects cell growth in suspension *versus* adherent condition. To mimic tumor heterogeneity, we co-cultured transgenic clones silenced for or overexpressing CD. We compared the growth kinetics of such mixed clones in 2D and 3D models in response to EGF, and we found that Over CD clone was advantaged for the growth in suspension, while the CD knocked-down clone was favored for the adherent growth as 2D. The fact that CD plays a dual role in cancer cell growth in 2D and 3D conditions indicates that during clonal evolution subclones expressing different level of CD may arise, which confers survival and growth advantages depending on the metastatic step. Epigenetic regulation of CD expression and activity could be an additional strategy to cure this, and likely, other neoplasms.

Keywords: cancer; 3D neurosphere; lysosome; cell adhesion; clonal evolution, metastasis, tumor heterogeneity.

Citation: Lastname, F.; Lastname, F.; Lastname, F. Title. *Cells* **2022**, *11*, x. https://doi.org/10.3390/xxxxx

Academic Editor: Firstname Lastname

Received: date
Accepted: date
Published: date

1. Introduction

Neuroblastoma (NB) is one of the most common solid tumors affecting children, and it accounts for 15% of cancer-related deaths [1]. It is an embryonal malignancy of the autonomic nervous. NB may present with heterogeneous phenotype and clinical outcome with some tumors exhibiting (relative) good prognosis even not requiring intervention (as for neonatally diagnosed ones) and others exhibiting an early aggressive and metastatic behavior with multiple organ dysfunction and high mortality [1]. In individuals with high-risk disease the 5-year survival rate is less than 50%; even after radiation therapy the loco-regional relapse is still high (50%) and these patients have a 5-year survival of only 8% [2,3]. The hyperactivation of oncogenic signaling pathways, such as epidermal growth factor receptor/mitogen-activated protein kinase (EGFR/MAPK), as well as the overexpression of EGF family ligands, exert an important role in NB growth and progression [4-6]. Since the high expression of EGFR has been associated with enhanced tumor growth and chemoresistance in neuroblastoma, the pharmacologic inhibition of EGFR is a clinical approach widely used for cancer treatment. However, some tyrosine kinase inhibitors are not effective on MAPK pathway [7], leaving uncovered an important issue to solve. Recently, we demonstrated that lysosomal cathepsin D (CD), a ubiquitous soluble aspartic endopeptidase, contrasts neuroblastoma cell proliferation [8]. The high expression of CD reduced the sensitivity to EGF stimulation and diminished ERK 1/2 activation

in human NB cells cultured in 2D condition. Accordingly, data retrieved from *in silico* transcriptome analysis showed a better prognosis and longer overall survival in NB patients with high *EGFR* and high *CTSD* levels [8].

Cancer shows a wide genetic heterogeneity and during tumor evolution different clones compete for survival and overtake each-other. Multicellular 3D models more accurately resemble the *in vivo* tumor condition [9] and neurospheres may mimic clusters of metastatic cells which disseminate in secondary sites.

Whether and how the expression of cathepsin D plays a role in the switch from adherent to suspended growth of NB remains to be elucidated. We found different level of CD expression in 2D and 3D NB culture systems. We used engineered NB cells in which CD was overexpressed (Over CD clone) or knocked-down (KD-CD clone) [8]. High expression of CD suppressed the proliferation of adherent NB cells, yet it conferred a survival and growth advantage to free-floating spheroids. Intriguingly, when these spheroids were switched to grow on solid substrate, mimicking the adhesion in a metastatic site, the KD-CD clone grew faster and acquired the proliferative advantage over the other. Thus, high CD expression favors the survival of floating-spheroids, but it is detrimental for the growth in adherent condition. This noteworthy, in Sham-transfected clone, which retains the ability to modulate protein expression, the cellular level of CD increased when grown in suspension and decreased when grown in adhesion.

These findings highlight a dual role of CD in NB cell growth and suggest that this lysosomal protease is epigenetically regulated during the reversible transition for adherent-to-suspended-to-adherent growth of metastatic clones. It follows that epigenetic modulation of CD expression could be a valuable complementary strategy for preventing NB metastasis.

2. Materials and Methods

Cell culture and treatments

Human neuroblastoma SH-SY5Y cells were obtained from the American Type Culture Collection (cod. CRL-2266, ATCC, Rockville, MD). SH-SY5Y cells were maintained in standard conditions as previously described [8]. Treatments included 20 ng/ml Epidermal Growth Factor (EGF, cod. E5036; Sigma-Aldrich Corp. St. Louis, MO, USA), dissolved in 10 mM acetic acid, and 100 μM Pepstatin A, inhibitor of the aspartic protease CD (PstA, cod. P4265; Sigma-Aldrich Corp.). SH-SY5Y stable transfectant clones (Sham, knockdown CD (KD-CD), and overexpressing CD (Over CD) were generated in our laboratory [8] and have been cultivated alone or in combination for coculture experiments both in 2D and 3D systems, in different proportions: 50% KD-CD + 50% Over CD cells (ratio 1:1), 25% KD-CD + 75% Over CD (ratio 1:3) and 75% KD-CD + 25% Over CD cells (ratio 3:1). In two-dimensional system (2D), cells were plated at a density of 40,000 cells/cm^2 in Petri P60, whereas for 3D cultures 1,000,000 cells were seeded in non-adherent Petri dishes for each experimental condition.

Cell counting and doubling time calculation

Cells were seeded in 12-well plates (20,000 – 50,000 cells/cm^2), let adhere for 24 hours and then treated with 20 ng/ml EGF. Medium was refreshed every day. At each time point, cells were collected and counted in triplicate with Trypan Blue solution. Cell counting was performed following the protocol previously described [8]. Doubling time (Dt) was calculated through the free software Doubling Time Online Calculator (http://www.doubling-time.com/compute.php).

Clonogenic assay

Cells were seeded in 6-well (MW6) plates at the density of 2000 cells/well, treated with EGF and cultivated for 10 days to allow colony formation [10]. Newly colonies were stained with 0.5% crystal violet solution as previously described [8]. Images of each experimental condition were acquired, and the number of colonies formed was estimated by photometric measurements with CellCounter software (v0.2.1.).

Antibodies

The following primary antibodies were employed for western blotting: mouse anti-β-tubulin (1:1000, cod. T5201; Sigma-Aldrich Corp.), mouse anti-β-actin (1:2000, cod. A5441; Sigma-Aldrich Corp.), mouse anti-cathepsin D (1:100, cod. IM03; Calbiochem, St. Louis, MO, USA), mouse anti-histone H3 (1:500, cod. 61475; Active Motif, Carlsbad, CA, USA). Secondary antibodies used for western blot analysis were the following: Horse Radish Peroxidase-conjugated goat anti-mouse IgG (1:10,000, cod. 170–6516; Bio-Rad, Hercules, CA, USA), Horse Radish Peroxidase-conjugated goat anti-rabbit IgG (1: 10,000, cod. 170–6515: Bio-Rad, Hercules, CA, USA). The primary antibodies employed for immunofluorescence staining are listed below: mouse anti-CD (1:100, cod. IM03; Calbiochem), rabbit anti-p27 (1:100, cod. 2552; Cell Signaling, Danvers, MA, USA), rabbit anti-Ki-67 (1:100, cod. HPA001164; Sigma-Aldrich). The secondary antibodies were goat-Anti Rabbit IgG Alexa FluorTM Plus 488 (1:1000, cod. A32731; Invitrogen, Waltham, MA, USA) and Goat-Anti Mouse IgG Alexa FluorTM Plus 555 (1:1000, cod. A32727; Invitrogen).

Western blotting

SH-SY5Y Sham, KD-CD and Over CD transfectant clones were seeded at a density of 40,000 cells/cm^2 for coculture experiments on sterile P60 Petri dishes and let adhere. For the experiment with SH-SY5Y Sham grown in two-dimensional condition, cells were plated at a density of 4000 cells/Petri and cultivated for 7 days. At the end, cells were collected in RIPA Buffer (0.5% Deoxycholate, 1% NP-40, 0.1% Sodium Dodecyl Sulfate in PBS solution) supplemented with protease inhibitor cocktail and phosphatase inhibitors (0.5 M sodium fluoride NaF and 0.2 M sodium orthovanadate Na3VO4) and homogenized, as previously reported [8]. Protein content concentration was determined by Bradford assay and samples were denatured with 5X Leammli sample buffer at 95 °C for 10 minutes [8]. The bands were detected using Enhanced Chemiluminescence reagents (ECL, cod. NEL105001EA; Perkin Elmer, Waltham, MA, USA) and developed with the Chemi-Doc XRS instrument (BioRad, Hercules, CA, USA). Western blotting data were reproduced three times independently. Intensity of the bands was estimated by densitometry using Quantity One Software (BioRad, Hercules, CA, USA).

Immunofluorescence

SH-SY5Y transfectants clones were plated on sterile coverslips at the density of 30,000 cells/cm^2, let adhere and grow at least 24 hours before treatment. The coverslips were fixed and processed for immunofluorescence staining as previously described [8]. After the incubation with primary antibodies, the coverslips were washed three times with 0.1% Triton-PBS and incubated for 1 hour at room temperature with Goat-Anti Rabbit IgG Alexa FluorTM Plus 488 or Goat-Anti Mouse IgG Alexa FluorTM Plus 555 secondary antibodies, as appropriate. Nuclei were stained with the UV fluorescent dye DAPI (4′,6-diamidino-2-phenylindole). Secondary antibodies and DAPI were dissolved in 0.1% Triton-PBS + 10% FBS. Lastly, coverslips were mounted onto glasses using SlowFade antifade reagent (cod. S36936; Life Technologies, Paisley, UK) and data acquired by fluorescence microscopy

(Leica DMI6000, Leica Microsystems, Wetzlar, Germany). Different microscopic fields were randomly chosen, and representative pictures of selected fields were shown.

3D spheroid forming assay

3D multicellular spheroids were cultured based on our previous work [11]. Cells were cultured in specific P35 Petri dishes coated with 120 mg/mL Poly 2-hydroxyethyl methacrylate (Poly-HEMA, cod. P3932; Sigma-Aldrich) to prevent cell adhesion. Poly-HEMA was dissolved in 95% ethanol solution under rotation overnight at 50°C. The day after, the stock solution was diluted in 95% ethanol. Petri dishes were coated with 1.3 ml of diluted Poly-HEMA and left under the biological hood to completely dry. 1,000,000 cells/Petri were seeded and maintained in culture for 7 days. Fresh medium was added every 48 hours and supplemented with 20 ng/ml EGF or 100 μM PstA, as indicated. Spheroid's growth was monitored by taking pictures at phase contrast microscope (magnification 20x, Zeiss AXIOVERT 40 CFL) at each time-point. The 3D culture quantification was performed through ImageJ software, which calculates the area of spheroids, indicated as Arbitrary Unit (A.U.). In a 3D-to-2D experiment, 500,000 cells were initially plated in Poly-HEMA-coated Petri and let grow as neurospheres until the third day, and then 3D cell aggregates were collected, centrifuged, and reseeded in adherent Petri dishes. The adhesion and growth capacity of SH-SY5Y transfectant clones were monitored up to 72 hours by imaging. Finally, after 72 hours of culture in adherent condition, cells were harvested in RIPA Buffer and processed for western blot analysis.

Statistical analysis

Statistical analysis was performed with GraphPad Prism 6.0 software (San Diego, CA, USA). Bonferroni's multiple comparison test after one-way/two-way ANOVA analysis (unpaired, two-tailed) was employed. Significance was considered as follow: **** $p < 0.0001$; *** $p < 0.001$; ** $p < 0.01$; * $p < 0.05$. Data are reported as average ± S.D.

3. Results

3.1. Neuroblastoma cells grown as 2D or 3D express different level of cathepsin D

We checked whether CD expression is differently modulated in NB cells depending on whether growing adherent in 2D or in suspension in 3D culture conditions. We employed Pepstatin A (PstA) as a specific inhibitor of CD to determine its contribution to NB growth in both anchorage-dependent and anchorage-independent conditions (Figure 1A). The enzymatic inhibition of CD increased the growth of adherent cells compared to untreated control, whereas it reduced the size of multicellular spheroids. In fact, their size was 4-times smaller compared to that of untreated neurospheres with active CD (Figure 1B). Thus, in the absence of adhesion signals CD confers survival and growth advantage, which is nullified by PstA, indicating that this advantage is dependent on the proteolytic activity of CD. By western blotting it was shown that CD protein content was upregulated (almost five times) in NB spheroids compared to the cells grown as 2D (Figure 1C). Thus, CD is differently modulated in NB cells cultured in anchorage-dependent and anchorage-independent conditions and its activity is necessary for the growth in the latter condition.

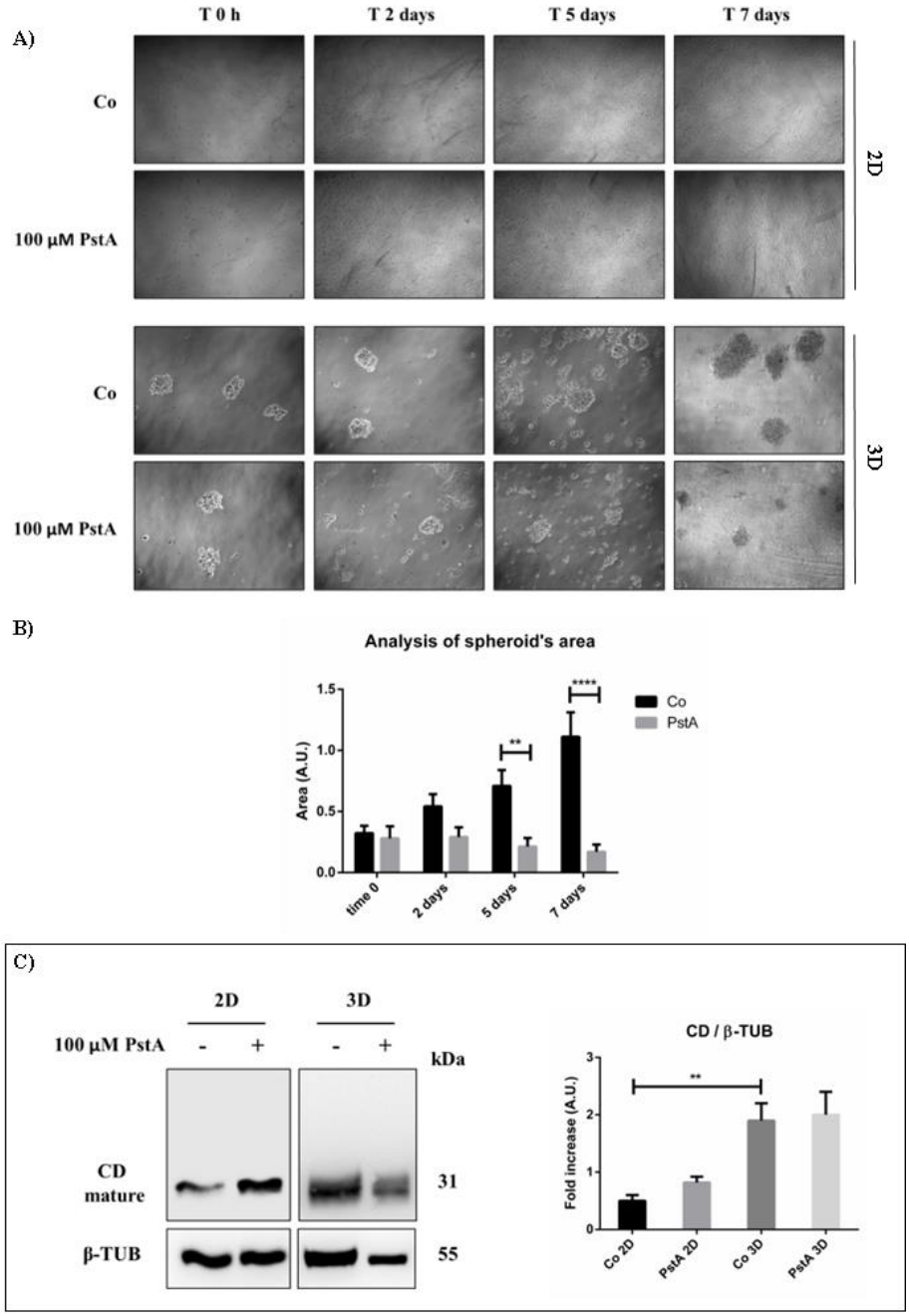

Figure 1. **Cathepsin D expression differs in 2D and 3D NB cell cultures.** SH-SY5Y cells were seeded both in adherent and non-adherent Petri dishes, at 4000 cells/cm^2 and 1,000,000 cells/Petri, respectively, and let grow for 48 hours. Medium was refreshed every 48 hours, supplemented with 100 µM PstA where indicated. A) Cell growth was monitored at the phase-contrast microscope and images were acquired at the time point indicated (time 0 h, 2-,5- and 7-days). B) The quantification of 3D spheroid's size was performed with ImageJ software. The area is indicated as Arbitrary Unit (A.U.). Data represented the average ± S.D. calculated for at least 5 to 10 spheroids for each experimental condition in three separate experiments. C) Western blotting analysis of CD expression in 2D and 3D cell homogenates. The membrane was probed with β-tubulin as loading control. The blot is representative of three independent experiments. Densitometry of the bands is reported in the histogram. Significance was considered as follows: **** $p < 0.0001$; ** $p < 0.01$.

3.2. Cathepsin D expression differentially affects the 2D and 3D growth of neuroblastoma cells

To better assess the role of CD in anchorage-dependent and anchorage-independent growth of NB we took advantage of human neuroblastoma SH-SY5Y stable transfectant clones engineered in our laboratory that are silenced for (knocked-down, KD-CD) or over-express (over CD) this protease [8]. The effectiveness of such genetic manipulations is here confirmed by the immunofluorescence staining of CD shown in Figure 2A. It appears obvious that CD is highly expressed in Over CD clone while it is barely detectable in KD-CD clone. Next, we examined their proliferative potential in 2D cultures. KD-CD clone displayed the highest while Over CD clone displayed the lowest proliferation rate, compared to Sham-transfected clone (Figure 2B). Accordingly, the doubling time (Dt) of Over CD clone was approximately 50% increased (from 38 h to 56 h) while the Dt of KD-CD was approximately 30% reduced (from 38 h to 29 h) compared to that reported for Sham-transfected counterpart (Table 1).

Table 1. Doubling time calculated for SH-SY5Y Sham, KD-CD and Over CD clones.

Clone	Doubling Time
Sham	37.6 ± 1.7
KD-CD	29.3 ± 1.2
Over CD	55.6 ± 1.1

Then, we assayed the growth rate of these clones cultured as 3D spheroids for up to 7 days. CD-overexpressing cells showed a greater ability to survive and grow in suspension, forming spheroids that are 12-times larger than those of KD-CD (Figure 2C).

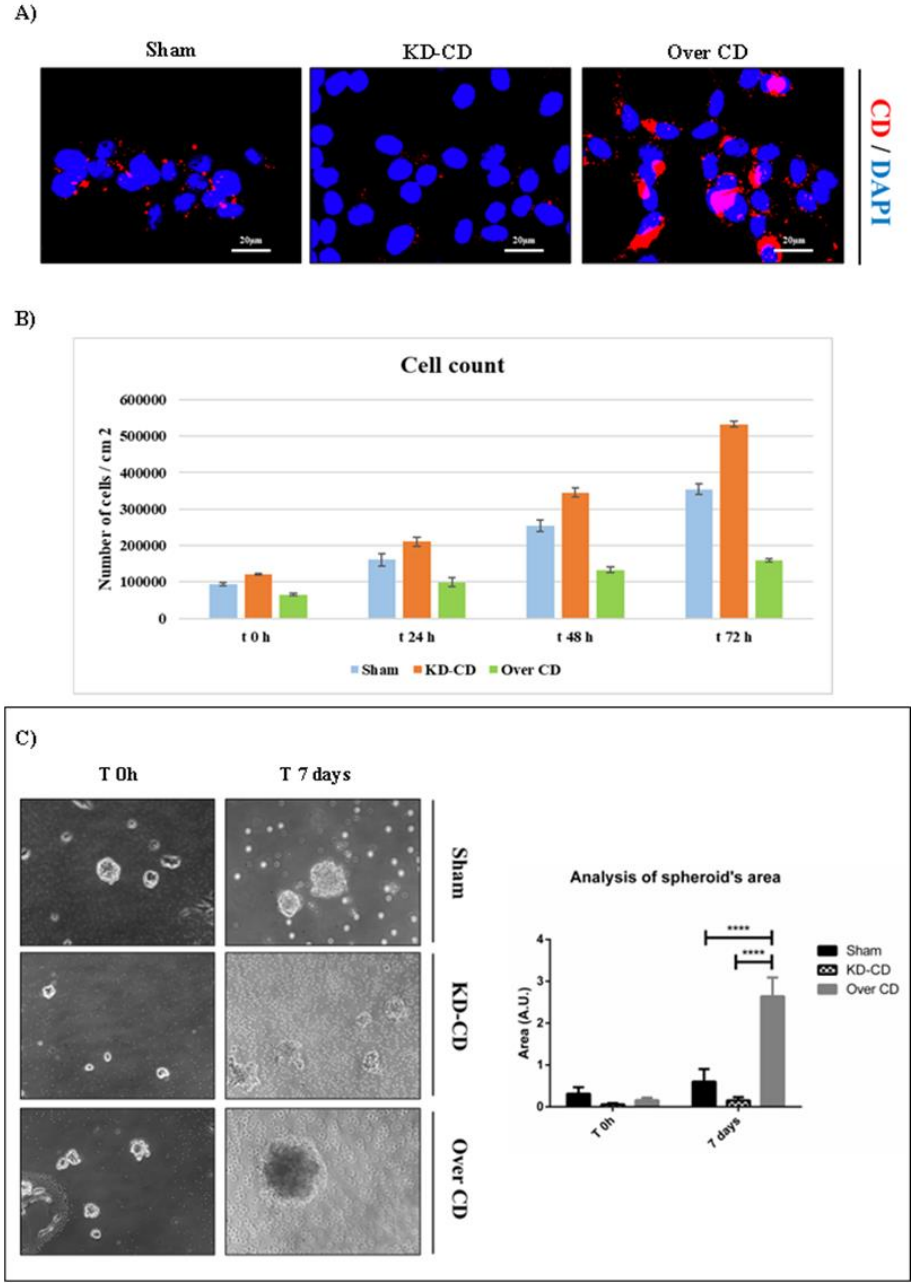

Figure 2. SH-SY5Y Sham, KD-CD and Over CD clones show different growth rates. A) Immunofluorescence performed on SH-SY5Y clones. Cells were seeded on sterile coverslips and then fixed and stained for CD (red); nuclei were marked with the UV fluorescent dye DAPI. Scale bar = 20 μm; magnification = 63x. B) Graph representing cell count. Cell counting was performed in triplicate for each experimental condition. C) **3D cultures of neuroblastoma clones.** SH-SY5Y Sham, KD-CD and Over CD cells were seeded on non-adherent Petri dishes and maintained in culture for 7 days. New fresh medium was replaced every 48 hours. The 3D spheroid's growth was monitored at the phase-contrast microscope and pictures were acquired. The quantification of 3D spheroid's size was performed with ImageJ software. The area was indicated as Arbitrary Unit (A.U.). Data represented the average ± S.D. calculated for at least 5 to 10 spheroids for each condition in three separate experiments. Significance was considered as follow: **** $p < 0.0001$.

3.3. Cathepsin D overexpression contrasts while cathepsin D silencing enhances Epidermal growth factor-induced cell growth

Colony assay confirmed that transgenic SH-SY5Y cells KD for CD had higher while those overexpressing CD had lower proliferation rate compared to Sham-transfected counterpart (Figure 3 A-B). EGFR stimulation exacerbates the growth and the aggressive behavior of NBs [7]. The administration of 20 ng/ml EGF, which is in the range of cell growth stimulation [12], markedly increased the colony forming ability of CD knockdown cells (Figure 3A). When stimulated with EGF, the colony formation increased differently in the three clones, with an increment of 3.4-fold, of 4.5-fold, and of 3-fold for Sham-transfected, KD-CD, and Over CD, respectively (Figure 3A-B). Particularly, the number of newly formed colonies in EGF-treated KD-CD clone was 3- and 8.8- times higher compared to Sham and Over CD, respectively. These data definitively confirm that in adherent 2D condition low or null expression of CD favors NB cell growth.

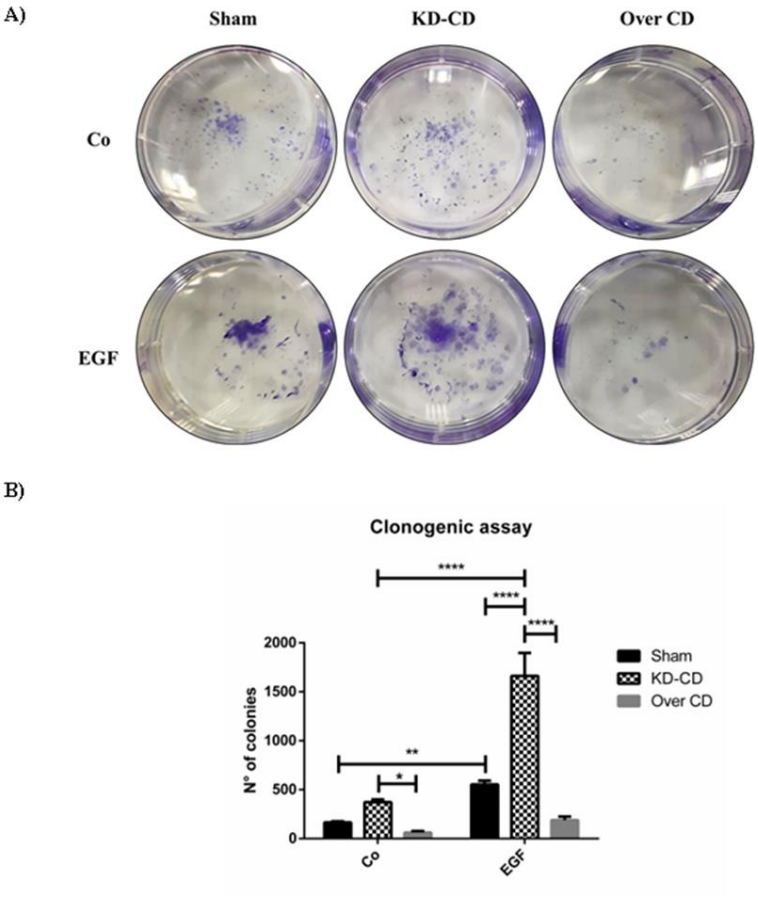

Figure 3. EGF stimulation of neuroblastoma growth depends on cellular level of cathepsin D. A) Clonogenic assay performed on SH-SY5Y transgenic clones upon stimulation with 20 ng/ml EGF. Colonies were stained as described in the Materials and Methods section. B) Cell growth and number of colonies were estimated through photometric measurements and CellCounter Software and are shown in the graph. Data ± S.D. are representative of three independent replicates. Significance was considered as follow: **** $p < 0.0001$; ** $p < 0.01$; * $p < 0.05$.

3.4. Knocked-down CD clone overtakes Over CD clone in EGF-stimulated growth of mixed cultures

Tumor evolution is characterized by the presence of multiple cancer clones with different genetic background and these clones compete for survival and overtake each-other. We hypothesized that during malignant progression NB could develop subclones expressing different level of CD, which then would respond differently to EGF. To mimic such tumor heterogeneity, we have mixed at different ratios clones overexpressing or silenced for CD

and tested which one would take advantage to grow over the other in the absence or in the presence of EGF stimulation. In pure cultures, EGF greatly stimulated the growth of KD-CD and to a much lesser extent that of Over CD, as expected (Figure 4A). When the clones were mixed in different proportion of KD-CD and of Over CD at 1:1 or 1:3 or 3:1 ratio, the cocultures stimulated with EGF showed a higher growth rate when the KD-CD clone was highly represented (Figure 4A). Immunofluorescence staining of Ki-67, a proliferative nuclear marker, and of $p27^{Kip1}$, a cyclin-dependent kinase inhibitor that prevents entering the cell cycle, corroborated these findings. To distinguish the two populations of KD-CD and Over CD in the mixed cultures, we co-stained the cells with an anti-CD antibody. In pure cultures, EGF strongly increased the expression of nuclear Ki-67 and decreased the levels of p27 in KD-CD cells, and conversely high level of p27 and low level of Ki-67 were observed in Over CD cells (Figure 4B). In cocultures, especially in 1:1 and 3:1 ratio of KD-CD vs Over CD, we observed high expression of Ki-67 in CD-silenced cells that were the most represented ones, indicating that these cells took advantage to grow over the others.

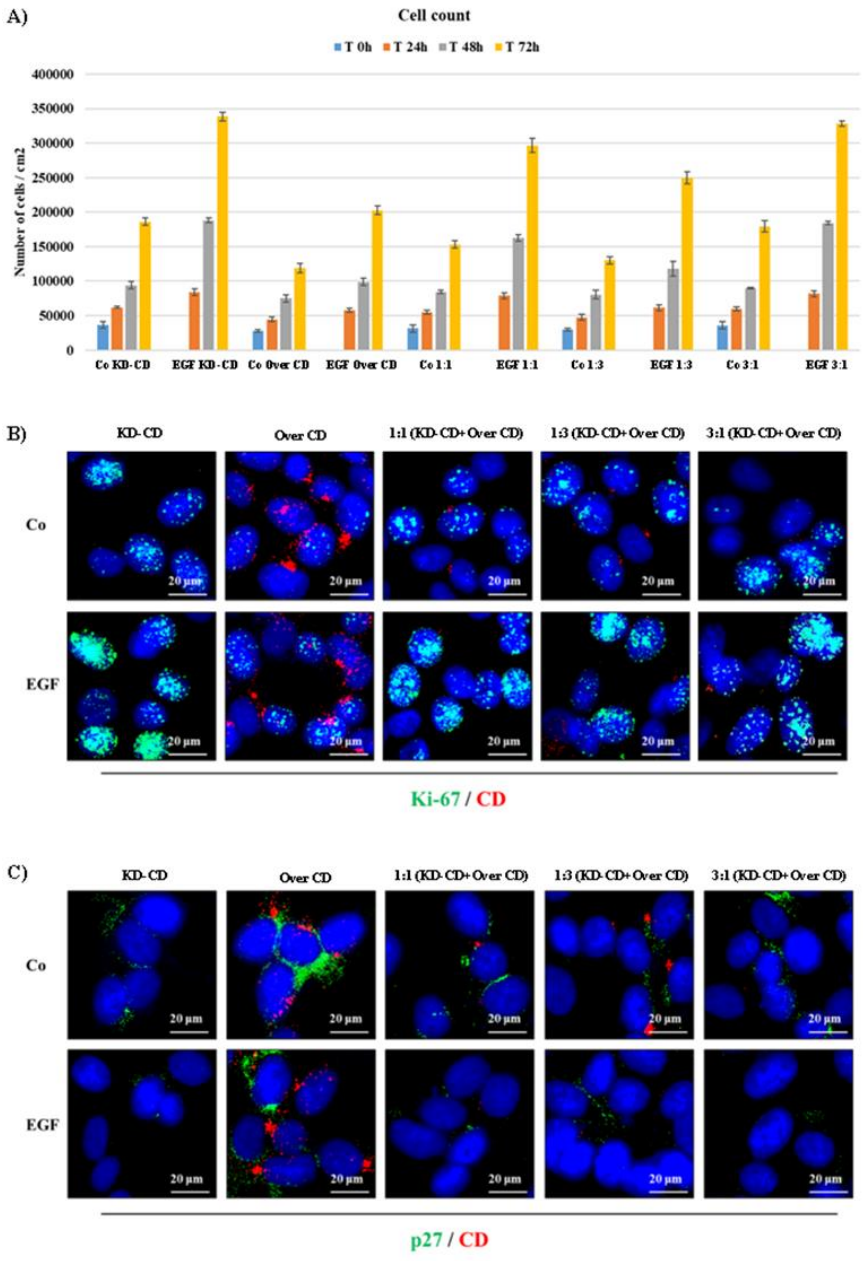

267

Figure 4. CD knockdown clone expresses high level of nuclear Ki-67 proliferation marker and reduced p27 cell cycle inhibitor. A) Cell counting of viable cells of KD-CD or Over CD or a mix of both at the ratio indicated, in the absence or the presence of EGF. Medium was renewed and EGF added every 24 h. The cells were cultivated for 24, 48 and 72 h. B-C) Immunofluorescence double staining of CD and Ki-67 or p27 in SH-SY5Y KD-CD, Over CD and mixed cultures at different ratio: 50% KD-CD + 50% Over CD cells (1:1), 25% KD-CD + 75% Over CD (1:3) and 75% KD-CD + 25% Over CD cells (3:1). Fresh medium was replaced every day and EGF was added as indicated. After 72h of treatment, cells were fixed and stained for Ki-67 (green) / CD (red) (B) and p27 (green) / CD (red) (C). Scale bar = 20 μm; magnification = 63x. Representative images of different fields for each experimental condition are shown.

We further assessed the level of cellular CD expressed in the mixed clones (Figure 5). Over CD clone expresses approximately 25-folds more CD than KD-CD clone, in which CD is indeed barely expressed. In the absence of EGF stimulation, after 72 hours the mixed culture of the two clones at (KD-CD vs Over CD) 1:1, 1:3 and 3:1 ratio demonstrated a progressive reduction of the total content of CD. However, at 1:1 ratio the total content of CD is reduced by some 30% and not by 50% as one would expect. Also, comparing the two opposite proportion of the clones (1:3 *versus* 3:1) it appears that the reduction of CD in the whole homogenate is not reflecting the proportion of the clones (Figure 5A). Together with data in Figure 4 and in agreement with our previous findings [8], the possible explanation is that in the mixed co-cultures Over CD cells are viable though in a resting phase while the KD-CD cells are proliferating. This supposes that with time the latter clone would overtake the former. To accelerate this process, we exposed the clones to EGF. We previously reported [8] that Over CD cells resist while KD-CD cells respond to the growth promoting effect of EGF. In fact, EGF greatly stimulated the growth of KD-CD clone which overtook that of CD-overexpressing cells in the cultures mixed at any ratio (Figure 5B-C). It is worth nothing that this effect is now evident at the 1:1 ratio, and even at the 1:3 ratio in which the number of Over CD seeded at time zero was 3-folds that of KD-CD cells.

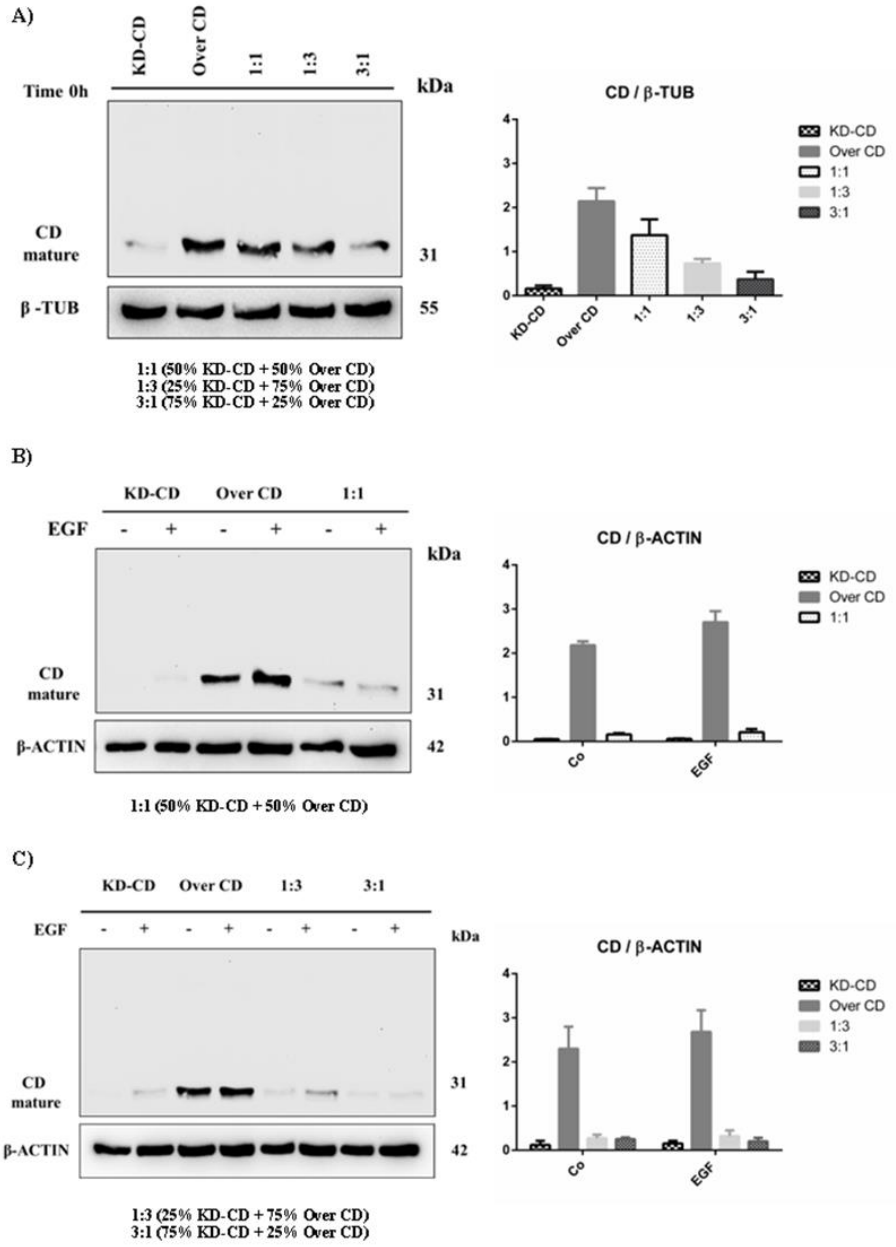

Figure 5. Analysis of cathepsin D protein content in SH-SY5Y mixed clones. Western Blotting showing the expression of cathepsin D in pure cultures (KD-CD and Over CD) and in mixed cocultures: 50% KD-CD + 50% Over CD cells (1:1), 25% KD-CD + 75% Over CD (1:3) and 75% KD-CD + 25% Over CD cells (3:1). A) Samples were collected at time 0h, before EGF treatment and processed for western blot analysis of cathepsin D. B) and C) Cells were cultured for 72 hours and medium was renewed and EGF re-added every day. Membranes were probed with β-tubulin and β-actin as loading control. All blots are representative of three independent experiments. Densitometry of the bands is reported in the histogram.

3.5. Cathepsin D overexpression increases the survival of NB spheroids cultivated in suspension

Neurospheres can be assumed as clusters of cells representing metastatic clones at the step of detachment from the primary tumor and, possibly, circulating in body fluids. At this point, it was necessary to determine the role of CD in the EGF-induced proliferation of the two clones expressing CD at different levels cultivated in suspension. To mimic tumor heterogeneity for CD expression, we co-cultured the two clones KD-CD and Over CD in

different proportion as detailed above. Representative images and quantification of the spheroid's growth are shown in Figure 6. In pure cultures, EGF stimulated the growth of Over CD neurospheres to a larger extent compared to the KD-CD neurospheres. This effect was observed also in mixed clones at the ratio 1:1 and 1:3, but not at the ratio 3:1 in which the Over CD clone is less represented. Particularly, EGF increased the dimension of Over CD neurospheres by 2-folds compared to those formed by KD-CD. The growth curves of each condition (shown in Figure 6C) suggest that as the Over CD cell population overcomes the other, the spheroid's size increases as well.

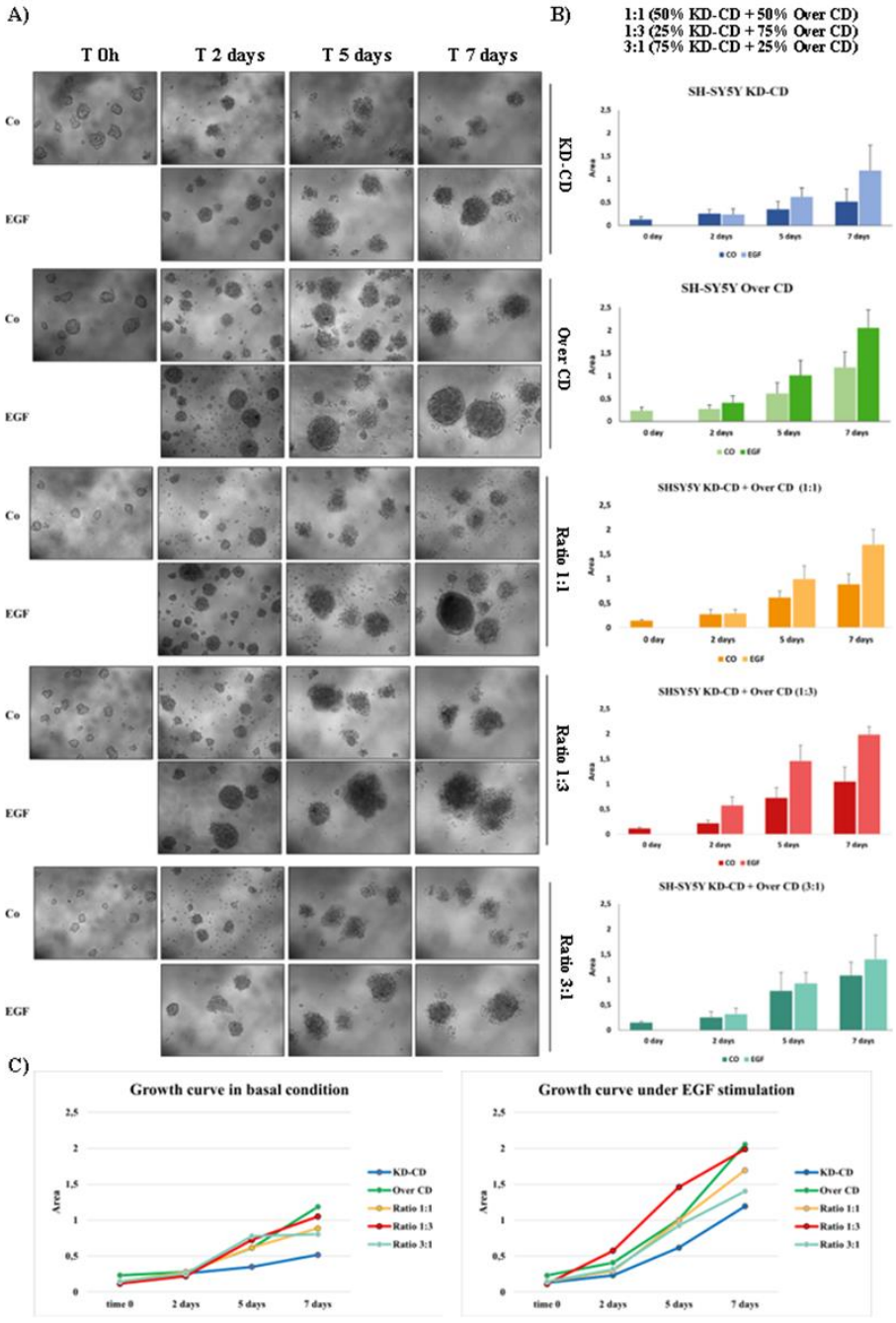

Figure 6. Monitoring of spheroid formation in pure and mixed clones cocultured in the absence or presence of EGF. SH-SY5Y KD-CD, Over CD and cocultures (50% KD-CD + 50% Over CD cells (1:1), 25% KD-CD + 75% Over CD (1:3) and 75% KD-CD + 25% Over CD cells (3:1)) were plated on non-adherent Petri dishes and let grow for 48 hours to allow spheroid formation. Cells were

cultured for 7 days after the first treatment. At time 0h, cells were incubated with EGF and re-treated in fresh medium at day 2 and 5. A) The 3D spheroid growth was monitored at the phase-contrast microscope and images were acquired at different time points (time 0h, 2-, 5- and 7-days). B) Quantification of spheroid's size was obtained through ImageJ software. The area is indicated as Arbitrary Unit (A.U.). Data represent the average ± S.D. calculated for at least 5 to 10 spheroids for each condition in three separate experiments. C) Graphs representing the growth curves of spheroids in control and EGF-treated conditions.

To have a more objective measure, we assayed the expression of histone H3 in a standard volume of cell homogenate that was equal for each sample. The H3 protein is one of the main histones composing chromatin structure and can be assumed as an indirect readout of cell number. The western blotting (Figure 7A) shows high level of histone H3 in pure Over CD culture and in the mixed culture at the ratio 1:1 and 1:3, both in EGF-treated and untreated conditions. In EGF-treated pure cultures, the level of histone H3 in Over CD was 3-folds that in KD-CD cells. As a definitive confirmation of which subpopulation gained growth advantage in the mixed cultures we assayed the CD protein content in spheroid's homogenates (Figure 7B). In pure KD-CD culture as well as in mixed 3:1 culture (where the KD-CD clone is predominant), and to a lesser extent in the mixed 1:1 culture, it is not observed an increase of CD content upon stimulation with EGF, indicating that the absence of CD makes the cells less able to grow in suspension and to respond to EGF. By contrast, in the pure and in the 1:3 mixed culture (containing the Over CD in higher proportion), it is appreciable the increase of CD content upon EGF stimulation, indicating that this subclone took advantage for growth in suspension.

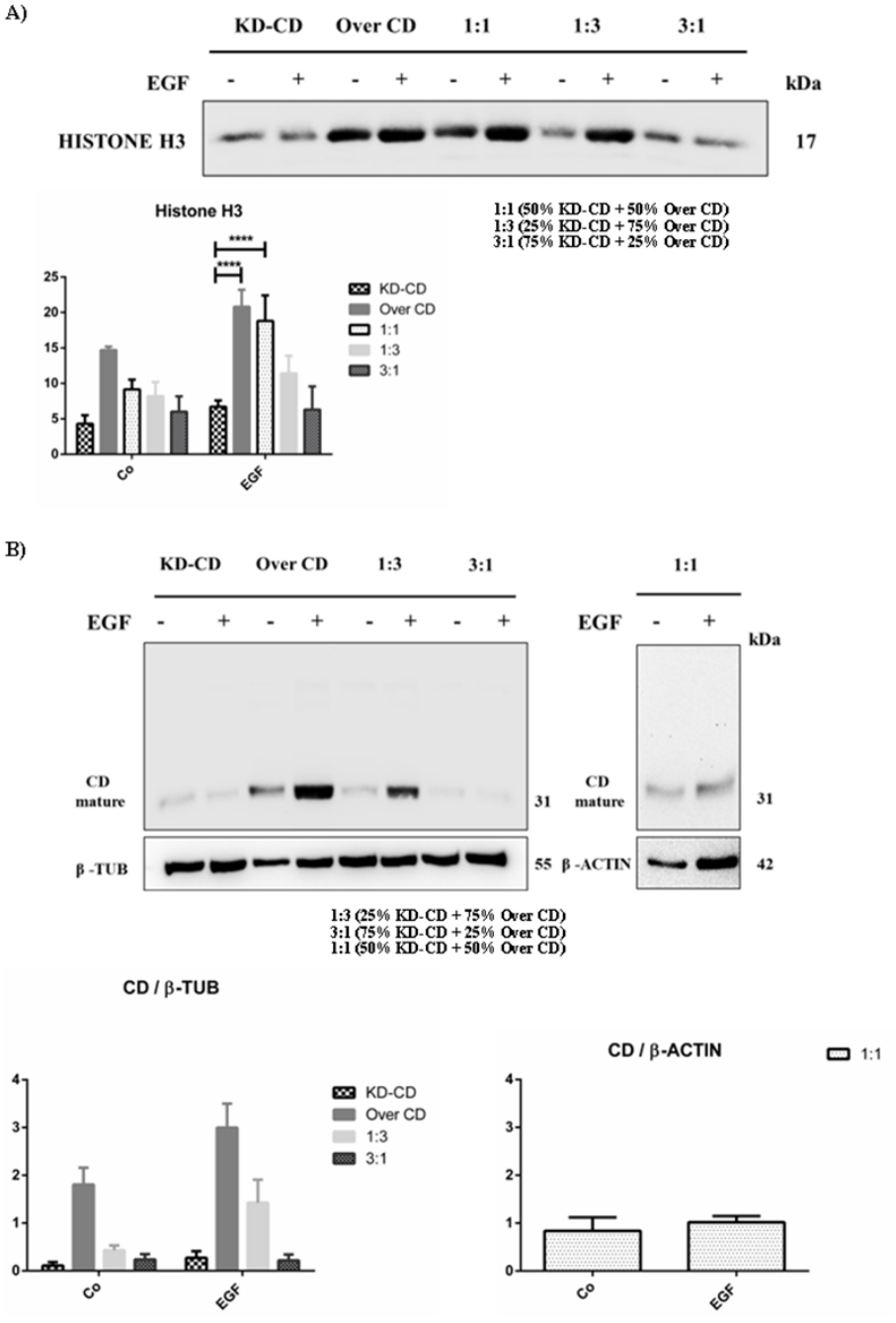

Figure 7. SH-SY5Y Over CD shows a greater ability to grow in suspension compared to KD-CD cells. SH-SY5Y 3D spheroids of pure clones or clones mixed at the indicated ratio were cultured for 7 days in the absence or presence of EGF. Homogenates were assayed by western blotting for the protein histone H3 (panel A) and CD (panel B). Histone H3 was measured in an equal volume of cell homogenate for each sample. The filters were stripped and re-probed for β-tubulin and β-actin proteins, as loading control. Blots are representative of three independent experiments. Densitometry of the bands is reported in the histograms.

3.6. Suspended SH-SY5Y clone knocked-down for cathepsin D rescues the ability to grow in adherent condition

In vivo, small clusters of circulating tumor cells can reach distant organs where they have to attach and grow for forming secondary metastasis. To mimic *in vitro* such situation, the spheroids of suspended cells, from either pure or mixed clones, were placed in culture

Petri dishes for attachment and let them grow for 72 hours. The cultures were imaged at 24, 48 and 72 h (Figure 8A-B).

It is apparent that KD-CD cells, either cultured as pure clone or mixed with Over CD cells at any ratio displayed the greatest ability to adhere and grow onto a solid matrix, giving rise to secondary colonies. By contrast, Over CD cells which were the most actively proliferating in suspension were less prone to attach and rescue the growth as adherent colonies. We measured the CD content in the attached colonies as an indirect marker of the prominent subclone in the pure and mixed populations (Figure 8C). Whatever the relative proportion in the starting co-culture of spheroids (i.e., at either 1:1, 1:3 and 3:1 ratio), the KD-CD clone became prevalent in the adherent colonies, as indicated by the very low content of CD in the whole homogenates. This confirms that overexpression of CD limits the anchorage-dependent growth of neuroblastoma cells, also reported in [8].

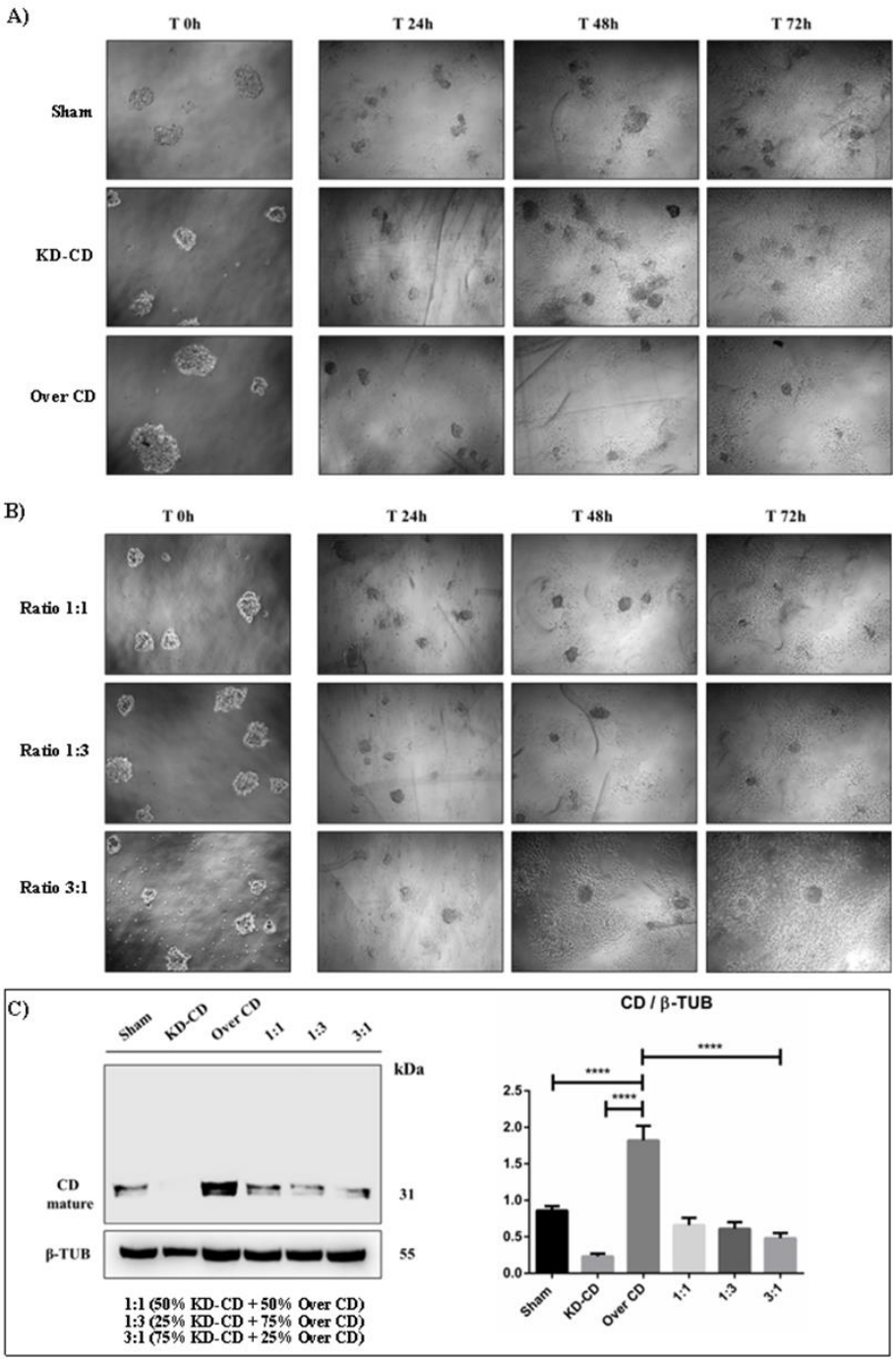

Figure 8. CD knocked-down SH-SY5Y cells rescue the ability to grow in adherent condition. SH-SY5Y Sham, KD-CD, Over CD and mixed cocultures, 50% KD-CD + 50% Over CD cells (1:1), 25% KD-CD + 75% Over CD (1:3) and 75% KD-CD + 25% Over CD cells (3:1) were seeded in non-adherent Petri dishes and let grow for 72 hours to allow spheroid formation (500,000 cells/Petri). The third day, (indicated in Figure as Time 0h), neurospheres were collected, resuspended in fresh medium, plated in adherent Petri dishes and maintained in culture for other 72 hours. New fresh medium was replaced every day. Cell homogenates were processed for western blot analysis. A) and B) Images were acquired at the phase-contrast microscope every day to monitor cell attachment and growth. C) Western blotting analysis of CD in cell homogenates. The membrane was stripped and re-probed for β-tubulin as loading control. The blot is representative of three independent experiments. Densitometry of the bands is reported in the histogram.

4. Discussion

Neuroblastoma is the most common extracranial solid tumor of childhood responsible for over 15% of cancer-related deaths [2,13]. Despite recent advances in multimodal therapeutic strategy, including EGFR targeting, NB continues to cause high mortality. NB tumorigenesis and progression are driven by the overexpression and hyperactivation of oncogenic signaling pathways that are not efficiently counteracted by inhibitory pathways. A better understanding of the regulatory mechanisms downstream growth factor receptors may help the development of novel targets and effective therapeutics.

The conventional 2D cellular model often does not adequately resemble the complexity of the tumor mass. Neuroblastoma cells grown as 3D aggregates (multicellular spheroids) much closer recapitulate the *in vivo* structure of cancers and possess features in common with primary tumors, including cells in different proliferative and metabolic state, also due to growth factor, nutrient, and oxygen availability [14,15]. Important phenotypic and metabolic differences, including migration, proliferation, and response to toxic drugs, have been reported when comparing the neuroblastoma cells cultured in adhesion as 2D monolayer or in suspension as 3D spheroids [16-18]. The type of culture system influences the proteome [17]. Changing in signaling cascades, like PI3K/AKT/mTOR and EGFR/MAPK, two central regulators of cell growth, survival, and metabolism, have been well documented [19-22]. We have previously demonstrated that high expression of the lysosomal protease CD is a predictor of good prognosis in neuroblastoma patients bearing high levels of *EGFR* [8]. *In silico* transcriptome analysis was corroborated by *in vitro* studies revealing that high intracellular CD reduces ERK 1/2 activation and inhibits EGF-induced cell growth. Whether and how CD impacts differentially on the 2D or 3D growth of neuroblastomas remains to be determined. In this work, we took advantage of transgenic neuroblastoma SH-SY5Y cells either knocked-down for (KD-CD) or overexpressing CD (Over CD) available in our laboratory to address this issue. Strikingly, we found that overexpression of CD while inhibiting NB growth in 2D cultures it was instead beneficial for the growth in 3D. Accordingly, NB cells enhanced the expression of CD when the culture was switched from adherent to suspended condition. We exploited our CD-engineered clones for understanding the role of CD in culture conditions that recapitulate *in vitro* the steps of metastatic spreading, that is the transition from adherent to suspended to adherent growth. Additionally, to mimic the tumor heterogeneity arising from clonal evolution that could lead to clones expressing CD at different levels, we tested the growth ability under EGF stimulation of mixtures at different ratio of the two clones. Briefly, we found that upregulation of CD expression is mandatory to guarantee the survival and proliferation of the cells in suspension while it is mandatory to downregulate its expression for allowing adherence and anchorage-dependent growth of the tumor cells. Thus, we may conclude that CD expression is epigenetically modulated during the metastatic cascade. To our knowledge, this is the first evidence for such a role of CD in neuroblastomas. We anticipate that the present findings likely hold also for other tumor models.

Collectively, we have uncovered a novel function of CD in the metastatic spreading of tumors. This finding may have a translational relevance, and we propose CD as a biomarker for metastatic neuroblastomas and for the stratification of patients in a view of personalized medicine. Further to be considered, epigenetic modulation of CD expression could be a valuable complementary strategy for preventing NB metastasis.

Author Contributions: Conceptualization, E.S. and C.I.; methodology and data curation, E.S., G.C., C.V., A.E. and A.F.; visualization, E.S. and G.C.; writing—original draft preparation, E.S.; writing—review and editing, C.I. supervision, C.I. All authors have read and agreed to the published version of the manuscript.

Funding: This research received no external funding.

Institutional Review Board Statement: Not applicable.

Informed Consent Statement: Not applicable.

Data Availability Statement: Not applicable.

Acknowledgments: ES and AE are recipients of a PhD fellowship granted by the Italian Ministry of Education, University and Research (MIUR, Rome, Italy). The fluorescence microscope was donated by Comoli, Ferrari & SpA (Novara, Italy). Thanks to Associazione per la Ricerca Medica Ippocrate-Rhazi (ARM-IR, Novara, Italy) for the support.

Conflicts of Interest: The authors declare no conflict of interest.

References

1. Davidoff AM. Neonatal Neuroblastoma. Clin Perinatol. 2021 Mar;48(1):101-115. doi: 10.1016/j.clp.2020.11.006. Epub 2021 Jan 12. PMID: 33583499.
2. Siegel RL, Miller KD, Fuchs HE, Jemal A. Cancer Statistics, 2021. CA Cancer J Clin. 2021 Jan;71(1):7-33. doi: 10.3322/caac.21654. Epub 2021 Jan 12. Erratum in: CA Cancer J Clin. 2021 Jul;71(4):359. PMID: 33433946.
3. Zhao Q, Liu Y, Zhang Y, Meng L, Wei J, Wang B, Wang H, Xin Y, Dong L, Jiang X. Role and toxicity of radiation therapy in neuroblastoma patients: A literature review. Crit Rev Oncol Hematol. 2020 May;149:102924. doi: 10.1016/j.critrevonc.2020.102924. Epub 2020 Mar 3. PMID: 32172225.
4. Wells A. EGF receptor. Int J Biochem Cell Biol. 1999 Jun;31(6):637-43. doi: 10.1016/s1357-2725(99)00015-1. PMID: 10404636.
5. Tang CK, Lippman ME. EGF family receptors and their ligands in human cancer. In: O'Malley BW, editor. Hormones and signaling. vol. I. San Diego (CA): Academic Press; 1998. p. 113–65.
6. Sasaki T, Hiroki K, Yamashita Y. The role of epidermal growth factor receptor in cancer metastasis and microenvironment. Biomed Res Int. 2013;2013:546318. doi: 10.1155/2013/546318. Epub 2013 Aug 7. PMID: 23986907; PMCID: PMC3748428.
7. Ho R, Minturn JE, Hishiki T, Zhao H, Wang Q, Cnaan A, Maris J, Evans AE, Brodeur GM. Proliferation of human neuroblastomas mediated by the epidermal growth factor receptor. Cancer Res. 2005 Nov 1;65(21):9868-75. doi: 10.1158/0008-5472.CAN-04-2426. PMID: 16267010.
8. Secomandi E, Salwa A, Vidoni C, Ferraresi A, Follo C, Isidoro C. High Expression of the Lysosomal Protease Cathepsin D Confers Better Prognosis in Neuroblastoma Patients by Contrasting EGF-Induced Neuroblastoma Cell Growth. Int J Mol Sci. 2022 Apr 26;23(9):4782. doi: 10.3390/ijms23094782. PMID: 35563171.
9. Pozzi S, Scomparin A, Israeli Dangoor S, Rodriguez Ajamil D, Ofek P, Neufeld L, Krivitsky A, Vaskovich-Koubi D, Kleiner R, Dey P, Koshrovski-Michael S, Reisman N, Satchi-Fainaro R. Meet me halfway: Are in vitro 3D cancer models on the way to replace in vivo models for nanomedicine development? Adv Drug Deliv Rev. 2021 Aug;175:113760. doi: 10.1016/j.addr.2021.04.001. Epub 2021 Apr 7. PMID: 33838208.
10. Thongchot S, Vidoni C, Ferraresi A, Loilome W, Khuntikeo N, Sangkhamanon S, Titapun A, Isidoro C, Namwat N. Cancer-Associated Fibroblast-Derived IL-6 Determines Unfavorable Prognosis in Cholangiocarcinoma by Affecting Autophagy-Associated Chemoresponse. Cancers (Basel). 2021 Apr 28;13(9):2134. doi: 10.3390/cancers13092134. PMID: 33925189; PMCID: PMC8124468.
11. Ferraresi A, Esposito A, Girone C, Vallino L, Salwa A, Ghezzi I, Thongchot S, Vidoni C, Dhanasekaran DN, Isidoro C. Resveratrol Contrasts LPA-Induced Ovarian Cancer Cell Migration and Platinum Resistance by Rescuing Hedgehog-Mediated Autophagy. Cells. 2021 Nov 17;10(11):3213. doi: 10.3390/cells10113213. PMID: 34831435; PMCID: PMC8625920.
12. Chiu B, Mirkin B, Madonna MB. Mitogenic and apoptotic actions of epidermal growth factor on neuroblastoma cells are concentration-dependent. J Surg Res. 2006 Oct;135(2):209-12. doi: 10.1016/j.jss.2006.04.018. Epub 2006 Jul 26. PMID: 16872636.

13. Matthay KK, Maris JM, Schleiermacher G, Nakagawara A, Mackall CL, Diller L, Weiss WA. Neuroblastoma. Nat Rev Dis Primers. 2016 Nov 10;2:16078. doi: 10.1038/nrdp.2016.78. PMID: 27830764.
14. Nothdurfter D, Ploner C, Coraça-Huber DC, Wilflingseder D, Müller T, Hermann M, Hagenbuchner J, Ausserlechner MJ. 3D bioprinted, vascularized neuroblastoma tumor environment in fluidic chip devices for precision medicine drug testing. Biofabrication. 2022 Apr 12;14(3). doi: 10.1088/1758-5090/ac5fb7. PMID: 35333193.
15. Chilamakuri R, Agarwal S. Dual Targeting of PI3K and HDAC by CUDC-907 Inhibits Pediatric Neuroblastoma Growth. Cancers (Basel). 2022 Feb 20;14(4):1067. doi: 10.3390/cancers14041067. PMID: 35205815; PMCID: PMC8870466.
16. Zingales V, Torriero N, Zanella L, Fernández-Franzón M, Ruiz MJ, Esposito MR, Cimetta E. Development of an in vitro neuroblastoma 3D model and its application for sterigmatocystin-induced cytotoxicity testing. Food Chem Toxicol. 2021 Nov;157:112605. doi: 10.1016/j.fct.2021.112605. Epub 2021 Oct 9. PMID: 34634377.
17. Hall MK, Burch AP, Schwalbe RA. Functional analysis of N-acetylglucosaminyltransferase-I knockdown in 2D and 3D neuroblastoma cell cultures. PLoS One. 2021 Nov 8;16(11):e0259743. doi: 10.1371/journal.pone.0259743. PMID: 34748597; PMCID: PMC8575246.
18. Hartwig F, Köll-Weber M, Süss R. Preclinical In Vitro Studies with 3D Spheroids to Evaluate Cu(DDC)2 Containing Liposomes for the Treatment of Neuroblastoma. Pharmaceutics. 2021 Jun 17;13(6):894. doi: 10.3390/pharmaceutics13060894. PMID: 34204205; PMCID: PMC8234124.
19. Riedl A, Schlederer M, Pudelko K, Stadler M, Walter S, Unterleuthner D, Unger C, Kramer N, Hengstschläger M, Kenner L, Pfeiffer D, Krupitza G, Dolznig H. Comparison of cancer cells in 2D vs 3D culture reveals differences in AKT-mTOR-S6K signaling and drug responses. J Cell Sci. 2017 Jan 1;130(1):203-218. doi: 10.1242/jcs.188102. Epub 2016 Sep 23. PMID: 27663511.
20. Pickl M, Ries CH. Comparison of 3D and 2D tumor models reveals enhanced HER2 activation in 3D associated with an increased response to trastuzumab. Oncogene. 2009 Jan 22;28(3):461-8. doi: 10.1038/onc.2008.394. Epub 2008 Nov 3. PMID: 18978815.
21. Weigelt B, Lo AT, Park CC, Gray JW, Bissell MJ. HER2 signaling pathway activation and response of breast cancer cells to HER2-targeting agents is dependent strongly on the 3D microenvironment. Breast Cancer Res Treat. 2010 Jul;122(1):35-43. doi: 10.1007/s10549-009-0502-2. Epub 2009 Aug 22. PMID: 19701706; PMCID: PMC2935800.
22. Ekert JE, Johnson K, Strake B, Pardinas J, Jarantow S, Perkinson R, Colter DC. Three-dimensional lung tumor microenvironment modulates therapeutic compound responsiveness in vitro implication for drug development. PLoS One. 2014 Mar 17;9(3):e92248. doi: 10.1371/journal.pone.0092248. PMID: 24638075; PMCID: PMC3956916.

Research Article under drafting and to be submitted to the peer-reviewed Journal *Oncogene*

Lysosomal Cathepsin D Contrasts the Malignant Phenotype of Neuroblastoma Cells through the Proteolytic Cleavage of Oncogenic Annexin A2: Role of Chaperone-Mediated Autophagy

Introduction

Cathepsin D is a soluble aspartic endopeptidase localized in the endosomes and lysosomes of mammalian cells (Barrett, 1979). It accomplishes the degradation of extracellular proteins internalized by endocytosis or phagocytosis as well as of intracellular proteins delivered to lysosomes by autophagy (Castino *et al.,* 2003). Thanks to its intracellular functions, CD promotes protein homeostasis and, consequently, regulates cell growth. CD plays multiple roles in tumorigenesis, affecting cell proliferation, invasion, angiogenesis and apoptosis, known as hallmarks of cancer. Overexpression of the *CTSD* gene along with defective segregation in the acidic compartments lead to abnormal secretion of the precursor proCD, which can be found in the culture media and body fluids of tumor bearers (Vignon *et al.,* 1986; Isidoro *et al.,* 1995a; Isidoro *et al.,* 1995b; Reid *et al.,* 1986). The hypersecretion of proCD elicits the oncogenic activities. Cancer and stromal cells secrete huge amount of the precursor through active exocytosis or following necrosis. In the tumor microenvironment, the acid pH allows proCD to become the active "*pseudo*-CD" after a partial proteolysis, thus favoring cancer cell invasion and neo-angiogenesis (Nicotra *et al.,* 2010; Benes *et al.,* 2008). Moreover, extracellular CD acts as an autocrine and paracrine growth factor for an unknown receptor, triggering RAS/MAPK and PI3K/AKT pathway activation (Laurent-Matha *et al.,* 2005; Pranjol *et al.,* 2018). In neuroblastoma cells, secreted proCD exerts an anti-apoptotic function, promotes cell survival and contributes to doxorubicin resistance (Sagulenko *et al.,* 2008).

CD secretion increases the malignant behavior of cancer cells and simultaneously curbs intracellular functions.

In our previous findings, we have described for the first time a novel anti-proliferative role of cathepsin D in downregulating the pro-oncogenic MAPK signaling pathway in neuroblastoma cells. CD contrasts EGF-induced cancer cell growth and confers better prognosis to neuroblastoma patients (Secomandi, Salwa, *et al.,* 2022).

Lysosomal cathepsin D accomplishes bulk protein degradation and mediates the activation of hormones and their precursors as well as the inactivation of mature growth factors through extensive lysosomal proteolysis (Berg *et al.,* 1995). Besides protein degradation, CD exerts post-translational

modifications on cytosolic substrates, such as Annexin A1 (Sakaguchi *et al.,* 2007), affecting in turn cell proliferation.

The annexins belong to an evolutionary ancient and conserved family of Ca^{2+}-regulated phospholipid-binding proteins with up to 160 unique annexins in more than 65 different species (Moss and Morgan, 2004). Annexin A2 (ANXA2), a 36 kDa protein, contains a conserved segment of 70 amino acids that binds negatively charged phospholipids in a Ca^{2+}-dependent manner (Moss and Morgan, 2004). Annexin A2 NH_2-terminal domain contains a binding site for S100A10 (p11) and for tissue plasminogen activator (t-Pa); the C-terminal domain carries the binding site for F-actin (Filipenko and Waisman, 2001), heparin (Kassam *et al.,* 1997) and plasminogen (Hajjar *et al.,* 1994). The core of the protein binds to calcium and to cell membranes. Annexin A2 is involved in different biological processes including exocytosis, endocytosis, vesicle budding, lipid raft, calcium homeostasis, cytoskeleton remodeling, signal transduction, protein assembly, transcription, and mRNA transport, as well as DNA replication and repair (Gerke and Moss, 2002).

Annexin A2 was frequently overexpressed in several types of aggressive malignancies such as colorectal cancer (Yang *et al.,* 2013), breast cancer (Shetty *et al.,* 2012), lung cancer (Yao *et al.,* 2009), gastric carcinoma (Zhang Q. *et al.,* 2012), pancreatic cancer (Takano *et al.,* 2008), glioblastoma, and neuroblastoma (Wang *et al.,* 2017). In pediatric NB, high annexin A2 is closely related to increased chemotherapy cycles, drug resistance, tumor metastasis and poor overall survival. Chemoresistance observed in neuroblastoma cell lines was associated to NF-κB activation and nuclear translocation (Wang *et al.,* 2017).

The activation of growth factor receptors triggers post-translational modifications of annexin proteins which alter their function and the binding with specific interactors. In respect of annexin A2, EGFR-induced Tyr23-phosphorylation enhances the oncogenic potential of ANXA2. In fact, phosphorylated annexin A2 interacts with STAT3 increasing its transcriptional activity (Yuan *et al.,* 2017). Consistently, the abrogation (knockdown/inhibition) of ANXA2 counteracts the malignant phenotypes of cancer cells (Chen *et al.,* 2015; Chen *et al.,* 2019; Sharma, 2019; Zhang *et al.,* 2015). Therefore, annexin A2 could be considered as a second messenger for signal transduction.

Lot of evidence suggest that annexin A2 may be a promising therapeutic target for cancer treatment. However, an effective and feasible approach aimed to abrogate its pro-tumorigenic activity has not yet been developed. Hence, the identification of molecular mechanisms controlling annexin A2 activity should give the opportunity to target it downstream, preventing its oncogenic-induced effects. Whether cathepsin D and annexin A2 are mechanistically linked and how this interaction may impinge on EGF-mediated neuroblastoma growth remain to be elucidated.

In the present work, we demonstrated that cathepsin D counteracts the malignant phenotypes of NB cells through the proteolytic cleavage of oncogenic annexin A2.

Results

1. High *CTSD* expression confers better prognosis to neuroblastoma patients bearing high *ANXA2_STAT3* mRNA

We have interrogated datasets from the TCGA database to determine the clinical relevance of *CTSD* status in pediatric neuroblastoma patients highly expressing *ANXA2_STAT3* mRNA. First, we studied the effects of *ANXA2* in pediatric neuroblastoma patients and thereby its functional role was determined by performing an *in-silico* transcriptomic analysis. Many studies reported that annexin A2 was highly expressed in neuroblastoma and in others malignant tumors (Wang *et al.,* 2017; Yang *et al.,* 2013; Shetty *et al.,* 2012; Yao *et al.,* 2009; Zhang X. *et al.,* 2012; Takano *et al.,* 2008). We retrieved the RNA-seq data (mRNA expression profile) from TCGA database (TARGET, 2018) and performed a co-expression analysis to identify the top significant differentially expressed genes (DEGs) that were positively (up-regulated genes in red-dots) and negatively (down-regulated genes in blue-dots) correlated with *ANXA2* in patients' samples, as represented in the Volcano plot (Figure 1A). Then, we focused on the genes that were positively correlated. Notably, these genes are involved in various biological processes, such as wound healing, cell migration, cell motility, interleukin-signaling, MAPK, JAK/STAT3, PI3K/AKT pathways, protein import into the nucleus (Figure 1B). Then, we extended our studies towards *STAT3* expression to evaluate its relationship with *ANXA2* (Figure 1B). In fact, based on Box-plot and Scatter plot we found that *ANXA2* mRNA expression is positively correlated with *STAT3* mRNA expression (Figure 1C, D).

Our previous findings showed that patients with high expression of *CTSD* and of *EGFR* exhibit a better prognosis (Secomandi, Salwa *et al.,* 2022). Therefore, we expected that *CTSD* acts as a positive biomarker for neuroblastoma. Next, we correlated *CTSD* expression with *ANXA2* and *STAT3* to analyze their prognostic values. We grouped the cases with high and low expression, and we analyzed the prognostic value in combinatorial groups of tumors based on the respective level of mRNA (Figure 1E). Kaplan-Meier overall survival curves indicated that patients with high *CTSD*, high *ANXA2* and *STAT3* showed a better prognosis, while the groups either with low *CTSD*, low *ANXA2* and high *STAT3* or high *ANXA2* and low *STAT3* exhibited worse prognosis (Figure 1E, F). These data suggested that *ANXA2* and *STAT3* overexpressing patients manifested a positive clinical outcome only when *CTSD* was high.

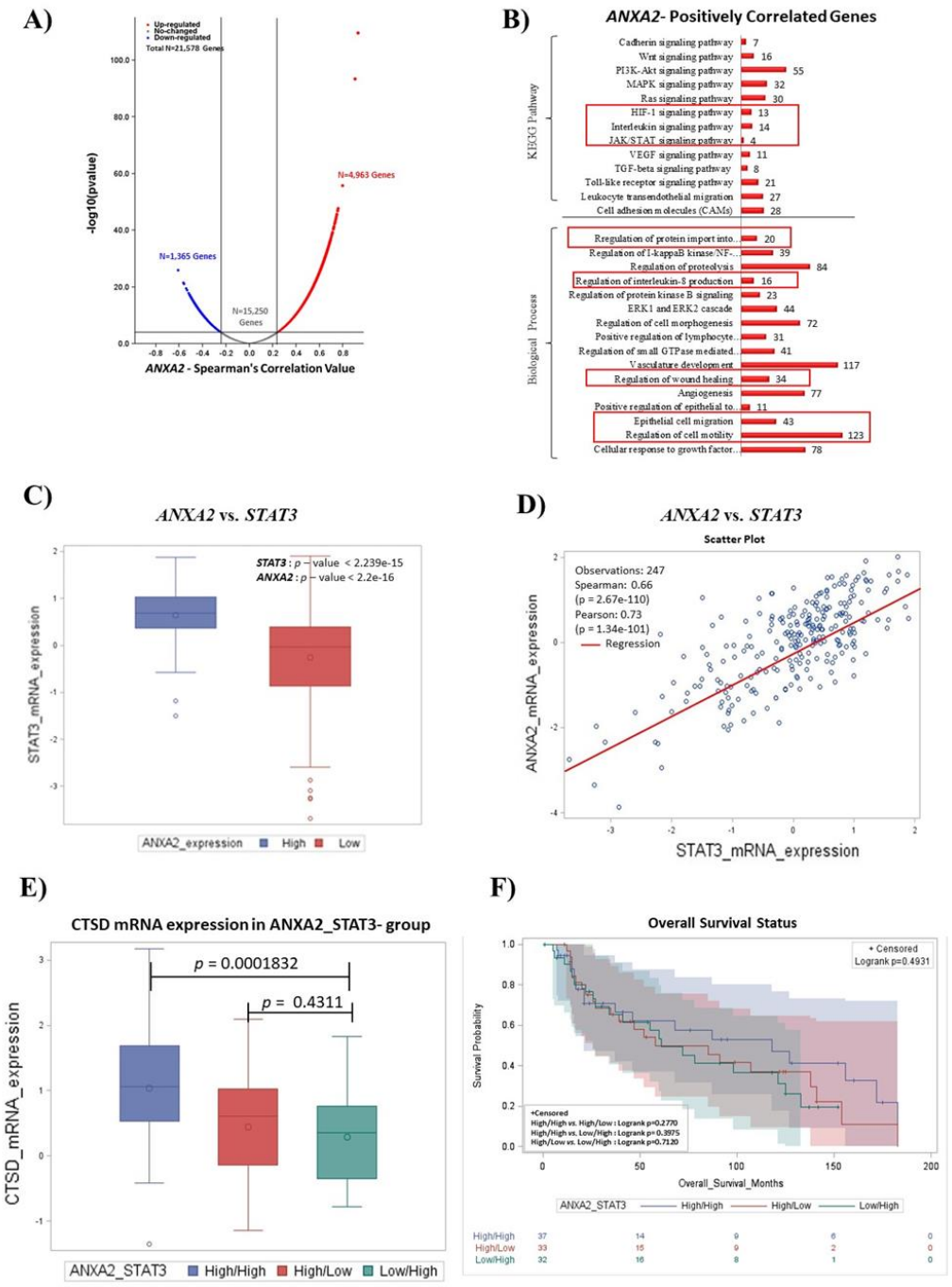

Figure 1. Neuroblastoma patients bearing high *CTSD* transcript level and high *ANXA2_STAT3* show a better prognosis.

2. Cathepsin D overexpression reduces STAT3 phosphorylation, nuclear translocation, and interaction with annexin A2

We found that patients with high *CTSD* and *ANXA2_STAT3* transcript levels showed a better prognosis and longer overall survival than those with high *ANXA2_STAT3* but low *CTSD*. These preliminary data provided the rationale to speculate that cathepsin D could be involved in annexin

A2-induced cell proliferation. Therefore, we tested our hypothesis in engineered neuroblastoma cells in which cathepsin D was overexpressed or knocked-down (Secomandi, Salwa *et al.,* 2022). We found that in the absence of cathepsin D, EGF increased the phosphorylation of the transcription factor STAT3 after 24 hours of treatment, as shown in Figure 2A. As confirmation of enhanced transcriptional activity, cyclin D1 a target gene of STAT3, was upregulated in CD-knockdown (KD-CD) cells upon EGF exposure (Figure 2B). Noteworthy, the immunofluorescence double staining highlighted an increased colocalization between annexin A2 (red) and phospho-STAT3 (green) and high level of nuclear STAT3 (Figure 2C) in KD-CD cells. Conversely, in CD-overexpressing cells we observed a reduction of STAT3 phosphorylation and nuclear translocation, even in the presence of EGF. ANXA2-STAT3 axis drives malignant phenotypic changes and mesenchymal transition in a variety of solid tumors (Matsumoto *et al.,* 2020; Wang *et al.,* 2015; Xiu *et al.,* 2016). The differential modulation among the clones let to hypothesize that cathepsin D may affect the overall amount of annexin A2 and its interaction with STAT3. To test our hypothesis, we analyzed protein content in SH-SY5Y clones through western blotting. We found a markedly reduction of annexin A2 level in Over CD, both in EGF-stimulated cells and untreated control, compared to that of KD-CD (Figure 2D). Cathepsin D overexpression not only downregulated the overall amount of annexin A2, but also impaired its association with phospho-STAT3, as indicated by the co-immunoprecipitation (Figure 2E). This effect was markedly evident upon 24 hours of EGF treatment.

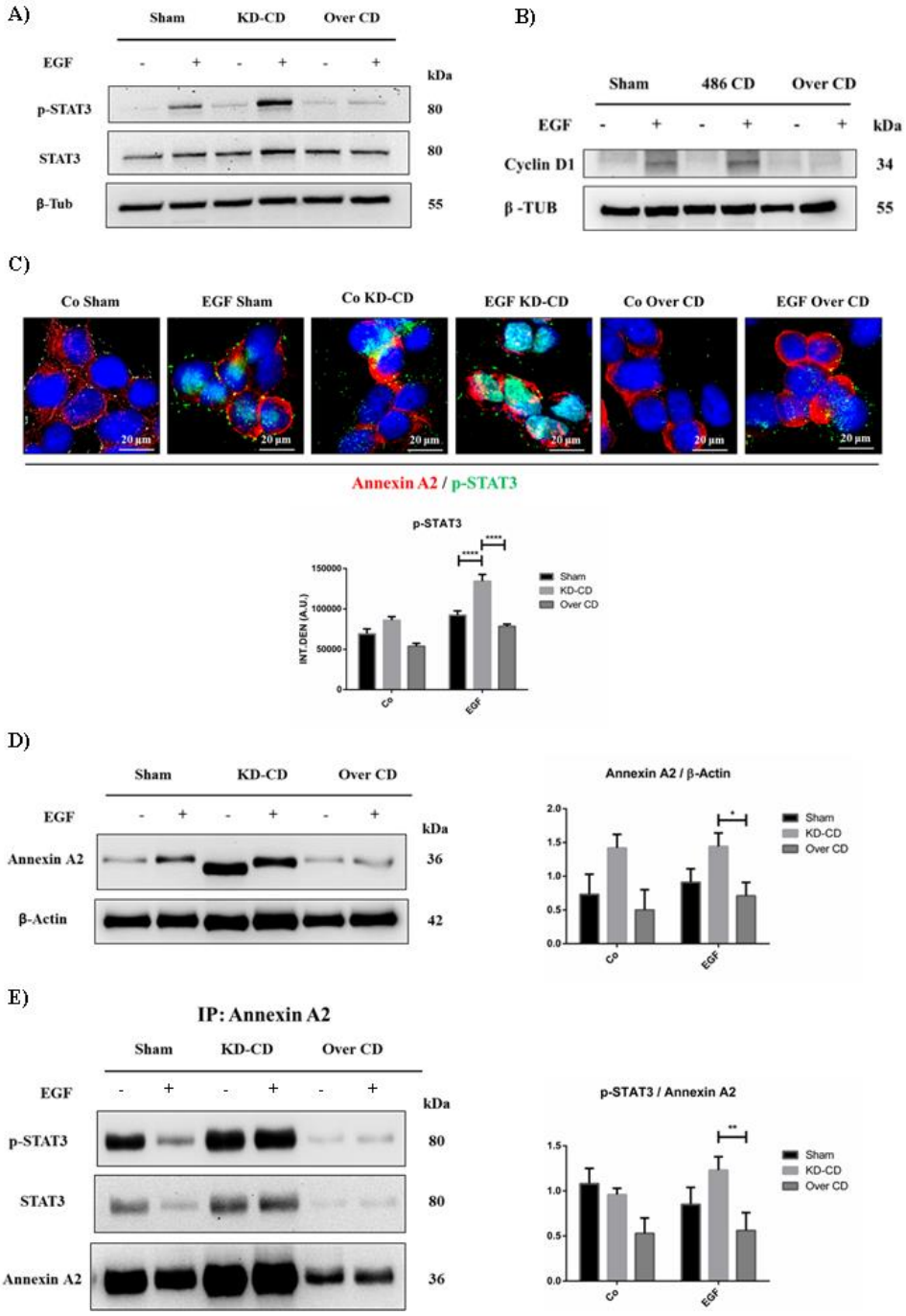

Figure 2. Cathepsin D overexpression reduces STAT3 phosphorylation and the binding with annexin A2.

3. Cathepsin D overexpression contrasts EGF-induced NB cell migration and invasion

The annexin A2-STAT3 axis is well known to enhance the malignant features of cancer cells. Thus, we analyzed the migratory and invasive potential of transfectant clones. We performed a scratch wound healing assay and we monitored cell migration through the phase-contrast microscope (Figure 3A). Previous results showed a reduction of phosphorylated STAT3 and annexin A2, and of protein-protein interaction in Over CD. Coherently, the migration rate of those cells after 96 hours was 3-

times less compared to KD-CD (Figure 3B). The rate of healing was calculated based on the distance between the two fronts of the wound using the ImageJ software (Figure 3B). KD-CD were the fastest to heal the wound, evident from 24 h incubation onward. In the presence of EGF almost 99% of the wound was healed by 96 hours, whereas the Over CD clone was rather insensitive to EGF stimulation, and the migration rate was approximately 37% in treated condition. Noteworthy, the absence of cathepsin D strongly accelerated the healing process, conversely its overexpression slowed down cell migration. Subsequently, KD-CD and Over CD clones were seeded in equal proportions (50% + 50%) on sterile coverslips, let grow to nearly confluence and subjected to scratch-wounding (Figure 4A, B). Cells were treated with EGF for 48 hours. Coverslips were fixed and processed for immunofluorescence staining of CD (marker for Over CD population) and of TWIST1, a transcription factor which promotes cell migration and acts as an oncogene in several cancers, including neuroblastoma (Martin *et al.,* 2005; Puisieux *et al.,* 2006). The Figure 4A showed high levels of TWIST1 in cells at the migration front upon EGF stimulation: these cells did not express cathepsin D, indicator of the KD-CD population that are characterized by the greatest migratory ability. Conversely, Over CD showed reduced motility, remained far from the wound, and expressed low level of TWIST1 (Figure 4B).

The transwell migration assay (Figure 4C) essentially confirmed the above observations, supporting the fact that EGF much more stimulated the motility of CD knockdown cells, (that are more sensitive to EGF stimulus), compared to that of Over CD when the two populations are co-cultured.

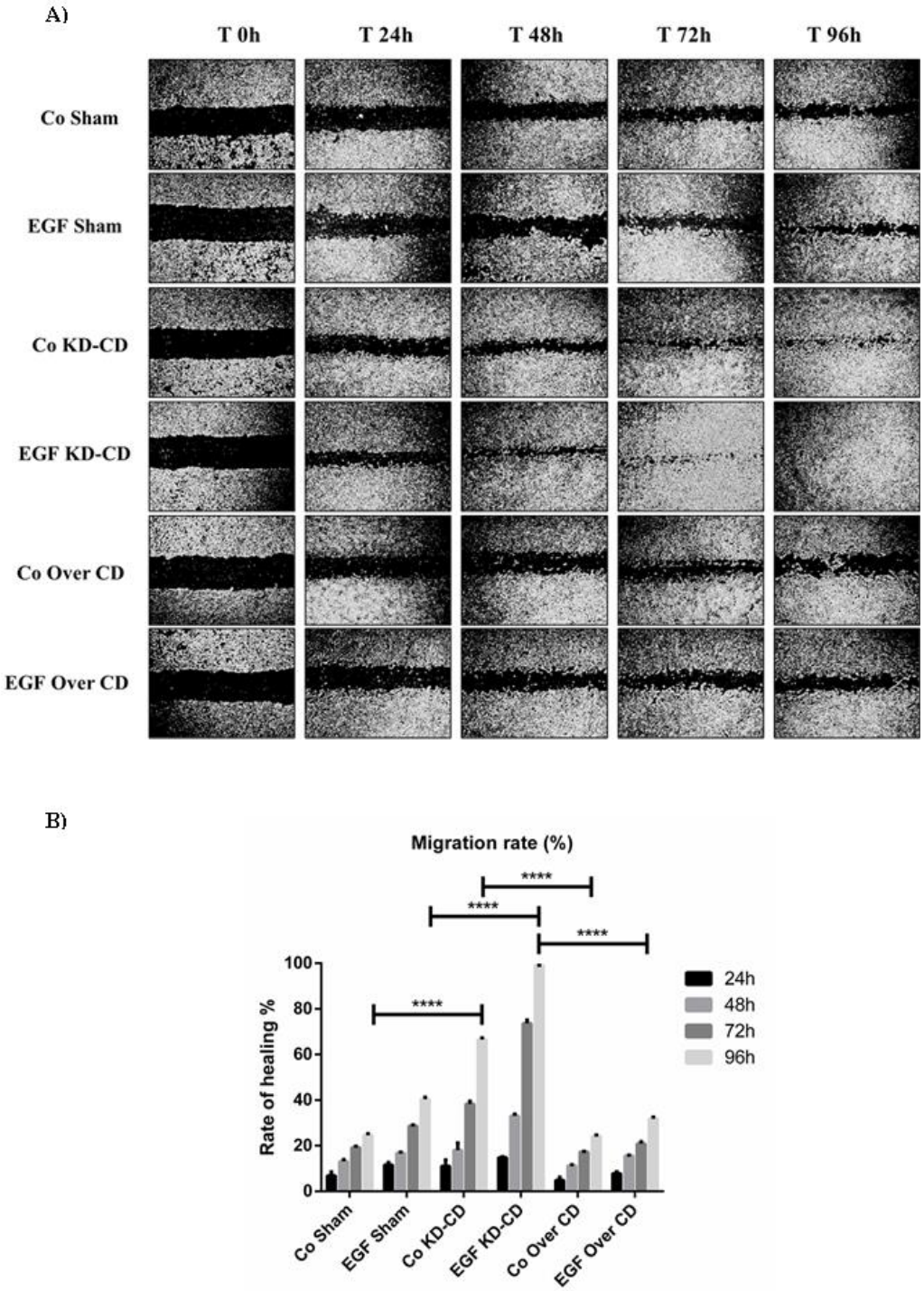

Figure 3. Cathepsin D overexpression slows down EGF-induced cell migration whereas CD knockdown increases cell motility.

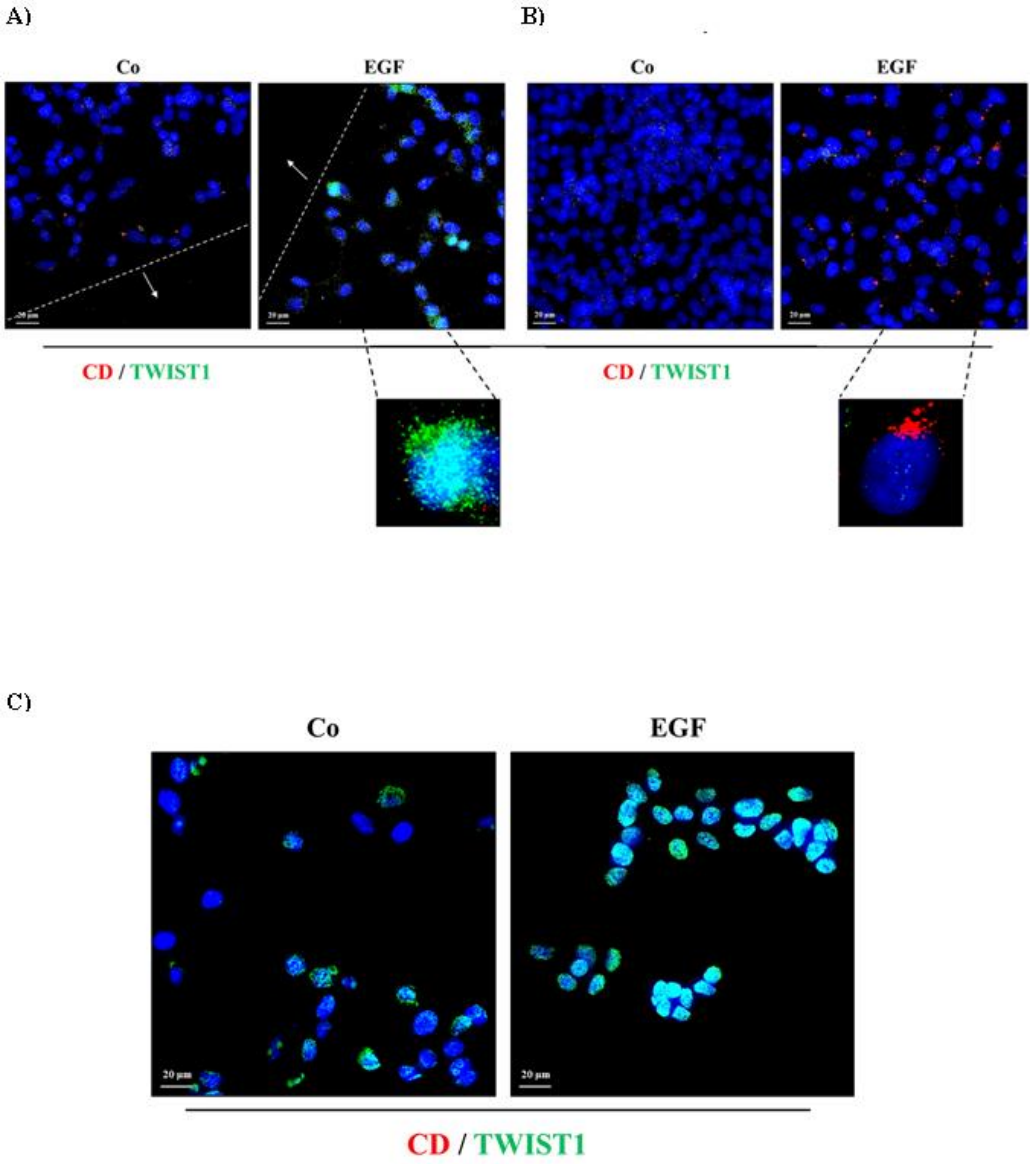

Figure 4. CD knocked-down cells show the highest invasive potential when stimulated with EGF in coculture with Over CD.

4. HSC70 competes with STAT3 for the binding with annexin A2

The Heat Shock Cognate protein 70 (HSC70) is the most abundant molecular chaperone activated by various cellular stresses, including starvation (Morimoto, 1998). Furthermore, HSC70 actively controls cell growth and survival by regulating the protein turnover and the catalytic activity of binding proteins (Frydman, 2001; Hartl and Hayer-Hartl, 2002). The HSC70-mediated recognition of cytosolic substrates occurs via the pentapeptide KFERQ that conduces proteins to the lysosomal membrane surface (Chiang *et al.,* 1989). The core domain of annexin A2 contains a KFERQ motif. It is well known that annexin A2 acts as a scaffold for signaling proteins, such as STAT3, and controls cell proliferation, epithelial-to-mesenchymal transition (EMT), invasion and migration (Wang *et al.,*

2015; Matsumoto *et al.,* 2020; Wang *et al.,* 2015; Xiu *et al.,* 2016). Increased HSC70 levels impaired the binding of annexin A2 with SHP2, a phosphatase that plays a pivotal role in the biological responses to growth factors, inhibiting EGF-induced cell proliferation (Yoo and Hayman, 2007). Since HSC70 acts as a molecular competitor with signaling proteins, we hypothesized that the chaperone may challenge annexin A2-STAT3 interaction, competing with STAT3 for annexin binding. Thus, we performed an immunofluorescence double staining for annexin A2 (marked in green) and HSC70 (in red) on SH-SY5Y clones seeded on sterile coverslips (Figure 5A). The short-term stimulation with EGF (45 minutes) enhanced their colocalization, as indicated by the increased yellow signal compared to untreated control, in all the clones. Annexin A2 and HSC70 interacted each other, regardless the presence of cathepsin D. The absence of nutrients (EBSS condition) was also capable of inducing HSC70/annexin A2 binding, yet to a lesser extent. The hypothesis that HSC70 may compete with STAT3 for binding was tested through the co-immunoprecipitation assay (Figure 5B). As confirmation, annexin A2 (extracted from cell homogenates with a specific primary antibody) interacted both with phosphorylated STAT3 and HSC70, in all the three clones. In control condition, any differences were detected between CD knockdown or CD overexpressing cells. The short-term stimulation with EGF slightly increased annexin A2/phospho-STAT3 interaction in KD-CD compared to that of Over CD. Next, me measured the protein content through western blotting and we found an increased HSC70 expression after EBSS-treatment (Figure 5C). EGF triggered tyrosine-23 (Tyr23) phosphorylation of annexin A2 in Sham, KD-CD and Over CD clones. In EBSS condition we detected two distinct bands of ANXA2 only in CD-expressing cells. Intriguingly, in KD-CD clone no fragments were observed.

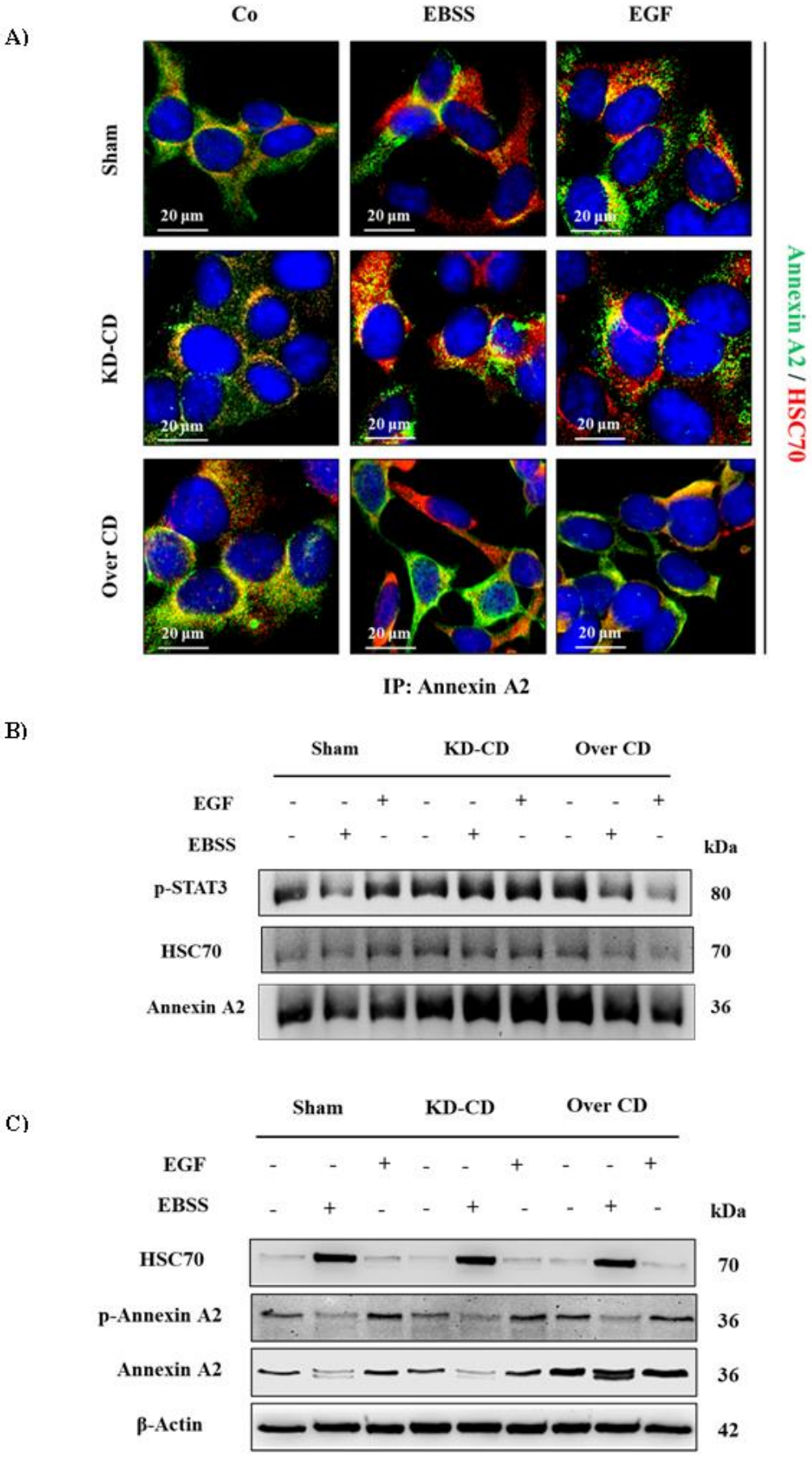

Figure 5. Assessment of annexin A2/HSC70 interaction in SH-SY5Y clones.

5. EGF triggers the lysosomal internalization of annexin A2 through chaperone-mediated autophagy

We know from the literature that HSC70 regulates the degradation of intracellular proteins and regulates cell homeostasis (Agarraberes *et al.,* 1997; Yoo and Hayman, 2006; Yoo and Hayman, 2007). Upon selective recognition, HSC70 drives substrates to the lysosomal membrane surface and the Lysosome-Associated Membrane Protein type 2A (LAMP2A) mediates their internalization. This type of selective lysosomal degradation is called chaperone-mediated autophagy (Mizushima and Komatsu, 2011). After inducing ANXA2 phosphorylation and interaction with HSC70, EGF triggered its translocation into the lysosomes, as indicated by the increased colocalization between LAMP2 and phospho-annexin A2 (Figure 6A). Therefore, we wondered whether annexin A2 and cathepsin D may interact within the lysosomes. To test this hypothesis, we performed an immunofluorescence for cathepsin D (red channel) and annexin A2 (green channel) on fixed Sham cells. The short-term stimulation with EGF (45 minutes) markedly increased their colocalization, which was barely detectable in EBSS condition (Figure 6B). The co-immunoprecipitation (Figure 6C) confirmed the above findings and demonstrated that annexin A2 is a substrate of lysosomal cathepsin D. To be noted, the western blot previously performed highlighted the presence of a smaller fragment of annexin A2 in CD-expressing cells (Figure 5C). At this point, our aims were to explore in detail the significance of cathepsin D-annexin A2 interaction and to assess whether a post-translational modification could affect any cellular phenotypes.

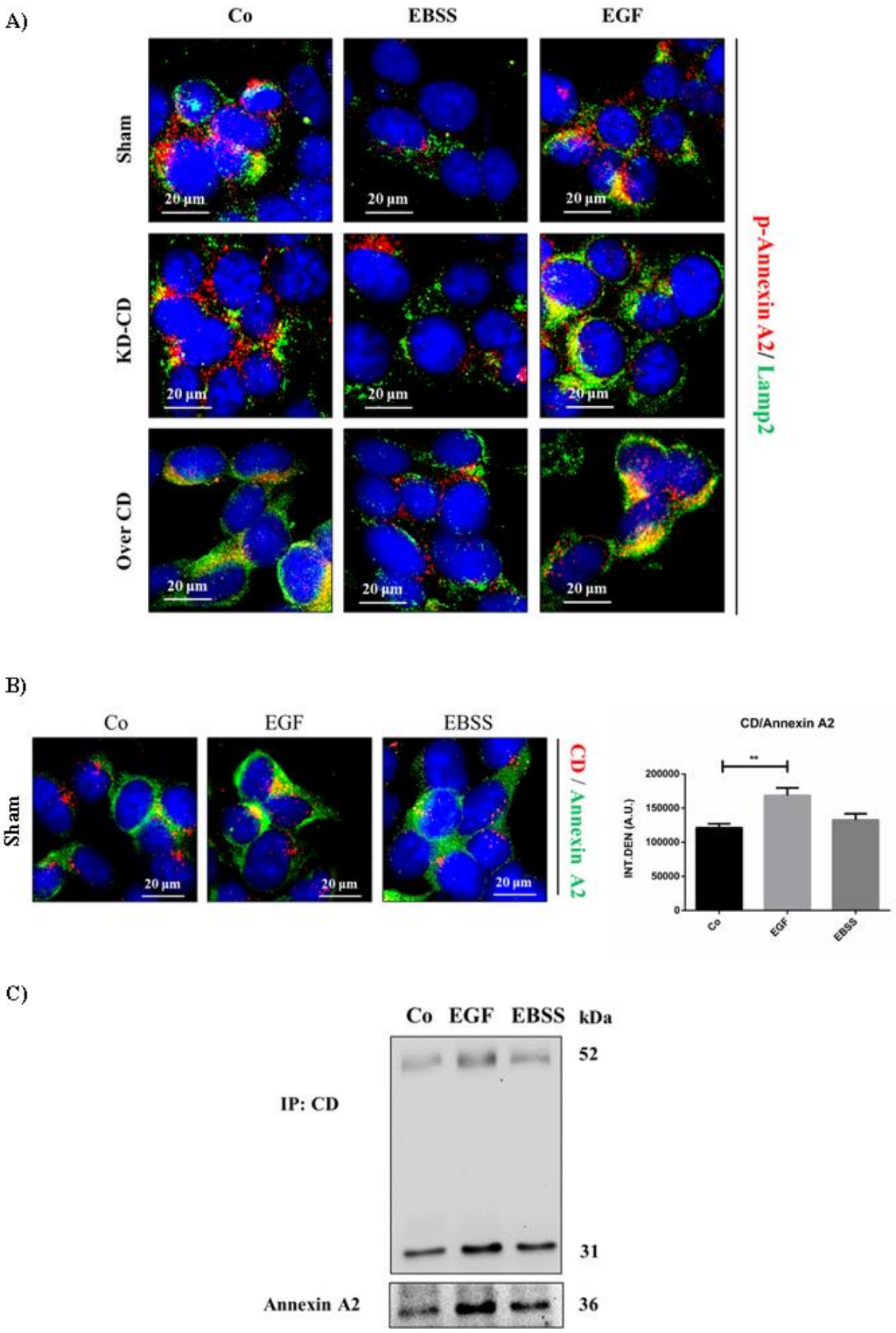

6. Annexin A2 interacts with cathepsin D after Lamp2-mediated lysosomal internalization.

6. Cathepsin D mediates proteolytic cleavages of annexin A2 generating smaller peptides

We sought to reproduce *in vitro* CD/ANXA2 binding and to test the effects deriving from this interaction. Firstly, we measured CD protein content in Sham treated with Pepstatin A and in KD-CD incubated with EGF and EBSS. As expected, in knockdown cells CD was barely detectable (Figure 7A). In the same experimental conditions, we detected the full-length form of annexin A2 (Figure 7B). Then, we performed the *in vitro* protease assay (Figure 7C, D), in which immunoprecipitated cathepsin D (extracted from Over CD homogenates) was added to Sham and KD-CD-derived samples. An incubation of 3 hours at 37 °C was carried out and then samples were processed for western blot analysis. In the panel 7C, we showed the addition of exogenous cathepsin D in Sham and KD-CD. Interestingly, in these conditions, different smaller peptides besides the full-length form of annexin A2 were clearly detectable, below 36 kDa (Figure 7D). The fragments were generated by the proteolytic activity of cathepsin D. Membranes were further incubated with an anti-annexin antibody recognizing the first 49 amino acids at the N-terminal of the sequence and the same bands were detected.

Data previously reported have identified a reduction of nuclear phospho-STAT3 (Figure 2A, B) and a limited binding affinity for annexin A2 in Over CD cells (Figure 2D). These results let us to hypothesize that the proteolytic cleavage may generate peptides unable to bind STAT3 and to drive its nuclear translocation.

Our results identified for the first time a post-translational modification of annexin A2 as a direct substrate of lysosomal cathepsin D. The proteolytic cleavage of ANXA2 may hamper its oncogenic activities and counteract the malignant phenotypes of neuroblastoma cells.

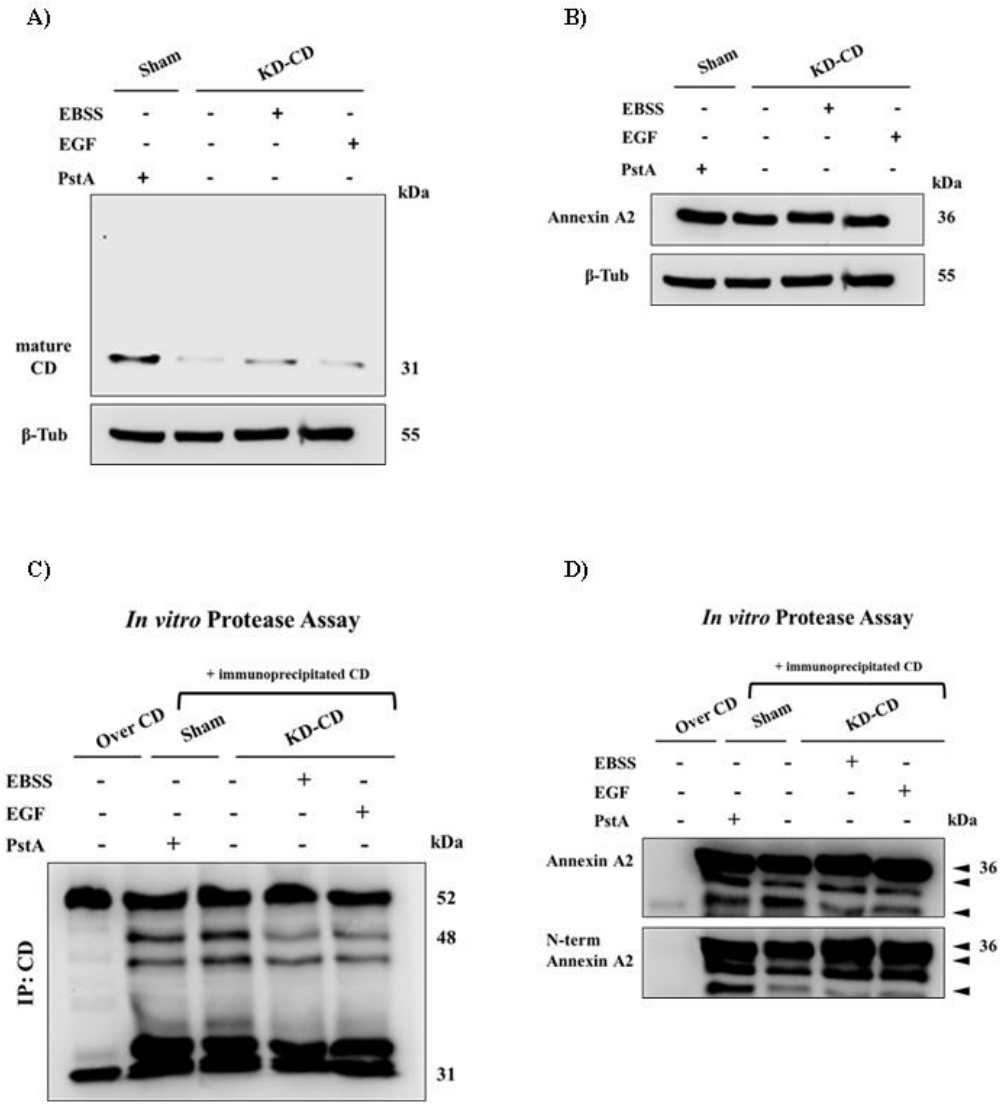

Figure 7. The proteolytic activity of cathepsin D generates annexin A2-derived fragments.

7. siRNA-mediated silencing of ANXA2 inhibits the migration and proliferation of CD-knockdown cells

To prove that the proteolytic cleavage of annexin A2 hampers its oncogenic activities, and consistent with this interpretation Over CD cells showed in fact reduced cell proliferation, migration and invasion, we expect to observe the same behavior in KD-CD cells silenced for ANXA2. Thus, we proceeded by transfecting the CD knocked-down clone with siANXA2. As confirmation, the siRNA transfection strongly reduced NB cell migration and this effect was evident from 24 hours onward (Figure 8A). siANXA2 silencing greatly slowed down the healing of the wound even in the presence of EGF, in fact the 80% of the heal was still open at 96 hours. In control condition (Co-Duplex), the migration rate was approximately 80% upon 96 h of EGF stimulation. The efficiency of siRNA transfection was shown in Figure 8B. Knockdown of ANXA2 significantly suppressed the colony-forming ability of KD-CD cells, a reduction of 2.1 times was observed in EGF-treated condition (Figure 8C). Conversely, the normal expression of endogenous annexin A2 (which remained unprocessed because of the absence of CD) enhanced cell proliferation and colony formation.

Our previous findings demonstrated that high cathepsin D inhibits MAPK signaling activation and contrasts EGF-induced neuroblastoma cell growth (Secomandi, Salwa *et al.,* 2022). Here, we described a molecular mechanism through which CD exerts an anti-proliferative activity.

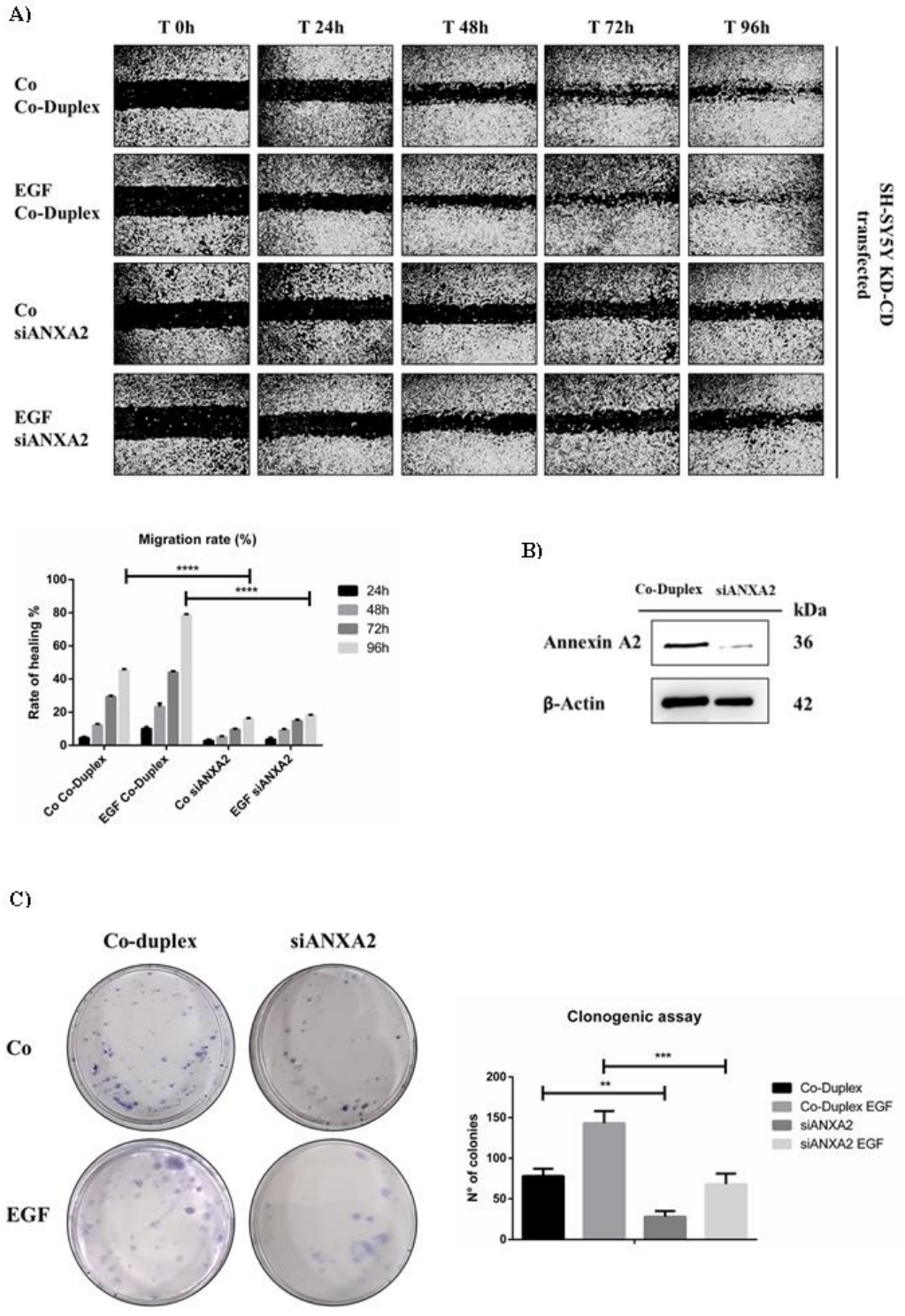

Figure 8. Knockdown of ANXA2 suppresses KD-CD cell migration and colony formation.

Discussion

Annexin A2 is a calcium-dependent phospholipid-binding protein involved in various cellular processes, including cell proliferation, adhesion, migration, invasion, and angiogenesis (Gerke and Moss, 2002). Overexpression of ANXA2 was observed in many tumor types and it was correlated to cancer progression and poor prognosis for patients (Zhang X. *et al.,* 2012; Lokman *et al.,* 2011). In pathological conditions the molecular mechanisms controlling its functions and localization could be dysregulated.

In the present study, we described for the first time a post-translational modification of annexin A2 which inhibited its oncogenic activities. The lysosomal enzyme cathepsin D exerted proteolytic cleavages within ANXA2 amino acid sequence, releasing peptides with reduced binding affinity for STAT3.

Cathepsin D is a soluble aspartic endopeptidase resident within the acidic endosomal-lysosomal compartments of mammalian cells. CD mediates the degradation of extracellular proteins as well as intracellular molecules delivered to lysosomes by autophagy (Castino *et al.,* 2003). This function is associated to the maintenance of cellular homeostasis and, consequently, cell growth control (Lockwood and Shier, 1977;). CD overexpression along with defective segregation in the acidic compartments induce an aberrant secretion of the precursor proCD (Isidoro *et al.,* 1995c), event associated to increased tumor size, grading and chemoresistance in a variety of malignancies (Cunat *et al.,* 2004; Leto *et al.,* 2004). The extracellular secretion of proCD elicits oncogenic activities missing the intracellular functions. Our previous findings demonstrated that high cathepsin D exerts anti-proliferative effects on neuroblastoma cells, inhibiting the activation of MAPK signaling in response to EGF (Secomandi, Salwa, *et al.,* 2022). Here, we described how CD hampers the oncogenic activity of annexin A2, contrasting the malignant behavior of NB cells. The HSC70-mediated lysosomal internalization of full-length annexin, through chaperone-mediated autophagy, reduced the pool of free protein able to interact with STAT3 and drive its nuclear translocation. Hence, the importance of the proteolytic cleavage, which altered annexin's structure hampering its oncogenic potential. In fact, Over CD showed reduced growth, migratory and invasive potential compared to CD-knockdown clone. The present study described a novel tumor-suppressive role of lysosomal cathepsin D. Getting insight into the molecular mechanisms regulating cell growth will be helpful to identify new targets and to stratify patients based on CD expression. The employment of stimulators of cathepsin D synthesis and activity could benefit neuroblastoma prognosis.

Chapter 5

Discussion and Conclusions

Cathepsin D is a soluble aspartic endopeptidase resident in acidic cellular compartments, where it accomplishes the degradation of extra- and intra-cellular proteins, delivered to lysosome by autophagy, as well as the proteolytic modification of substrates (Castino *et al.,* 2003). These functions are associated with protein homeostasis and affect cellular processes, including cell growth (Isidoro *et al.,* 1995c; Lockwood and Shier *et al.,* 1977). The defective maturation, localization and function of cathepsin D influence its activities and cell behavior. It is well established that the abnormal secretion of the precursor proCD, that can be found in culture media and body fluids of tumor bearers, elicits oncogenic activities (Nicotra *et al.,* 2010; Laurent-Matha *et al.,* 2005; Pranjol *et al.,* 2018; Benes *et al.,* 2008; Jha *et al.,* 2019; Sagulenko *et al.,* 2008). proCD may undergo autoactivation in the acidic tumor microenvironment where it degrades the extracellular matrix, releasing active growth factors and promoting cell growth and angiogenesis (Nicotra *et al.,* 2010; Jha *et al.,* 2019). Therefore, it is crucial that cathepsin D is correctly segregated to perform its proper functions.

First, we reported that patients bearing a neuroblastoma that expresses high level of CD benefit from a better prognosis and longer overall survival. On the opposite, individuals with high *EGFR* and *CTSD* manifested the worst clinical outcome. Accordingly, two-thirds of patients at INSS Stage 4 present with a low level of *CTSD* expression. This indicates that neuroblastomas with CD deficiency grow and progress faster than neuroblastomas highly expressing CD (Secomandi, Salwa *et al.,* 2022).

When cathepsin D is retained intracellularly can control cell cycle, downregulate EGFR/MAPK signaling and inhibit NB cell proliferation. In this context, it is of relevance that SH-SY5Y overexpressing CD showed high p21 and were less responsive to EGF stimulation, whereas SH-SY5Y knocked-down for CD were basally more proliferative and more responsive to EGF stimulation. Notably, Sham-transfected SH-SY5Y cells, which retain the ability to modify protein level, responded to EGF by increasing cell proliferation, along with downregulating the level of endogenous CD. To our knowledge this is the first report showing such an effect of EGF on CD expression in cancer cells.

The conventional 2D cellular model often does not adequately reproduce the dynamic conditions and relations present within the tumor mass. Cancer shows a wide genetic heterogeneity and during tumor evolution different clones compete for survival and overtake each-other. Multicellular 3D models much closely resemble the *in vivo* tumor structure (Pozzi *et al.,* 2021) and neurospheres may mimic clusters of metastatic cells which disseminate in secondary sites. Important molecular and phenotypic

differences between cancer cells cultured as 2D monolayers, or in suspension as 3D spheroids, have been reported. These alterations result from changing in signaling cascades, metabolic processes and different access to nutrients and growth factors (Zingales *et al.,* 2021; Hall *et al.,* 2021; Hartwig *et al.,* 2021; Riedl *et al.,* 2017; Pickl and Ries, 2009; Weigelt *et al.,* 2010; Ekert *et al.,* 2014).

In the second part of the work, we investigated whether and how cathepsin D plays a role in the metastatic process and to recapitulate *in vitro* the steps of metastatic spreading, we switched the type of culture system. We employed neuroblastoma SH-SY5Y transgenic clones engineered for overexpressing or silencing CD expression, cultivated alone and in combination for mimicking tumor heterogeneity. Interestingly, we found that high levels of cathepsin D favor the survival of floating spheroids. However, when these neurospheres were switched to grow onto solid substrate, mimicking the formation of a secondary metastasis, CD downregulation is necessary to allow adhesion and proliferation in anchorage-dependent condition. In fact, KD-CD clone grew faster, forming wide secondary colonies and overtook the Over CD clone in mixed cocultures. To be noted, Sham transgenic clone reduced the intracellular level of CD when grown in adhesion, further supporting the fact that cathepsin D can be differentially regulated during the reversible transition for adherent-to-suspended-to-adherent growth of metastatic clones.

Lastly, we described a molecular mechanism through which CD exerts an anti-proliferative activity by processing oncogenic annexin A2. Accumulating evidence suggest that interactions between annexin A2 and bindings proteins, such as STAT3, play an important role in cancer progression and metastasis. Here, we found that the proteolytic cleavage of annexin A2, exerted by lysosomal cathepsin D, reduced the binding affinity of ANXA2 for the transcription factor STAT3. In accordance, cell proliferation, migration and invasion were counteracted by CD overexpression, which reduced the pool of free full-length annexin A2, even when cells were stimulated to grow by EGF. As confirmation, siRNA-mediated silencing of ANXA2 in CD knocked-down cells, rescued the phenotypes.

Collectively, our results may have a translational relevance and we propose cathepsin D as a possible biomarker for the stratification of neuroblastoma patients in view of personalized medicine. In this respect, testing the effects of cathepsin D stimulators in CD low-expressing tumors could represent a novel therapeutic strategy to ameliorate patients' outcome. These patients could in fact benefit from a therapy combining EGFR inhibitors with a drug inducing the expression and/or stimulating the activity of cathepsin D, such as the nutraceutical resveratrol (Trincheri *et al.,* 2007).
In conclusion, we have uncovered novel anti-proliferative roles of intracellular cathepsin D that mihgt be exploited to ameliorate neuroblastoma treatment, and likely other neoplasms.

Chapter 6

References

1. Agarraberes FA, Terlecky SR, Dice JF. An intralysosomal hsp70 is required for a selective pathway of lysosomal protein degradation. J Cell Biol. 1997 May 19;137(4):825-34. doi: 10.1083/jcb.137.4.825. PMID: 9151685; PMCID: PMC2139836.
2. Attiyeh EF, London WB, Mossé YP, Wang Q, Winter C, Khazi D, McGrady PW, Seeger RC, Look AT, Shimada H, Brodeur GM, Cohn SL, Matthay KK, Maris JM; Children's Oncology Group. Chromosome 1p and 11q deletions and outcome in neuroblastoma. N Engl J Med. 2005 Nov 24;353(21):2243-53. doi: 10.1056/NEJMoa052399. PMID: 16306521.
3. Authier F, Métioui M, Bell AW, Mort JS. Negative regulation of epidermal growth factor signaling by selective proteolytic mechanisms in the endosome mediated by cathepsin B. J Biol Chem. 1999 Nov 19;274(47):33723-31. doi: 10.1074/jbc.274.47.33723. PMID: 10559264.
4. Azizkhan RG, Shaw A, Chandler JG. Surgical complications of neuroblastoma resection. Surgery. 1985 May;97(5):514-7. PMID: 3992477.
5. Baldwin ET, Bhat TN, Gulnik S, Hosur MV, Sowder RC 2nd, Cachau RE, Collins J, Silva AM, Erickson JW. Crystal structures of native and inhibited forms of human cathepsin D: implications for lysosomal targeting and drug design. Proc Natl Acad Sci U S A. 1993 Jul 15;90(14):6796-800.
6. Barr EK, Applebaum MA. Genetic Predisposition to Neuroblastoma. Children (Basel). 2018 Aug 31;5(9):119. doi: 10.3390/children5090119. PMID: 30200332; PMCID: PMC6162470.
7. Barrett AJ. Cathepsin D: the lysosomal aspartic proteinase. Ciba Found Symp. 1979;(75):37-50. doi:10.1002/9780470720585.ch3.
8. Beckwith JB, Perrin EV. In Situ Neuroblastomas: A contribution to the natural history of neural crest tumors. Am J Pathol. 1963 Dec;43(6):1089-104. PMID: 14099453; PMCID: Pmc1949785.
9. Benes P, Vetvicka V, Fusek M. Cathepsin D--many functions of one aspartic protease. Crit Rev Oncol Hematol. 2008 Oct;68(1):12-28. doi: 10.1016/j.critrevonc.2008.02.008. Epub 2008 Apr 8. PMID: 18396408; PMCID: PMC2635020.
10. Berg T, Gjøen T, Bakke O. Physiological functions of endosomal proteolysis. Biochem J. 1995 Apr 15;307 (Pt 2)(Pt 2):313-26. doi: 10.1042/bj3070313. PMID: 7733863; PMCID: PMC1136650.
11. Braig F, Kriegs M, Voigtlaender M, Habel B, Grob T, Biskup K, Blanchard V, Sack M, Thalhammer A, Ben Batalla I, Braren I, Laban S, Danielczyk A, Goletz S, Jakubowicz E, Märkl B, Trepel M, Knecht R, Riecken K, Fehse B, Loges S, Bokemeyer C, Binder M. Cetuximab Resistance in Head and Neck Cancer Is Mediated by EGFR-K521 Polymorphism. Cancer Res. 2017 Mar 1;77(5):1188-1199. doi: 10.1158/0008-5472.CAN-16-0754. Epub 2016 Dec 28. PMID: 28031227.
12. Brodeur GM, Hogarty MD, Mosse YP, et al. Neuroblastoma. In: Pizzo PA, Poplack DG, editors. Principles and practice of pediatric oncology. 6th edition. Philadelphia: Lippincott; 2011. p. 886–922.
13. Brodeur GM, Pritchard J, Berthold F, Carlsen NL, Castel V, Castelberry RP, De Bernardi B, Evans AE, Favrot M, Hedborg F, et al. Revisions of the international criteria for

neuroblastoma diagnosis, staging, and response to treatment. J Clin Oncol. 1993 Aug;11(8):1466-77. doi: 10.1200/JCO.1993.11.8.1466. PMID: 8336186.
14. Brodeur GM, Seeger RC, Schwab M, Varmus HE, Bishop JM. Amplification of N-myc in untreated human neuroblastomas correlates with advanced disease stage. Science. 1984 Jun 8;224(4653):1121-4. doi: 10.1126/science.6719137. PMID: 6719137.
15. Brodeur GM. Neuroblastoma: biological insights into a clinical enigma. Nat Rev Cancer. 2003 Mar;3(3):203-16. doi: 10.1038/nrc1014. PMID: 12612655.
16. Burkhardt JK, Hester S, Lapham CK, Argon Y. The lytic granules of natural killer cells are dual function organelles combining secretory and pre-lysosomal compartments. J Cell Biol. 1990 Dec;111(6 Pt 1):2327-40. PubMed PMID: 2277062; PubMed Central PMCID: PMC2116378.
17. Canuel M, Korkidakis A, Konnyu K, Morales CR. Sortilin mediates the lysosomal targeting of cathepsins D and H. Biochem Biophys Res Commun. 2008 Aug 22;373(2):292-7. doi: 10.1016/j.bbrc.2008.06.021.
18. Castino R, Bellio N, Nicotra G, Follo C, Trincheri NF, Isidoro C. Cathepsin D-Bax death pathway in oxidative stressed neuroblastoma cells. Free Radic Biol Med. 2007;42(9):1305–1316. doi: 10.1016/j.freeradbiomed. 2006.12.030.
19. Castino R, Démoz M, Isidoro C. Destination 'lysosome': a target organelle for tumour cell killing? J Mol Recognit. 2003 Sep-622 Oct;16(5):337-48. doi: 10.1002/jmr.643. PMID: 14523947.
20. Castino R, Peracchio C, Salini A, Nicotra G, Trincheri NF, Démoz M, Valente G, Isidoro C. Chemotherapy drug response in ovarian cancer cells strictly depends on a cathepsin D-Bax activation loop. J Cell Mol Med. 2009 Jun;13(6):1096-109. doi: 10.1111/j.1582-4934.2008.00435.x.Epub 2008 Jul 24.
21. Castino R. Isidoro C. (2008). The transport of soluble lysosomal hydrolases from Golgi complex to lysosomes. In The Golgi Apparatus, A. a. P. Mironov, M, ed. (SpringerWienNewYork), pp. 402-413.
22. Cavaillès V, Augereau P, Rochefort H. Cathepsin D gene is controlled by a mixed promoter, and estrogens stimulate only TATA-dependent transcription in breast cancer cells. Proc Natl Acad Sci U S A. 1993 Jan 1;90(1):203-7. PubMed PMID: 8419924; PubMed Central PMCID: PMC45628.
23. Chen CY, Lin YS, Chen CL, Chao PZ, Chiou JF, Kuo CC, Lee FP, Lin YF, Sung YH, Lin YT, Li CF, Chen YJ, Chen CH. Targeting annexin A2 reduces tumorigenesis and therapeutic resistance of nasopharyngeal carcinoma. Oncotarget. 2015 Sep 29;6(29):26946-59. doi: 10.18632/oncotarget.4521. PMID: 26196246; PMCID: PMC4694965.
24. Chen L, Lin L, Xian N, Zheng Z. Annexin A2 regulates glioma cell proliferation through the STAT3-cyclin D1 pathway. Oncol Rep. 2019 Jul;42(1):399-413. doi: 10.3892/or.2019.7155. Epub 2019 May 9. PMID: 31115554.
25. Chiang HL, Terlecky SR, Plant CP, Dice JF. A role for a 70-kilodalton heat shock protein in lysosomal degradation of intracellular proteins. Science. 1989;246(4928):382-385. doi:10.1126/science.2799391.
26. Colon NC, Chung DH. Neuroblastoma. Adv Pediatr. 2011;58(1):297-311. doi: 10.1016/j.yapd.2011.03.011. PMID: 21736987; PMCID: PMC3668791.

27. Crane JF, Trainor PA. Neural crest stem and progenitor cells. Annu Rev Cell Dev Biol. 2006;22:267-86. doi: 10.1146/annurev.cellbio.22.010305.103814. PMID: 16803431.
28. Cunat S, Hoffmann P, Pujol P. Estrogens and epithelial ovarian cancer. Gynecol Oncol. 2004 Jul;94(1):25-32. doi: 10.1016/j.ygyno.2004.03.026. PMID: 15262115.
29. Davidoff AM. Neonatal Neuroblastoma. Clin Perinatol. 2021 Mar;48(1):101-115. doi: 10.1016/j.clp.2020.11.006. Epub 2021 555 Jan 12. PMID: 33583499
30. Deiss LP, Galinka H, Berissi H, Cohen O, Kimchi A. Cathepsin D protease mediates programmed cell death induced by interferon-gamma, Fas/APO-1 and TNF-alpha. EMBO J. 1996 Aug 1;15(15):3861-70. PMID: 8670891; PMCID: PMC452079.
31. Delbrück R, Desel C, von Figura K, Hille-Rehfeld A. Proteolytic processing of cathepsin D in prelysosomal organelles. Eur J Cell Biol. 1994 Jun;64(1):7-14.
32. Démoz M, Castino R, Cesaro P, Baccino FM, Bonelli G, Isidoro C. Endosomal-lysosomal proteolysis mediates death signalling by TNFalpha, not by etoposide, in L929 fibrosarcoma cells: evidence for an active role of cathepsin D. Biol Chem. 2002 Jul-Aug;383(7-8):1237-48. doi: 10.1515/BC.2002.137.
33. Diment S, Leech MS, Stahl PD. Cathepsin D is membrane-associated in macrophage endosomes. J Biol Chem. 1988 May 15;263(14):6901-7. PubMed PMID: 3360812.
34. Dragonetti A, Baldassarre M, Castino R, Démoz M, Luini A, Buccione R, Isidoro C. The lysosomal protease cathepsin D is efficiently sorted to and secreted from regulated secretory compartments in the rat basophilic/mast cell line RBL. J Cell Sci. 2000 Sep;113 (Pt 18):328998.
35. Ekert JE, Johnson K, Strake B, Pardinas J, Jarantow S, Perkinson R, Colter DC. Three-dimensional lung tumor microenvironment modulates therapeutic compound responsiveness in vitro implication for drug development. PLoS One. 2014 Mar 17;9(3):e92248. doi: 10.1371/journal.pone.0092248. PMID: 24638075; PMCID: PMC3956916.
36. Emert-Sedlak L, Shangary S, Rabinovitz A, Miranda MB, Delach SM, Johnson DE. Involvement of cathepsin D in chemotherapy-induced cytochrome c release, caspase activation, and cell death. Mol Cancer Ther. 2005 May;4(5):733-42. doi: 10.1158/1535-7163.MCT-04-0301. PMID: 15897237.
37. Erickson AH, Blobel G. Early events in the biosynthesis of the lysosomal enzyme cathepsin D. J Biol Chem. 1979 Dec 10;254(23):11771-4.
38. Faust PL, Kornfeld S, Chirgwin JM. Cloning and sequence analysis of cDNA for human cathepsin D. Proc Natl Acad Sci U S A. 1985;82(15):4910-4914. doi:10.1073/pnas.82.15.4910.
39. Filipenko NR, Waisman DM. The C terminus of annexin II mediates binding to F-actin. J Biol Chem. 2001;276(7):5310-5315. doi:10.1074/jbc.M009710200.
40. Follo C, Castino R, Nicotra G, Trincheri NF, Isidoro C. Folding, activity and targeting of mutated human cathepsin D that cannot be processed into the double-chain form. Int J Biochem Cell Biol. 2007;39(3):638-49. doi: 10.1016/j.biocel.2006.11.010. Epub 2006 Nov 25. PMID: 17188016.
41. Follo C, Ozzano M, Montalenti C, Santoro MM, Isidoro C. Knockdown of cathepsin D in zebrafish fertilized eggs determines congenital myopathy. Biosci Rep. 2013;33(2):e00034. Published 2013 Apr 4. doi:10.1042/BSR20120100.

42. Follo C, Ozzano M, Mugoni V, Castino R, Santoro M, Isidoro C. Knock-down of cathepsin D affects the retinal pigment epithelium, impairs swim-bladder ontogenesis and causes premature death in zebrafish. PLoS One. 2011;6(7):e21908. doi:10.1371/journal.pone.0021908.
43. Fortenberry SC, Schorey JS, Chirgwin JM. Role of glycosylation in the expression of human procathepsin D. J Cell Sci. 1995 May;108 (Pt 5):2001-6. PMID: 7657720.
44. Frydman J. Folding of newly translated proteins in vivo: the role of molecular chaperones. Annu Rev Biochem. 2001;70:603-47. doi: 10.1146/annurev.biochem.70.1.603. PMID: 11395418.
45. Gerke V, Moss SE. Annexins: from structure to function. Physiol Rev. 2002;82(2):331-371. doi:10.1152/physrev.00030.2001.
46. Gieselmann V, Pohlmann R, Hasilik A, Von Figura K. Biosynthesis and transport of cathepsin D in cultured human fibroblasts. J Cell Biol. 1983 Jul;97(1):1-5.
47. Gigliotti AR, Di Cataldo A, Sorrentino S, Parodi S, Rizzo A, Buffa P, Granata C, Sementa AR, Fagnani AM, Provenzi M, Prete A, D'Ippolito C, Clerico A, Castellano A, Tonini GP, Conte M, Garaventa A, De Bernardi B. Neuroblastoma in the newborn. A study of the Italian Neuroblastoma Registry. Eur J Cancer. 2009 Dec;45(18):3220-7. doi: 10.1016/j.ejca.2009.08.020. Epub 2009 Sep 18. PMID: 19767197.
48. Gopalakrishnan MM, Grosch HW, Locatelli-Hoops S, Werth N, Smolenová E, Nettersheim M, Sandhoff K, Hasilik A. Purified recombinant human prosaposin forms oligomers that bind procathepsin D and affect its autoactivation. Biochem J. 2004 Nov 1;383(Pt. 3):507-15. doi: 10.1042/BJ20040175.
49. Goto S, Umehara S, Gerbing RB, Stram DO, Brodeur GM, Seeger RC, Lukens JN, Matthay KK, Shimada H. Histopathology (International Neuroblastoma Pathology Classification) and MYCN status in patients with peripheral neuroblastic tumors: a report from the Children's Cancer Group. Cancer. 2001 Nov 15;92(10):2699-708. doi: 10.1002/1097-0142(20011115)92:10<2699::aid-cncr1624>3.0.co;2-a. PMID: 11745206.
50. Granato M, Lacconi V, Peddis M, Lotti LV, Di Renzo L, Gonnella R, Santarelli R, Trivedi P, Frati L, D'Orazi G, Faggioni A, Cirone M. HSP70 inhibition by 2-phenylethynesulfonamide induces lysosomal cathepsin D release and immunogenic cell death in primary effusion lymphoma. Cell Death Dis. 2013 Jul 18;4:e730. doi:10.1038/cddis.2013.263. Erratum in: Cell Death Dis. 2014;5:e2154. Renzo, L D.
51. Hajjar KA, Jacovina AT, Chacko J. An endothelial cell receptor for plasminogen/tissue plasminogen activator. I. Identity with annexin II. J Biol Chem. 1994;269(33):21191-21197.
52. Hall MK, Burch AP, Schwalbe RA. Functional analysis of N-acetylglucosaminyltransferase-I knockdown in 2D and 3D neuroblastoma cell cultures. PLoS One. 2021 Nov 8;16(11):e0259743. doi: 10.1371/journal.pone.0259743. PMID: 34748597; PMCID: PMC8575246.
53. Hartl FU, Hayer-Hartl M. Molecular chaperones in the cytosol: from nascent chain to folded protein. Science. 2002 Mar 8;295(5561):1852-8. doi: 10.1126/science.1068408. PMID: 11884745.
54. Hartwig F, Köll-Weber M, Süss R. Preclinical In Vitro Studies with 3D Spheroids to Evaluate Cu(DDC)2 Containing Liposomes for the Treatment of Neuroblastoma. Pharmaceutics. 2021 Jun 17;13(6):894. doi: 10.3390/pharmaceutics13060894. PMID: 34204205; PMCID: PMC8234124.

55. Ho R, Minturn JE, Hishiki T, Zhao H, Wang Q, Cnaan A, Maris J, Evans AE, Brodeur GM. Proliferation of human neuroblastomas mediated by the epidermal growth factor receptor. Cancer Res. 2005 Nov 1;65(21):9868-75. doi: 10.1158/0008-5472.CAN-04-2426. PMID: 16267010.
56. Huang CC, Lee CC, Lin HH, Chang JY. Cathepsin S attenuates endosomal EGFR signalling: A mechanical rationale for the combination of cathepsin S and EGFR tyrosine kinase inhibitors. Sci Rep. 2016 Jul 8;6:29256. doi: 10.1038/srep29256. PMID: 27387133; PMCID: PMC4937378.
57. Ikeda H, Suzuki N, Takahashi A, Kuroiwa M, Nagashima K, Tsuchida Y, Matsuyama S. Surgical treatment of neuroblastomas in infants under 12 months of age. J Pediatr Surg. 1998 Aug;33(8):1246-50. doi: 10.1016/s0022-3468(98)90160-9. PMID: 9721996.
58. Isidoro C, Demoz M, De Stefanis D, Mainferme F, Wattiaux R, Baccino FM. Altered intracellular processing and enhanced secretion of procathepsin D in a highly deviated rat hepatoma. Int J Cancer. 1995 Jan 3;60(1):61-4. doi: 10.1002/ijc.2910600109. PMID: 7814153. (1995a).
59. Isidoro C, Démoz M, De Stefanis D, Baccino FM, Bonelli G. High levels of proteolytic enzymes in the ascitic fluid and plasma of rats bearing the Yoshida AH-130 hepatoma. Invasion Metastasis. 1995;15(3-4):116-24. PMID: 8621267. (1995b).
60. Isidoro C, Demoz M, De Stefanis D, Baccino FM, Bonelli G. Synthesis, maturation and extracellular release of procathepsin D as influenced by cell proliferation or transformation. Int J Cancer. 1995 Dec 11;63(6):866-71. doi: 10.1002/ijc.2910630619. PMID: 8847147. (1995c).
61. Isidoro C, Grässel S, Baccino FM, Hasilik A. Determination of the phosphorylation, uncovering of mannose 6-phosphate groups and targeting of lysosomal enzymes. Eur J Clin Chem Clin Biochem. 1991 Mar;29(3):165-71.
62. Isidoro C, Maggioni C, Démoz M, Pizzagalli A, Fra AM, Sitia R. Exposed thiols confer localization in the endoplasmic reticulum by retention rather than retrieval. J Biol Chem. 1996 Oct 18;271(42):26138-42. doi: 10.1074/jbc.271.42.26138.
63. Jha SK, Rauniyar K, Chronowska E, Mattonet K, Maina EW, Koistinen H, Stenman UH, Alitalo K, Jeltsch M. KLK3/PSA and cathepsin D activate VEGF-C and VEGF-D. Elife. 2019 May 17;8:e44478. doi: 10.7554/eLife.44478. PMID: 31099754; PMCID: PMC6588350.
64. Kågedal K, Zhao M, Svensson I, Brunk UT. Sphingosine-induced apoptosis is dependent on lysosomal proteases. Biochem J. 2001 Oct 15;359(Pt 2):335-43. doi: 10.1042/0264-6021:3590335. PMID: 11583579; PMCID: PMC1222151.
65. Kamihara J, Bourdeaut F, Foulkes WD, Molenaar JJ, Mossé YP, Nakagawara A, Parareda A, Scollon SR, Schneider KW, Skalet AH, States LJ, Walsh MF, Diller LR, Brodeur GM. Retinoblastoma and Neuroblastoma Predisposition and Surveillance. Clin Cancer Res. 2017 Jul 1;23(13):e98-e106. doi: 10.1158/1078-0432.CCR-17-0652. PMID: 28674118; PMCID: PMC7266051.
66. Kassam G, Manro A, Braat CE, Louie P, Fitzpatrick SL, Waisman DM. Characterization of the heparin binding properties of annexin II tetramer. J Biol Chem. 1997;272(24):15093-15100. doi:10.1074/jbc.272.24.15093.

67. Kholodenko IV, Kalinovsky DV, Doronin II, Deyev SM, Kholodenko RV. Neuroblastoma Origin and Therapeutic Targets for Immunotherapy. J Immunol Res. 2018 Jul 11;2018:7394268. doi: 10.1155/2018/7394268. PMID: 30116755; PMCID: PMC6079467.
68. Kim S, Chung DH. Pediatric solid malignancies: neuroblastoma and Wilms' tumor. Surg Clin North Am. 2006 Apr;86(2):469-87, xi. doi: 10.1016/j.suc.2005.12.008. PMID: 16580935.
69. Laurent-Matha V, Maruani-Herrmann S, Prébois C, Beaujouin M, Glondu M, Noël A, Alvarez-Gonzalez ML, Blacher S, Coopman P, Baghdiguian S, Gilles C, Loncarek J, Freiss G, Vignon F, Liaudet-Coopman E. Catalytically inactive human cathepsin D triggers fibroblast invasive growth. J Cell Biol. 2005 Jan 31;168(3):489-99. doi: 10.1083/jcb.200403078. Epub 2005 Jan 24. PMID: 15668295; PMCID: PMC2171724.
70. Leto G, Tumminello FM, Crescimanno M, Flandina C, Gebbia N. Cathepsin D expression levels in nongynecological solid tumors: clinical and therapeutic implications. Clin Exp Metastasis. 2004;21(2):91-106. doi: 10.1023/b:clin.0000024740.44602.b7. PMID: 15168727.
71. Li Z, Chen Y, Ren WU, Hu S, Tan Z, Wang Y, Chen Y, Zhang J, Wu J, Li T, Xu J, Ying X. Transcriptome Alterations in Liver Metastases of Colorectal Cancer After Acquired Resistance to Cetuximab. Cancer Genomics Proteomics. 2019 May-Jun;16(3):207-219. doi: 10.21873/cgp.20126. PMID: 31018951; PMCID: PMC6542644.
72. Liao HW, Hsu JM, Xia W, Wang HL, Wang YN, Chang WC, Arold ST, Chou CK, Tsou PH, Yamaguchi H, Fang YF, Lee HJ, Lee HH, Tai SK, Yang MH, Morelli MP, Sen M, Ladbury JE, Chen CH, Grandis JR, Kopetz S, Hung MC. PRMT1-mediated methylation of the EGF receptor regulates signaling and cetuximab response. J Clin Invest. 2015 Dec;125(12):4529-43. doi: 10.1172/JCI82826. Epub 2015 Nov 16. PMID: 26571401; PMCID: PMC4665782.
73. Lockwood TD, Shier WT. Regulation of acid proteases during growth, quiescence and starvation in normal and transformed cells. Nature. 1977 May 19;267(5608):252-4. doi: 10.1038/267252a0. PMID: 17074.
74. Lokman NA, Ween MP, Oehler MK, Ricciardelli C. The role of annexin A2 in tumorigenesis and cancer progression. Cancer Microenviron. 2011 Aug;4(2):199-208. doi: 10.1007/s12307-011-0064-9. Epub 2011 Mar 5. PMID: 21909879; PMCID: PMC3170418.
75. Look AT, Hayes FA, Nitschke R, McWilliams NB, Green AA. Cellular DNA content as a predictor of response to chemotherapy in infants with unresectable neuroblastoma. N Engl J Med. 1984 Jul 26;311(4):231-5. doi: 10.1056/NEJM198407263110405. PMID: 6738617.
76. Look AT, Hayes FA, Shuster JJ, Douglass EC, Castleberry RP, Bowman LC, Smith EI, Brodeur GM. Clinical relevance of tumor cell ploidy and N-myc gene amplification in childhood neuroblastoma: a Pediatric Oncology Group study. J Clin Oncol. 1991 Apr;9(4):581-91. doi: 10.1200/JCO.1991.9.4.581. PMID: 2066755.
77. Losty P, Quinn F, Breatnach F, O'Meara A, Fitzgerald RJ. Neuroblastoma--a surgical perspective. Eur J Surg Oncol. 1993 Feb;19(1):33-6. PMID: 8436238.
78. Maris JM. Recent advances in neuroblastoma. N Engl J Med. 2010 Jun 10;362(23):2202-11. doi: 10.1056/NEJMra0804577. PMID: 20558371; PMCID: PMC3306838.
79. Martin TA, Goyal A, Watkins G, Jiang WG. Expression of the transcription factors snail, slug, and twist and their clinical significance in human breast cancer. Ann Surg Oncol. 2005 Jun;12(6):488-96. doi: 10.1245/ASO.2005.04.010. Epub 2005 Apr 19. PMID: 15864483.
80. Masson O, Bach AS, Derocq D, Prébois C, Laurent-Matha V, Pattingre S, Liaudet-Coopman E. Pathophysiological functions of cathepsin D: Targeting its catalytic activity versus its

protein binding activity? Biochimie. 2010 Nov;92(11):1635-43. doi: 10.1016/j.biochi.2010.05.009.
81. Matsumoto Y, Ichikawa T, Kurozumi K, Otani Y, Fujimura A, Fujii K, Tomita Y, Hattori Y, Uneda A, Tsuboi N, Kaneda K, Makino K, Date I. Annexin A2-STAT3-Oncostatin M receptor axis drives phenotypic and mesenchymal changes in glioblastoma. Acta Neuropathol Commun. 2020 Apr 5;8(1):42. doi: 10.1186/s40478-020-00916-7. PMID: 32248843; PMCID: PMC7132881.
82. Meyers MB, Shen WP, Spengler BA, Ciccarone V, O'Brien JP, Donner DB, Furth ME, Biedler JL. Increased epidermal growth factor receptor in multidrug-resistant human neuroblastoma cells. J Cell Biochem. 1988 Oct;38(2):87-97. doi: 10.1002/jcb.240380203. PMID: 2464605.
83. Minarowska A, Minarowski L, Karwowska A, Gacko M. Regulatory role of cathepsin D in apoptosis. Folia Histochem Cytobiol. 2007;45(3):159-63. Review. PubMed PMID: 17951163.
84. Mizushima N, Komatsu M. Autophagy: renovation of cells and tissues. Cell. 2011 Nov 11;147(4):728-41. doi: 10.1016/j.cell.2011.10.026. PMID: 22078875.
85. Monclair T, Brodeur GM, Ambros PF, Brisse HJ, Cecchetto G, Holmes K, Kaneko M, London WB, Matthay KK, Nuchtern JG, von Schweinitz D, Simon T, Cohn SL, Pearson AD; INRG Task Force. The International Neuroblastoma Risk Group (INRG) staging system: an INRG Task Force report. J Clin Oncol. 2009 Jan 10;27(2):298-303. doi: 10.1200/JCO.2008.16.6876. Epub 2008 Dec 1. PMID: 19047290; PMCID: PMC2650389.
86. Morani F, Phadngam S, Follo C, et al. PTEN deficiency and mutant p53 confer glucoseaddiction to thyroid cancer cells: impact of glucose depletion on cell proliferation, cell survival, autophagy and cell migration. Genes Cancer. 2014 Jul;5(7-8):226-39.
87. Morimoto RI. Regulation of the heat shock transcriptional response: cross talk between a family of heat shock factors, molecular chaperones, and negative regulators. Genes Dev. 1998 Dec 15;12(24):3788-96. doi: 10.1101/gad.12.24.3788. PMID: 9869631.
88. Moss SE, Morgan RO. The annexins. Genome Biol. 2004;5(4):219. doi: 10.1186/gb-2004-5-4-219. Epub 2004 Mar 31. PMID: 15059252; PMCID: PMC395778.
89. Nakagawara A, Li Y, Izumi H, Muramori K, Inada H, Nishi M. Neuroblastoma. Jpn J Clin Oncol. 2018 Mar 1;48(3):214-241. doi: 10.1093/jjco/hyx176. PMID: 29378002.
90. Nicotra G, Castino R, Follo C, Peracchio C, Valente G, Isidoro C. The dilemma: does tissue expression of cathepsin D reflect tumor malignancy? The question: does the assay truly mirror cathepsin D misfunction in the tumor? Cancer Biomark. 2010;7(1):47-64. doi:10.3233/CBM-2010-014.
91. Nieto MA. The early steps of neural crest development. Mech Dev. 2001 Jul;105(1-2):27-35. doi: 10.1016/s0925-4773(01)00394-x. PMID: 11429279.
92. Nuchtern JG. Perinatal neuroblastoma. Semin Pediatr Surg. 2006 Feb;15(1):10-6. doi: 10.1053/j.sempedsurg.2005.11.003. PMID: 16458841.
93. Peaston AE, Gardaneh M, Franco AV, Hocker JE, Murphy KM, Farnsworth ML, Catchpoole DR, Haber M, Norris MD, Lock RB, Marshall GM. MRP1 gene expression level regulates the death and differentiation response of neuroblastoma cells. Br J Cancer. 2001 Nov 16;85(10):1564-71. doi: 10.1054/bjoc.2001.2144. PMID: 11720446; PMCID: PMC2363953.

94. Pickl M, Ries CH. Comparison of 3D and 2D tumor models reveals enhanced HER2 activation in 3D associated with an increased response to trastuzumab. Oncogene. 2009 Jan 22;28(3):461-8. doi: 10.1038/onc.2008.394. Epub 2008 Nov 3. PMID: 18978815.
95. Pozzi S, Scomparin A, Israeli Dangoor S, Rodriguez Ajamil D, Ofek P, Neufeld L, Krivitsky A, Vaskovich-Koubi D, Kleiner R, Dey P, Koshrovski-Michael S, Reisman N, Satchi-Fainaro R. Meet me halfway: Are in vitro 3D cancer models on the way to replace in vivo models for nanomedicine development? Adv Drug Deliv Rev. 2021 Aug;175:113760. doi: 10.1016/j.addr.2021.04.001. Epub 2021 Apr 7. PMID: 33838208.
96. Pranjol MZI, Gutowski NJ, Hannemann M, Whatmore JL. Cathepsin D non-proteolytically induces proliferation and migration in human omental microvascular endothelial cells via activation of the ERK1/2 and PI3K/AKT pathways. Biochim Biophys Acta Mol Cell Res. 2018 Jan;1865(1):25-33. doi: 10.1016/j.bbamcr.2017.10.005. Epub 2017 Oct 10. PubMed PMID: 29024694.
97. Puisieux A, Valsesia-Wittmann S, Ansieau S. A twist for survival and cancer progression. Br J Cancer. 2006 Jan 16;94(1):13-7. doi: 10.1038/sj.bjc.6602876. PMID: 16306876; PMCID: PMC2361066.
98. Raffaghello L, Conte M, De Grandis E, Pistoia V. Immunological mechanisms in opsoclonus-myoclonus associated neuroblastoma. Eur J Paediatr Neurol. 2009 May;13(3):219-23. doi: 10.1016/j.ejpn.2008.04.012. Epub 2008 Jun 20. PMID: 18571942.
99. Reid WA, Valler MJ, Kay J. Immunolocalization of cathepsin D in normal and neoplastic human tissues. J Clin Pathol. 1986 Dec;39(12):1323-30. doi: 10.1136/jcp.39.12.1323. PMID: 3543065; PMCID: PMC1140796.
100. Riedl A, Schlederer M, Pudelko K, Stadler M, Walter S, Unterleuthner D, Unger C, Kramer N, Hengstschläger M, Kenner L, Pfeiffer D, Krupitza G, Dolznig H. Comparison of cancer cells in 2D vs 3D culture reveals differences in AKT-mTOR-S6K signaling and drug responses. J Cell Sci. 2017 Jan 1;130(1):203-218. doi: 10.1242/jcs.188102. Epub 2016 Sep 23. PMID: 27663511.
101. Rijnboutt S, Stoorvogel W, Geuze HJ, Strous GJ. Identification of subcellular compartments involved in biosynthetic processing of cathepsin D. J Biol Chem. 1992 Aug 5;267(22):1566572.
102. Ritenour LE, Randall MP, Bosse KR, Diskin SJ. Genetic susceptibility to neuroblastoma: current knowledge and future directions. Cell Tissue Res. 2018 May;372(2):287-307. doi: 10.1007/s00441-018-2820-3. Epub 2018 Mar 27. Erratum in: Cell Tissue Res. 2021 Feb;383(2):905. PMID: 29589100; PMCID: PMC6893873.
103. Roberg K, Ollinger K. Oxidative stress causes relocation of the lysosomal enzyme cathepsin D with ensuing apoptosis in neonatal rat cardiomyocytes. Am J Pathol. 1998 May;152(5):1151-6. PMID: 9588882; PMCID: PMC1858594.
104. Saftig P, Hetman M, Schmahl W, et al. Mice deficient for the lysosomal proteinase cathepsin D exhibit progressive atrophy of the intestinal mucosa and profound destruction of lymphoid cells. EMBO J. 1995;14(15):3599–3608.
105. Sagulenko V, Muth D, Sagulenko E, Paffhausen T, Schwab M, Westermann F. Cathepsin D protects human neuroblastoma cells from doxorubicin-induced cell death. Carcinogenesis. 2008;29(10):1869–1877. doi:10.1093/carcin/bgn147.

106. Sakaguchi M, Murata H, Sonegawa H, Sakaguchi Y, Futami J, Kitazoe M, Yamada H, Huh NH. Truncation of annexin A1 is a regulatory lever for linking epidermal growth factor signaling with cytosolic phospholipase A2 in normal and malignant squamous epithelial cells. J Biol Chem. 2007 Dec 7;282(49):35679-86. doi: 10.1074/jbc.M707538200. Epub 2007 Oct 10. PMID: 17932043.
107. Sasaki T, Hiroki K, Yamashita Y. The role of epidermal growth factor receptor in cancer metastasis and microenvironment. Biomed Res Int. 2013;2013:546318. doi: 10.1155/2013/546318. Epub 2013 Aug 7. PMID: 23986907; PMCID: PMC3748428.
108. Scollon S, Anglin AK, Thomas M, Turner JT, Wolfe Schneider K. A Comprehensive Review of Pediatric Tumors and Associated Cancer Predisposition Syndromes. J Genet Couns. 2017 Jun;26(3):387-434. doi: 10.1007/s10897-017-0077-8. Epub 2017 Mar 29. PMID: 28357779.
109. Secomandi E, Salwa A, Vidoni C, Ferraresi A, Follo C, Isidoro C. High Expression of the Lysosomal Protease Cathepsin D Confers Better Prognosis in Neuroblastoma Patients by Contrasting EGF-Induced Neuroblastoma Cell Growth. Int J Mol Sci. 2022 Apr 26;23(9):4782. doi: 10.3390/ijms23094782. PMID: 35563171; PMCID: PMC9101173.
110. Sharma MC. Annexin A2 (ANX A2): An emerging biomarker and potential therapeutic target for aggressive cancers. Int J Cancer. 2019 May 1;144(9):2074-2081. doi: 10.1002/ijc.31817. Epub 2018 Oct 31. PMID: 30125343.
111. Shetty PK, Thamake SI, Biswas S, Johansson SL, Vishwanatha JK. Reciprocal regulation of annexin II and EGFR with Her-2 in Her-2 negative and herceptin-resistant breast cancer. PLoS One. 2012;7(9):e44299. doi:10.1371/journal.pone.0044299.
112. Shibata M, Kanamori S, Isahara K, Ohsawa Y, Konishi A, Kametaka S, Watanabe T, Ebisu S, Ishido K, Kominami E, Uchiyama Y. Participation of cathepsins B and D in apoptosis of PC12 cells following serum deprivation. Biochem Biophys Res Commun. 1998 Oct 9;251(1):199-203. doi: 10.1006/bbrc.1998.9422. PMID: 9790930.
113. Siegel MJ, Ishwaran H, Fletcher BD, Meyer JS, Hoffer FA, Jaramillo D, Hernandez RJ, Roubal SE, Siegel BA, Caudry DJ, McNeil BJ. Staging of neuroblastoma at imaging: report of the radiology diagnostic oncology group. Radiology. 2002 Apr;223(1):168-75. doi: 10.1148/radiol.2231010841. PMID: 11930063.
114. Siegel RL, Miller KD, Fuchs HE, Jemal A. Cancer Statistics, 2021. CA Cancer J Clin. 2021 Jan;71(1):7-33. doi: 10.3322/caac.21654. Epub 2021 Jan 12. Erratum in: CA Cancer J Clin. 2021 Jul;71(4):359. PMID: 33433946.
115. Sok JC, Coppelli FM, Thomas SM, Lango MN, Xi S, Hunt JL, Freilino ML, Graner MW, Wikstrand CJ, Bigner DD, Gooding WE, Furnari FB, Grandis JR. Mutant epidermal growth factor receptor (EGFRvIII) contributes to head and neck cancer growth and resistance to EGFR targeting. Clin Cancer Res. 2006 Sep 1;12(17):5064-73. doi: 10.1158/1078-0432.CCR-06-0913. PMID: 16951222.
116. Takano S, Togawa A, Yoshitomi H, et al. Annexin II overexpression predicts rapid recurrence after surgery in pancreatic cancer patients undergoing gemcitabine-adjuvant chemotherapy. Ann Surg Oncol. 2008;15(11):3157-3168. doi:10.1245/s10434-008- 0061-5.
117. Tamura S, Hosoi H, Kuwahara Y, Kikuchi K, Otabe O, Izumi M, Tsuchiya K, Iehara T, Gotoh T, Sugimoto T. Induction of apoptosis by an inhibitor of EGFR in neuroblastoma cells.

Biochem Biophys Res Commun. 2007 Jun 22;358(1):226-32. doi: 10.1016/j.bbrc.2007.04.124. Epub 2007 Apr 27. PMID: 17482563.

118. Tang CK, Lippman ME. EGF family receptors and their ligands in human cancer. In: O'Malley BW, editor. Hormones and signaling. vol. I. San Diego (CA): Academic Press; 1998. p. 113–65.

119. Thongchot S, Vidoni C, Ferraresi A, Loilome W, Khuntikeo N, Sangkhamanon S, Titapun A, Isidoro C, Namwat N. Cancer-Associated Fibroblast-Derived IL-6 Determines Unfavorable Prognosis in Cholangiocarcinoma by Affecting Autophagy-Associated Chemoresponse. Cancers (Basel). 2021 Apr 28;13(9):2134. doi: 10.3390/cancers13092134. PMID: 33925189; PMCID: PMC8124468.

120. Tomioka N, Oba S, Ohira M, Misra A, Fridlyand J, Ishii S, Nakamura Y, Isogai E, Hirata T, Yoshida Y, Todo S, Kaneko Y, Albertson DG, Pinkel D, Feuerstein BG, Nakagawara A. Novel risk stratification of patients with neuroblastoma by genomic signature, which is independent of molecular signature. Oncogene. 2008 Jan 17;27(4):441-9. doi: 10.1038/sj.onc.1210661. Epub 2007 Jul 16. PMID: 17637744.

121. Trincheri NF, Nicotra G, Follo C, Castino R, Isidoro C. Resveratrol induces cell death in colorectal cancer cells by a novel pathway involving lysosomal cathepsin D. Carcinogenesis. 2007 May;28(5):922-31. Epub 2006 Nov 20.

122. Vidoni C, Follo C, Savino M, Melone MA, Isidoro C. The Role of Cathepsin D in the Pathogenesis of Human Neurodegenerative Disorders. Med Res Rev. 2016;36(5):845-870. doi:10.1002/med.21394.

123. Vignon F, Capony F, Chambon M, Freiss G, Garcia M, Rochefort H. Autocrine growth stimulation of the MCF 7 breast cancer cells by the estrogen-regulated 52 K protein. Endocrinology. 1986 Apr;118(4):1537-45. doi: 10.1210/endo-118-4-1537. PMID: 3948791.

124. Von Figura K, Hasilik A. Lysosomal enzymes and their receptors. Annu Rev Biochem.1986;55:16793.

125. Wang T, Yuan J, Zhang J, Tian R, Ji W, Zhou Y, Yang Y, Song W, Zhang F, Niu R. Anxa2 binds to STAT3 and promotes epithelial to mesenchymal transition in breast cancer cells. Oncotarget. 2015 Oct 13;6(31):30975-92. doi: 10.18632/oncotarget.5199. PMID: 26307676; PMCID: PMC4741582.

126. Wang Y, Chen K, Cai Y, Cai Y, Yuan X, Wang L, Wu Z, Wu Y. Annexin A2 could enhance multidrug resistance by regulating NF-κB signaling pathway in pediatric neuroblastoma. J Exp Clin Cancer Res. 2017 Aug 16;36(1):111. doi: 10.1186/s13046-017-0581-6. PMID: 28814318; PMCID: PMC5559827.

127. Weigelt B, Lo AT, Park CC, Gray JW, Bissell MJ. HER2 signaling pathway activation and response of breast cancer cells to HER2-targeting agents is dependent strongly on the 3D microenvironment. Breast Cancer Res Treat. 2010 Jul;122(1):35-43. doi: 10.1007/s10549-009-0502-2. Epub 2009 Aug 22. PMID: 19701706; PMCID: PMC2935800.

128. Wells A. EGF receptor. Int J Biochem Cell Biol. 1999 Jun;31(6):637-43. doi: 10.1016/s1357-2725(99)00015-1. PMID: 10404636.

129. Xiu D, Liu L, Qiao F, Yang H, Cui L, Liu G. Annexin A2 Coordinates STAT3 to Regulate the Invasion and Migration of Colorectal Cancer Cells In Vitro. Gastroenterol Res Pract. 2016;2016:3521453. doi: 10.1155/2016/3521453. Epub 2016 May 4. PMID: 27274723; PMCID: PMC4870365.

130. Yang T, Peng H, Wang J, et al. Prognostic and diagnostic significance of annexin II in colorectal cancer. Colorectal Dis. 2013;15(7):e373-e381. doi:10.1111/codi.12207.
131. Yao H, Zhang Z, Xiao Z, et al. Identification of metastasis associated proteins in human lung squamous carcinoma using two-dimensional difference gel electrophoresis and laser capture microdissection. Lung Cancer. 2009;65(1):41-48. doi:10.1016/j.lungcan.2008.10.024.
132. Yoo JC, Hayman MJ. Annexin II binds to SHP2 and this interaction is regulated by HSP70 levels. Biochem Biophys Res Commun. 2007 May 18;356(4):906-11. doi: 10.1016/j.bbrc.2007.03.061. Epub 2007 Mar 19. PMID: 17395158; PMCID: PMC2034505.
133. Yoo JC, Hayman MJ. HSP70 binds to SHP2 and has effects on the SHP2-related EGFR/GAB1 signaling pathway. Biochem Biophys Res Commun. 2006 Dec 29;351(4):979-85. doi: 10.1016/j.bbrc.2006.10.152. Epub 2006 Nov 3. PMID: 17097051; PMCID: PMC1698467.
134. Yuan J, Yang Y, Gao Z, Wang Z, Ji W, Song W, Zhang F, Niu R. Tyr23 phosphorylation of Anxa2 enhances STAT3 activation and promotes proliferation and invasion of breast cancer cells. Breast Cancer Res Treat. 2017 Jul;164(2):327-340. doi: 10.1007/s10549-017-4271-z. Epub 2017 May 3. PMID: 28470457.
135. Zhang F, Wang Z, Yuan J, Wei X, Tian R, Niu R. RNAi-mediated silencing of Anxa2 inhibits breast cancer cell proliferation by downregulating cyclin D1 in STAT3-dependent pathway. Breast Cancer Res Treat. 2015 Sep;153(2):263-75. doi: 10.1007/s10549-015-3529-6. Epub 2015 Aug 8. PMID: 26253946.
136. Zhang Q, Ye Z, Yang Q, He X, Wang H, Zhao Z. Upregulated expression of annexin II is a prognostic marker for patients with gastric cancer. World J Surg Oncol. 2012;10:103. Published 2012 Jun 8. doi:10.1186/1477-7819-10-103.
137. Zhang X, Liu S, Guo C, Zong J, Sun MZ. The association of annexin A2 and cancers. Clin Transl Oncol. 2012 Sep;14(9):634-40. doi: 10.1007/s12094-012-0855-6. Epub 2012 Jul 24. PMID: 22855149.
138. Zhou Y, Li K, Zheng S, Chen L. Retrospective study of neuroblastoma in Chinese neonates from 1994 to 2011: an evaluation of diagnosis, treatments, and prognosis : a 10-year restrospective study of neonatal neuroblastoma. J Cancer Res Clin Oncol. 2014 Jan;140(1):83-7. doi: 10.1007/s00432-013-1535-9. Epub 2013 Nov 5. PMID: 24189916.
139. Zingales V, Torriero N, Zanella L, Fernández-Franzón M, Ruiz MJ, Esposito MR, Cimetta E. Development of an in vitro neuroblastoma 3D model and its application for sterigmatocystin-induced cytotoxicity testing. Food Chem Toxicol. 2021 Nov;157:112605. doi: 10.1016/j.fct.2021.112605. Epub 2021 Oct 9. PMID: 34634377.
140. Zuzarte-Luis V, Montero JA, Kawakami Y, Izpisua-Belmonte JC, Hurle JM. Lysosomal cathepsins in embryonic programmed cell death. Dev Biol. 2007;301(1):205-217. doi:10.1016/j.ydbio. 2006.08.008.

Appendix

In this section, I append the published papers regarding the other ongoing projects of the Laboratory and external collaborators in which I have participated.

cells

MDPI

Article

High *BECN1* Expression Negatively Correlates with *MS4A1* and *BCL2* Expression and Predicts Better Prognosis in Diffuse Large B-Cell Lymphoma: Role of Autophagy

Amreen Salwa[1†], Alessandra Ferraresi[1†], Eleonora Secomandi[1], Letizia Vallino[1], Riccardo Moia[2], Andrea Patriarca[2], Gianluca Gaidano[2*] and Ciro Isidoro[1*]

[1] Laboratory of Molecular Pathology, Department of Health Sciences, Università del Piemonte Orientale "A. Avogadro", Via Solaroli 17, 28100 Novara, Italy; salwa.amreen@uniupo.it (A.S.); alessandra.ferraresi@med.uniupo.it (A.F.); eleonora.secomandi@uniupo.it (E.S.); letizia.vallino@uniupo.it (L.V.);
[2] Division of Hematology, Department of Translational Medicine, Università del Piemonte Orientale, Via P. Solaroli 17, 28100 Novara, Italy; riccardo.moia@uniupo.it (RM); andrea.patriarca@uniupo.it (AP); gianluca.gaidano@med.uniupo.it (GG).
* Correspondence: ciro.isidoro@med.uniupo.it; Tel.: +39-0321-660507; Fax: +39-0321-620421
gianluca.gaidano@med.uniupo.it; Tel ++39-0321-660655; Fax: +39-0321-620421
† These authors have equally contributed and should be regarded as first author

Abstract: Diffuse large B-cell lymphoma (DLBCL) is characterized by high molecular and clinical heterogeneity. Autophagy, a lysosome-driven catabolic process devoted to macromolecular turnover, is fundamental for maintaining normal hematopoietic stem cells and progenitors' homeostasis, and its dysregulation plays a critical role in initiation and progression of hematological malignancies. One main regulator of autophagy is BECLIN1, which interacts with either BCL2, thus allowing apoptosis, or PI3KC3, thus promoting autophagy-dependent cell survival. BECLIN1 is coded by *BECN1*, a tumor suppressor gene. Altered expression of *BCL2* and *MS4A1* (CD20) correlates with lymphoma outcome, but its association with autophagy dysregulation remains to be elucidated. We interrogated the TCGA database to analyze how the expression of *BCL2*, *MS4A1* and *BECN1* impacts on DLBCL survival. The TCGA database contains full information for 48 DLBCL patients. DLBCL highly expressing *BCL2* and *MS4A1* showed poor prognosis, while DLBCL highly expressing *BECN1* showed better prognosis. The expression of *BCL2* and *MS4A1* positively correlated with oncogenic pathways (e.g., glucose transport, HIF1A signaling, JAK-STAT signaling, PI3K-AKT signaling, and mTOR signaling) and negatively correlated with autophagy-related processes. *BECN1* was highly expressed in a small number of patients showing longer survival, indicating that its expression could predict better prognosis. These findings unveil for the first time a link between the expression of *MS4A1* and *BCL2* and of *BECN1* and suggest that impairment of BECN1-dependent autophagy influences poor prognosis in DLBCL with high *MS4A1* and *BCL2* and low *BECN1* expression. Stimulating autophagy with drugs disrupting BECLIN1-BCL-2 interaction could be a valuable strategy for restoring chemosensitivity in DLBCL.

Keywords: personalized medicine; lymphoma; CD20; autophagy; overall survival; TCGA; prognosis, bioinformatics.

Citation: Salwa, A.; Ferraresi, A.; Secomandi, E. et al. Title. *Cells* **2022**, *11*, x. https://doi.org/10.3390/xxxxx

Academic Editor: Firstname Lastname

Received: date
Accepted: date
Published: date

Publisher's Note: MDPI stays neutral with regard to jurisdictional claims in published maps and institutional affiliations.

1. Introduction

Diffuse large B-cell lymphoma (DLBCL) is the most common subtype of B-cell non-Hodgkin lymphoma (B-NHL) in adults, accounting for 30-40% of cases globally [1-3]. DLBCL is characterized by the clonal proliferation of mature B-cell expressing the B-cell surface antigens CD19, CD20, CD22, and CD79a/b. DLBCL presents high clinical heterogeneity that reflects the molecular heterogeneity of gene expression [3-5].

Biomedicine & Pharmacotherapy 135 (2021) 111182

Contents lists available at ScienceDirect

Biomedicine & Pharmacotherapy

journal homepage: www.elsevier.com/locate/biopha

Original article

Halofuginone regulates keloid fibroblast fibrotic response to TGF-β induction

Pierre Marty [a,b], Brice Chatelain [b], Thomas Lihoreau [c], Marion Tissot [a], Zélie Dirand [a], Philippe Humbert [a], Clémence Senez [a], Eleonora Secomandi [d], Ciro Isidoro [d,**], Gwenaël Rolin [a,c,*]

[a] Univ. Bourgogne Franche-Comté, INSERM, EFS BFC, UMR1098, RIGHT Interactions Greffon-Hôte-Tumeur/Ingénierie Cellulaire et Génique, F-25000, Besançon, France
[b] Service de Chirurgie Maxillo-faciale, Stomatologie et Odontologie Hospitalière, CHU Besançon, F-25000, Besançon, France
[c] INSERM CIC-1431, CHU Besançon, F-25000, Besançon, France
[d] Laboratory of Molecular Pathology, Department of Health Sciences, Università del Piemonte Orientale "Amedeo Avogadro", Novara, Italy

ARTICLE INFO

Keywords:
Halofuginone
Keloid
Myofibroblasts
TGF-β1
Fibrosis

ABSTRACT

Keloids are characterized by increased deposition of fibrous tissue in the skin and subcutaneous tissue following an abnormal wound healing process. Although keloid etiology is yet to be fully understood, fibroblasts are known to be key players in its development. Here we analyze the antifibrotic mechanisms of Halofuginone (HF), a drug reportedly able to inhibit the TGF-β1-Smad3 pathway and to attenuate collagen synthesis, in an in-vitro keloid model using patient-derived Keloid Fibroblasts (KFs) isolated from fibrotic tissue collected during the "Scar Wars" clinical study (NCT NCT03312166). TGF-β1 was used as a pro-fibrotic agent to stimulate fibroblasts response under HF treatment. The fibrotic related properties of KFs, including survival, migration, proliferation, myofibroblasts conversion, ECM synthesis and remodeling, were investigated in 2D and 3D cultures. HF at 50 nM concentration impaired KFs proliferation, and decreased TGF-β1-induced expression of α-SMA and type I pro-collagen production. HF treatment also reduced KFs migration, prevented matrix contraction and increased the metallo-proteases/inhibitors (MMP/TIMP) ratio. Overall, HF elicits an anti-fibrotic contrasting the TGF-β1 stimulation of KFs, thus supporting its therapeutic use for keloid prevention and management.

1. Introduction

Since 2018, World Health Organization defines keloids as a member of a group of disorders *"characterized by increased deposition of fibrous tissue in the skin and subcutaneous tissue"* [1]. Accordingly, keloids are considered not just pathological scars, rather the outcome of an abnormal wound healing process with features similar to that of chronic inflammatory diseases and cancer [2]. Clinically, keloids present as a fibrotic tissue that proliferates beyond the primary injured area and persist over time without natural regression. Keloids may cause pain and pruritus, and seriously affect patient quality of life when they are located in visible areas [3]. Keloids may result from different skin injuries, including surgery, burns, trauma, piercing, and folliculitis, though their location appears mainly confined to chest, shoulders, neck and ears [4].

Despite the ample variety of treatments available, which include occlusive dressing, compressive therapy, cryotherapy, radiation, laser, and pharmacotherapies with steroids, mitomycin C, 5-FU, bleomycin, no effective therapeutic protocols or standardized guidelines have been published yet [5]. Surgery is commonly indicated in order to reduce keloid volume, despite the high recurrence rate after excision and the development of a fibrosis worse than the initial one [6]. The lack of effective treatments clearly reflects our poor understanding of keloid

Abbreviations: TGF-β1, transforming growth factor β1; ECM, extracellular matrix; SMADs, Mothers against decapentaplegic homolog; α-SMA, alpha-smooth muscle actin; MMP, matrix metalloproteinases; TIMP, tissue inhibitors of metalloproteinases; HF, Halofuginone; KF, keloid fibroblast; AUC, Area Under the Curve.

* Corresponding author at: Centre d'Investigation Clinique, Inserm CIC 1431, CHU de Besançon / Univ. Bourgogne Franche-Comté, INSERM, EFS BFC, UMR1098, RIGHT Interactions Greffon-Hôte-Tumeur/Ingénierie Cellulaire et Génique, F-25000, Besançon, France.
** Corresponding author at: Laboratory of Molecular Pathology, Department of Health Sciences, Università del Piemonte Orientale "Amedeo Avogadro", Novara, Italy.
E-mail addresses: ciro.isidoro@med.uniupo.it (C. Isidoro), grolin@chu-besancon.fr (G. Rolin).

https://doi.org/10.1016/j.biopha.2020.111182
Received 22 September 2020; Received in revised form 14 December 2020; Accepted 26 December 2020
Available online 1 February 2021

frontiers in Oncology

MINI REVIEW
published: 07 December 2020
doi: 10.3389/fonc.2020.599915

How Autophagy Shapes the Tumor Microenvironment in Ovarian Cancer

*Alessandra Ferraresi[1], Carlo Girone[1], Andrea Esposito[1], Chiara Vidoni[1], Letizia Vallino[1], Eleonora Secomandi[1], Danny N. Dhanasekaran[2] and Ciro Isidoro[1]**

[1] Laboratory of Molecular Pathology, Department of Health Sciences, Università del Piemonte Orientale "A. Avogadro", Novara, Italy, [2] Stephenson Cancer Center, The University of Oklahoma Health Sciences Center, Oklahoma City, OK, United States

Ovarian cancer (OC) is characterized by a high mortality rate due to the late diagnosis and the elevated metastatic potential. Autophagy, a lysosomal-driven catabolic process, contributes to the macromolecular turnover, cell homeostasis, and survival, and as such, it represents a pathway targetable for anti-cancer therapies. It is now recognized that the vascularization and the cellular composition of the tumor microenvironment influence the development and progression of OC by controlling the availability of nutrients, oxygen, growth factors, and inflammatory and immune-regulatory soluble factors that ultimately impinge on autophagy regulation in cancer cells. An increasing body of evidence indicates that OC carcinogenesis is associated, at least in the early stages, to insufficient autophagy. On the other hand, when the tumor is already established, autophagy activation provides a survival advantage to the cancer cells that face metabolic stress and protects from the macromolecules and organelles damages induced by chemo- and radiotherapy. Additionally, upregulation of autophagy may lead cancer cells to a non-proliferative dormant state that protects the cells from toxic injuries while preserving their stem-like properties. Further to complicate the picture, autophagy is deregulated also in stromal cells. Thus, changes in the tumor microenvironment reflect on the metabolic crosstalk between cancer and stromal cells impacting on their autophagy levels and, consequently, on cancer progression. Here, we present a brief overview of the role of autophagy in OC hallmarks, including tumor dormancy, chemoresistance, metastasis, and cell metabolism, with an emphasis on the bidirectional metabolic crosstalk between cancer cells and stromal cells in shaping the OC microenvironment.

Keywords: cancer, cell metabolism, dormancy, cytokines, chemoresistance, autophagy, cancer associated fibroblasts, inflammatory stroma

OPEN ACCESS

Edited by:
Ana Preto,
University of Minho, Portugal

Reviewed by:
Lucie Brisson,
Inserm UMR1069 Équipe Nutrition, Croissance et Cancer, France
Maria Letizia Taddei,
University of Florence, Italy

****Correspondence:***
Ciro Isidoro
ciro.isidoro@med.uniupo.it

Specialty section:
This article was submitted to Cancer Metabolism, a section of the journal Frontiers in Oncology

Received: *28 August 2020*
Accepted: *03 November 2020*
Published: *07 December 2020*

Citation:
Ferraresi A, Girone C, Esposito A, Vidoni C, Vallino L, Secomandi E, Dhanasekaran DN and Isidoro C (2020) How Autophagy Shapes the Tumor Microenvironment in Ovarian Cancer. Front. Oncol. 10:599915. doi: 10.3389/fonc.2020.599915

INTRODUCTION

Ovarian cancer (OC) emerges as the eighth most commonly diagnosed cancer among women worldwide and the leading cause of death among gynecological malignancies (1). Epithelial ovarian cancers are characterized by extensive genomic instability with mutations in several oncogenes and tumor suppressor genes including *BRAF, KRAS, TP53, BRCA1/2,* and *PTEN,* among others, that identify different subtypes with different behaviors and prognoses (2). The current therapy for OC

Seminars in Cancer Biology 66 (2020) 34–44

Contents lists available at ScienceDirect

Seminars in Cancer Biology

journal homepage: www.elsevier.com/locate/semcancer

Review

Epigenetic targeting of autophagy for cancer prevention and treatment by natural compounds

Chiara Vidoni[a,1], Alessandra Ferraresi[a,1], Eleonora Secomandi[a], Letizia Vallino[a], Danny N. Dhanasekaran[b], Ciro Isidoro[a,*]

[a] Laboratory of Molecular Pathology, Department of Health Sciences, Università del Piemonte Orientale "A. Avogadro", Via Solaroli 17, 28100, Novara, Italy
[b] Stephenson Cancer Center, The University of Oklahoma Health Sciences Center, Oklahoma City, OK, USA

ARTICLE INFO

Keywords:
Herb
Therapy
Cell metabolism
miRNA
Long non coding RNA

ABSTRACT

Despite the undeniable progress made in the last decades, cancer continues to challenge the scientists engaged in searching for an effective treatment for its prevention and cure. One of the malignant hallmarks that characterize cancer cell biology is the altered metabolism of sugars and amino acids. Autophagy is a pathway allowing the macromolecular turnover via recycling of the substrates resulting from the lysosomal degradation of damaged or redundant cell molecules and organelles. As such, autophagy guarantees the proteome quality control and cell homeostasis. Data from *in vitro*, in animals and in patients researches show that dysregulation of autophagy favors carcinogenesis and cancer progression, making this process an ineluctable target of cancer therapy. The autophagy process is regulated at genetic, epigenetic and post-translational levels. Targeting autophagy with epigenetic modifiers could represent a valuable strategy to prevent or treat cancer. A wealth of natural products from terrestrial and marine living organisms possess anti-cancer activity. Here, we review the experimental proofs demonstrating the ability of natural compounds to regulate autophagy in cancer via epigenetics. The hope is that in the near future this knowledge could translate into effective intervention to prevent and cure cancer.

1. Introduction

Cancer is a cell proliferative disorder that compromises the structural and functional relationships between organs and that eventually impacts on the whole organism homeostasis, often causing death of the affected patient. Our knowledge on the molecular and cellular events that underlie the process of carcinogenesis has greatly increased in the last decades, yet this knowledge only in rare cases could translate in satisfactory treatments of cancer. The therapy with traditional chemicals may lead to initial shrinkage of the tumoral mass, yet on long term it results in selecting resistant clones that persist in a dormant state and later give rise to relapse. Regrettably, radio- and chemotherapy have systemic deleterious effects that frequently discourage the patients to continue the therapy. Also, these treatments may themselves introduce DNA damages and gene mutations leading to secondary tumors [1,2]. The targeted molecular therapy with specific antibodies [3] or kinase inhibitors [4] and, more recently, the CAR-T immunotherapy [5] bring the promise to treat cancers more successfully, yet with side effects that remain to be determined on long run.

At any rate, because of the multifaceted character of solid tumors [6] and of the complex contribution of the microenvironment in tumor development and progression [7] to have chance of success the therapeutic strategy must include compounds that can target more than just one single malignant feature.

Targeting cancer cell metabolism is one option returned to fashion since it was first proposed a century ago. In this respect, autophagy has gained much interest in the last twenty years among scientists looking for novel anti-cancer therapeutic strategies [8]. The term "autophagy" means 'self-eating' and was coined by Christian De Duve in the early sixties to mean the process by which the cell literally eats and degrades its own constituents within the lysosomes [9]. The cellular substrates can be transferred into the lysosomes via three pathways, which identify the three types of autophagy for degradation: macro-autophagy, micro-autophagy and chaperone-mediated autophagy [10]. Of these three types, the first is by far the most relevant for the macromolecular turnover because of the amount and the dimension of the cellular

Abbreviations: ATG genes, autophagy related genes; DNMT, DNA methyltransferase; EGCG, EpiGalloCatechin-3-Gallate; HAT, histone acetyltransferase; HDAC, histone deacetylase; HMT, histone methyltransferase; LSD1, Lysine-specific histone demethylase 1

* Corresponding author at: Dipartimento di Scienze della Salute, Università del Piemonte Orientale "A. Avogadro", Via P. Solaroli 17, 28100, Novara, Italy.
E-mail address: ciro.isidoro@med.uniupo.it (C. Isidoro).

[1] These authors have equally contributed and should be regarded as first co-authors.

https://doi.org/10.1016/j.semcancer.2019.04.006
Received 14 February 2019; Received in revised form 16 April 2019; Accepted 30 April 2019
Available online 02 May 2019
1044-579X/

Journal of Traditional and Complementary Medicine 10 (2020) 217–229

Contents lists available at ScienceDirect

Journal of Traditional and Complementary Medicine

journal homepage: http://www.elsevier.com/locate/jtcme

Modulation of non-coding RNAs by resveratrol in ovarian cancer cells: *In silico* analysis and literature review of the anti-cancer pathways involved

Letizia Vallino [a, 1], Alessandra Ferraresi [a, 1], Chiara Vidoni [a], Eleonora Secomandi [a], Andrea Esposito [a], Danny N. Dhanasekaran [b], Ciro Isidoro [a, *]

[a] Laboratory of Molecular Pathology, Department of Health Sciences, Università del Piemonte Orientale "A. Avogadro", Via Solaroli 17, 28100, Novara, Italy
[b] Stephenson Cancer Center, The University of Oklahoma Health Sciences Center, Oklahoma City, OK, USA

ARTICLE INFO

Article history:
Received 29 January 2020
Received in revised form
12 February 2020
Accepted 17 February 2020
Available online 4 March 2020

Keywords:
Nutraceutical
Cancer
Epigenetics
Cell metabolism
Warburg effect
Autophagy

ABSTRACT

Background and aim: Non-coding RNAs control cell functioning through affecting gene expression and translation and their dysregulation is associated with altered cell homeostasis and diseases, including cancer. Nutraceuticals with anti-cancer therapeutic potential have been shown to modulate non-coding RNAs expression that could impact on the expression of genes involved in the malignant phenotype.
Experimental procedure: Here, we report on the microarray profiling of microRNAs (miRNAs) and long non-coding RNAs (lncRNAs) and on the associated biochemical pathways and functional processes potentially modulated in OVCAR-3 ovarian cancer cells exposed for 24 h to Resveratrol (RV), a nutraceutical that has been shown to inhibit carcinogenesis and cancer progression in a variety of human and animal models, both *in vitro* and *in vivo*. Diana tools and Gene Ontology (GO) pathway analyses along with Pubmed literature search were employed to identify the cellular processes possibly affected by the dysregulated miRNAs and lncRNAs.
Results and conclusion: The present data consistently support the contention that RV could exert anti-neoplastic activity via non-coding RNAs epigenetic modulation of the pathways governing cell homeostasis, cell proliferation, cell death and cell motility.

1. Introduction

Ovarian cancer remains among the deadliest gynecological cancer in women worldwide. Based on a recent statistic, it is predicted that in 2019 in US there will be more than 22,000 new cases of ovary cancer, with about 14,000 deaths that represent 5% of all deaths for cancer.[1] Ovarian cancer is frequently diagnosed in the late stage because it develops asymptomatically in the early stage and manifests its presence after it has spread in the peritoneum and distant organs.[2] In most cases, surgery and chemotherapy elicit an initial good response, which however is followed by relapse of chemoresistant clones that inevitably lead to death the patient.[3,4] The tumor microenvironment, with its unique composition in stromal- and immune cell-derived cytokines and of blood and lymphatic vessels that determine the availability of nutrients, growth factors and oxygen, plays a pivotal role in ovarian cancer cell metabolism and progression.[5–12]

There is an urgent need for understanding the molecular history of ovarian carcinogenesis in order to identify novel pharmacologic targets. Numerous oncogenes and tumor suppressor driver genes are found mutated in chemoresistant ovarian cancers.[13] In addition to these mutations, also the altered epigenetic regulation of oncogenes and tumor suppressor genes contributes to ovarian carcinogenesis.[14,15] Epigenetic regulation of carcinogenic driver genes

Abbreviations: miRNA, microRNA; lncRNA, long non-coding RNA; RV, Resveratrol; GO, Gene Ontology; EMT, Epithelial to Mesenchymal Transition; TCGA, The Cancer Genome Atlas.

* Corresponding author. Dipartimento di Scienze della Salute, Università del Piemonte Orientale "A. Avogadro", Via P. Solaroli 17, 28100, Novara, Italy. Tel.: +39 0321 660 507.
E-mail address: ciro.isidoro@med.uniupo.it (C. Isidoro).

Peer review under responsibility of The Center for Food and Biomolecules, National Taiwan University.

[1] These authors have equally contributed and should be regarded as first co-authors.

https://doi.org/10.1016/j.jtcme.2020.02.006

Vidoni et al. Cell Communication and Signaling (2019) 17:98
https://doi.org/10.1186/s12964-019-0414-7

Cell Communication and Signaling

RESEARCH Open Access

Autophagy drives osteogenic differentiation of human gingival mesenchymal stem cells

Chiara Vidoni[1], Alessandra Ferraresi[1], Eleonora Secomandi[1], Letizia Vallino[1], Chiara Gardin[2], Barbara Zavan[2,3], Carmen Mortellaro[4] and Ciro Isidoro[1*]

Abstract

Background/aim: Autophagy is a macromolecular degradation process playing a pivotal role in the maintenance of stem-like features and in the morpho-functional remodeling of the tissues undergoing differentiation. In this work we investigated the involvement of autophagy in the osteogenic differentiation of mesenchymal stem cells originated from human gingiva (HGMSC). METHODS: To promote the osteogenic differentiation of HGMSCs we employed resveratrol, a nutraceutical known to modulate autophagy and cell differentiation, together with osteoblastic inductive factors. Osteoblastic differentiation and autophagy were monitored through western blotting and immunofluorescence staining of specific markers.

Results: We show that HGMSCs can differentiate into osteoblasts when cultured in the presence of appropriate factors and that resveratrol accelerates this process by up-regulating autophagy. The prolonged incubation with dexamethasone, β-glycerophosphate and ascorbic acid induced the osteogenic differentiation of HGMSCc with increased expression of autophagy markers. Resveratrol (1 μM) alone elicited a less marked osteogenic differentiation yet it greatly induced autophagy and, when added to the osteogenic differentiation factors, it provoked a synergistic effect. Resveratrol and osteogenic inductive factors synergistically induced the AMPK-BECLIN-1 pro-autophagic pathway in differentiating HGMSCs, that was thereafter downregulated in osteoblastic differentiated cells. Pharmacologic inhibition of BECLIN-1-dependent autophagy precluded the osteogenic differentiation of HGMSCs.

Conclusions: Autophagy modulation is instrumental for osteoblastic differentiation of HGMSCs. The present findings can be translated into the regenerative cell therapy of maxillary / mandibular bone defects.

Keywords: AMPK, BECLIN-1, Phytotherapy, Osteoblast, Resveratrol

Background

Bone resorption, bone wound healing and osteo-integration of implants remain major clinical challenges in orthopedics and dentistry. An attractive solution is exploiting the regenerative potential of Mesenchymal Stem Cells (MSCs) isolated from adult tissues that could differentiate into osteoblasts and chondrocytes [1–3]. In this context, interest recently arose for MSCs from the lamina propria of the gingiva (GMSCs), that represents an easily accessible source from which MSCs can be isolated with minimally invasive techniques [4–6]. GMSCs can be propagated in vitro for long-time while maintaining a stable phenotype and can be induced to differentiate into the osteogenic lineage employing a variety of substances, including herbal-derived polyphenols [7–11].

Recently, interest arose for the potential of resveratrol (RV, trans 3,5,4′ trihydroxy-stylbene), a naturally occurring polyphenol, to prevent and cure bone loss-related diseases [12, 13]. RV shows anti-inflammatory [14] and anti-osteoclastic activities [15, 16] while showing osteoblastic differentiation promoting activities on MSCs [17–21].

* Correspondence: ciro.isidoro@med.uniupo.it
[1]Laboratory of Molecular Pathology, Department of Health Sciences, Università del Piemonte Orientale "A. Avogadro", Via P. Solaroli 17, 28100 Novara, Italy
Full list of author information is available at the end of the article

Chapter 18

Methods for Monitoring Macroautophagy in Pancreatic Cancer Cells

Chiara Vidoni, Alessandra Ferraresi, Christian Seca, Eleonora Secomandi, and Ciro Isidoro

Abstract

Macroautophagy is a catabolic process through which redundant, aged, or damaged cellular structures are first enclosed within double-membrane vesicles (called autophagosomes), and thereafter degraded within lysosomes. Macroautophagy provides a primary route for the turnover of macromolecules, membranes and organelles, and as such plays a major role in cell homeostasis. As part of the stress response, autophagy is crucial to determine the cell fate in response to extracellular or intracellular injuries. Autophagy is involved in cancerogenesis and in cancer progression. Here we illustrate the essential methods for monitoring autophagy in pancreatic cancer cells.

Key words Pancreatic cancer, Autophagy, LC3, p62, Autophagosome, Lysosome

1 Introduction

1.1 Autophagy at a Glance

Macroautophagy (from now on simply autophagy) is a lysosome-driven degradation process that allows for the elimination of cellular macrostructures (i.e., membranes, organelles, macromolecules) [1]. The autophagy process comprises of three steps. The first step consists in the formation of the autophagosome, a double-membrane vesicle that engulfs the cellular structures or molecules that must be degraded [2]. This step is associated with the post-translational insertion within the inner and outer membranes of the autophagosome of the LC3-II protein. LC3-II arises from the proteolytic processing of the cytosolic precursor MAP-LC3 (Macrotubule Associated Protein Light Chain 3) that generates the soluble LC3-I isoform, which is subsequently conjugated with PhosphatydilEthanolamine (PE) [3]. In this step, the autophagy substrates are sequestered within the autophagosomes through the binding to specific receptors (e.g., p62/SQSTM1) [4, 5]. In the second step, the autophagosome fuses with numerous endosomes

Gloria H. Su (ed.), *Pancreatic Cancer: Methods and Protocols*, Methods in Molecular Biology, vol. 1882,
https://doi.org/10.1007/978-1-4939-8879-2_18,

Chapter 7

Acknowledgments

Un ringraziamento speciale è dedicato al mio Professore Ciro Isidoro che ha reso possibile questo lavoro. E' stato il mio mentore fin dai tempi della mia tesi triennale, e ha contribuito fortemente al mio accrescimento e maturazione, sia in ambito scientifico, sia personale.

Porterò con me, con grande piacere e orgoglio, i Suoi preziosi insegnamenti.

Naturalmente ringrazio di cuore tutto il Laboratorio di Patologia Molecolare! Noi non siamo solo colleghi ma una grande squadra di amici. Ognuno di voi, sia materialmente, sia con un sorriso e un grande supporto morale, ha contribuito alla realizzazione della presente tesi. Vi voglio bene ragazzi!

"Talent wins games, but ***teamwork and intelligence win championships****"*

(Michael Jordan)